Dissertation

submitted to the

Combined Faculties for the Natural Sciences and for Mathematics

of the Ruperto-Carola University of Heidelberg, Germany

for the degree of

Doctor of Natural Sciences

presented by

Lennard Ganß, M.Sc.

born in: Kassel

Oral-examination: …….

Oncogenic potential of HPV E6 and E7 and evaluation of treatment strategies inhibiting their effects

Referees: apl. Prof. Dr. Martin Müller

Prof. Dr. Magnus von Knebel Doeberitz

Acknowledgements

First of all, I thank Prof. Magnus von Knebel Doeberitz for giving me the opportunity to complete my PhD thesis in his group. His exciting ideas and motivating guidance supported me during every step of the project. I was always welcome to discuss important questions with him and I am very grateful to his encouraging enthusiasm. Thank you Magnus!

Moreover, I want to thank Dr. Svetlana Vinokurova for her advice and patience especially during the beginning of this project. I am also very grateful to Prof. Dr. Stefan Duensing who supported me in the design of several experiments and provided his laboratory and microscope for the analyses. In particular, I also thank Dr. Johannes Gebert and Dr. Jennifer Lee for providing the HCT116 master cell clone and for guiding me during the first steps of the project. Without their help the completion of this thesis would not have been possible.

Especially, I want to thank the members of my Thesis Advisory Committee (TAC): Prof. Dr. Magnus von Knebel Doeberitz, Prof. Dr. Martin Müller and Prof. Dr. Martina Muckenthaler. Due to their expertise and external view on the project, their comments and advices during our TAC meetings were always very helpful and encouraging.

In addition, I am very grateful to Dr. Matthias Kloor, Prof. Dr. Jürgen Kopitz and Dr. Elena-Sophie Prigge for inspiring discussions and for sharing their expertise during all phases of this thesis.

As a friendly, but motivating atmosphere is the key to successful projects, I want to thank all the members of the Department for Applied Tumor Biology. Of course, special thanks go to my friends in the office: Katharina Urban, Simon Kalteis, Dr. Mine Özcan, Dr. Eva-Maria Katzenmaier, Dr. Malwina Michalak, Fabia Fricke and Dr. Ana-Ligia Gutierrez. Thank you for the unique atmosphere, for the work-related and -unrelated support and for the pleasant time inside and outside the laboratory.

I also want to thank Maximilian Stich for his unshakable enthusiasm and his never-ending motivation. Thank you for a very fruitful time in the lab.

Last but not least, I am very grateful to my family: my father Heinrich, my mother Irmtraud, my brother Jan-Hendrik and my sister Annekathrin. Thank you for your everlasting support and for always believing in me.

Most importantly, I want to finally thank Jennifer Meyer for her unlimited support and understanding. Thank you for your patience, your motivating advices and for encouraging me to accomplish my goals.

Table of Contents

Abstract

Persistent infections with high-risk human papillomaviruses (hr-HPVs) may cause cervical and other types of cancer. The key event for the transformation of hr-HPV-infected cells into malignant tumor cells is the deregulated expression of the hr-HPV oncogenes E6 and E7. Both gene products interfere with cell cycle checkpoints, inhibit DNA damage repair and induce chromosomal instability. Deregulation of hr-HPV oncogene expression as well as transformation of the host cells are driven by the hypermethylation of specific CpG dinucleotides in the viral and host cellular genome. Thereby, the HPV E2-mediated control of E6 and E7 transcription is disrupted and the expression of host cellular tumor suppressive genes and microRNAs is prevented. Therefore, we hypothesized that the application of demethylating agents might re-establish these regulatory mechanisms reducing the hr-HPV oncogene expression and inhibiting cell proliferation.

To test this hypothesis, the demethylating agent 5-aza-2'-deoxycytidine (DAC) was applied to a panel of six HPV-transformed cell lines. DAC treatment significantly decreased the expression of the HPV oncogenes. As a consequence, the levels of E6 and E7 target proteins, including p53 and p21, increased repressing cell proliferation and colony formation. In addition, the application of DAC strongly induced the expression of tumor suppressive miR-375, which was shown to target and degrade E6 and E7 transcripts. In conclusion, the presented data demonstrate the effectiveness of DAC in the treatment of HPV-transformed cells and suggest its testing in clinical trials.

In addition to the evaluation of treatment strategies, the present thesis aimed to study the effects of HPV oncogene expression on chromosomal stability, gene expression patterns and DNA methylation levels. For this, chromosomally stable HCT116 cells were used as a model system to generate clones allowing the inducible HPV 16 E6 and E7 expression. Immortalization of HCT116 cells, which is characterized by microsatellite instability, can be clearly distinguished from HPV-driven immortalization, which depends on the induction of chromosomal instability. Therefore, HCT116 cells represent an ideal

model system to study the HPV 16 oncogene-mediated induction of chromosomal instability.

Induction of HPV 16 oncogene expression affected the chromosomal stability of HCT116 cells by causing abnormal centrosome and spindle pole numbers, by inducing DNA damage and by increasing the number of aneuploid cells. Furthermore, a panel of genes was found to be differentially expressed after induction of HPV 16 oncogene expression potentially representing candidate genes and indicating pathways that might play a role during the transformation of HPV-infected cells. Taken together, HPV 16 oncogene expression seems to increase the genomic variability in the cell population presumably elevating the risk for the generation of highly proliferative subclones over time.

Zusammenfassung

Persistierende Infektionen mit humanen Papillomviren der Hochrisiko-Typen (hr-HPVs) können die Entstehung von Zervixkarzinomen und anderen Tumoren hervorrufen. Die maligne Transformation von hr-HPV-infizierten Zellen wird durch eine unkontrollierte Überexpression der Onkogene E6 und E7 ausgelöst, wodurch vor allem der Zellzyklus beschleunigt, DNA Reparaturmechanismen gehemmt und chromosomale Instabilität induziert wird. Die Regulation der Onkogenexpression und die Transformation infizierter Zellen werden maßgeblich durch die verstärkte Methylierung bestimmter CpG Dinukleotide im Virus- und Wirtszellgenom beeinflusst, wodurch die HPV E2-abhängige Kontrolle der HPV Onkogenexpression gestört und die Expression wichtiger tumor-suppressiver Gene und mikroRNAs verhindert wird. Dies lässt vermuten, dass die Anwendung demethylierender Substanzen zur Behandlung HPV-transformierter Zellen die genannten Regulationsmechanismen wiederherstellt und dadurch die HPV Onkogenexpression, sowie die Zellproliferation inhibiert.

Zur Überprüfung dieser Hypothese wurden in dieser Studie sechs HPV-transformierte Zelllinien mit der demethylierenden Substanz 5-Aza-2'-desoxycytidin (DAC) behandelt. Die Behandlung führte zu einer signifikanten Reduktion der HPV Onkogenexpression, zu einer erhöhten Konzentration der Bindungspartner von E6 und E7, wie beispielsweise p53 und p21, und schließlich zur Hemmung der Zellproliferation. Zusätzlich ließ sich eine starke Expression der tumor-suppressiven miR-375 detektieren, die E6 und E7 Transkripte bindet und deren Abbau auslöst. Die Behandlung von HPV-transformierten Zellen mit der demethylierenden Substanz DAC erscheint somit als ein vielversprechender Ansatz, um die HPV Onkogenexpression und die Proliferation der Zellen zu verhindern.

Neben der Erforschung von Behandlungsstrategien, zielte diese Arbeit darauf ab, den Einfluss der HPV Onkogene auf die chromosomale Stabilität, sowie auf das Genexpressions- und DNA Methylierungsmuster genauer zu untersuchen. Als Modellsystem wurde dafür die chromosomal stabile Zelllinie HCT116 ausgewählt und mittels rekombinanten Kassettenaustauschs zur induzierbaren HPV 16

Onkogenexpression manipuliert. Die Immortalisierung von HCT116 Zellen beruht auf deren Mikrosatelliten-Instabilität und kann daher eindeutig vom HPV-induzierten Transformationsprozess unterschieden werden, der auf einer chromosomalen Instabilität der Wirtszellen basiert. Die Expression der HPV 16 Onkogene bedingte eine Erhöhung des Anteils der Zellen mit abnormalen Centrosomen und der Mitosen mit aberranten Spindelpolen, eine Zunahme von DNA Schädigungen, sowie eine Steigerung aneuploider Zellen und beeinträchtigte somit die chromosomale Stabilität der Zellen. Darüber hinaus wurden nach der HPV 16 E6 und E7 Expression einige differentiell exprimierte Gene identifiziert, die möglicherweise eine Rolle während der Transformation HPV-infizierter Zellen spielen könnten. Die Expression der HPV Onkogene scheint somit die genomische Variabilität der Zellpopulation zu erhöhen, wodurch die Entstehung von stärker proliferierenden Subklonen mit der Zeit gefördert würde.

Abbreviations

A	Adenosine	hr-HPV	High-risk human papillomavirus
AmpR	Ampicillin resistance gene	lr-HPV	Low-risk human papillomavirus
Bidest.	Bidestillatus	Hyg	Hygromycin B
BSA	Bovine serum albumin	HygTK	Hygromycin B phosphotransferase thymidine kinase
C	Cytosine	IF	Immunofluorescence
CIN	Cervical intraepithelial neoplasia	IRES	Internal ribosomal entry site
CMV	Cytomegalovirus	LTR	Long terminal repeat
CNV	Copy number variation	mAb	Monoclonal antibody
DAC	5-aza-2`-deoxycytidine	MCS	Multiple cloning site
DMEM	Dulbecco`s modified eagle medium	min	Minutes
DMSO	Dimethyl sulfoxide	MLH1	MutL homolog 1
DNA	Deoxyribonucleic acid	MMLV	Moloney Murine Leukemia Virus
DNMT	DNA methyltransferase	MMR	Mismatch repair
ddNTPs	Dideoxynucleotide triphosphates	MSI	Microsatellite instability
dNTPs	Deoxynucleotide triphosphates	MSP	Methylation-specific qPCR
Dox	Doxycycline	NHK	Normal human foreskin keratinocytes
DSB	DNA double-strand break	nt	Nucleotide
DTT	1,4-Dithiothreitol	ori	Origin of replication
E2BS	E2 binding site	ORF	Open reading frame
E. coli	Escherichia coli	pAb	Polyclonal antibody
ECL	Enhanced chemiluminescence	PAGE	Polyacrylamide gel electrophoresis
EDTA	Ethylenediaminetetraacetic acid	PBS	Phosphate buffered saline
EtOH	Ethanol	PCR	Polymerase chain reaction
FACS	Fluorescence-activated cell sorting	P_{tet}bi	Bidirectional dox-inducible promoter
FBS	Fetal bovine serum	RIPA	Radioimmunoprecipitation
FFPE	Formalin-fixed paraffin-embedded	RMCE	Recombination-mediated cassette exchange
Flp	Flippase	miRNA	Micro ribonucleic acid
G	Guanosine	mRNA	Messenger ribonucleic acid
Gan	Ganciclovir	rpm	Rounds per minute
h	Hours	RT	Reverse transcription
HNPCC	Hereditary nonpolyposis colorectal cancer	RT-qPCR	Reverse transcription quantitative polymerase chain reaction
HPV	Human papillomavirus	rtTA	Reverse transcriptional transactivator

s	Seconds	TBP	TATA-binding protein
SCC	Squamous cell carcinoma	tet	Tetracycline
S.O.C.	Super optimal broth with catabolite repression	U	Uracile
SV40	Simian-Virus 40	URR	Upstream regulatory region
T	Thymidine	UV	Ultraviolet
TBE	Tris-borate-ethylendiaminetetraacetic acid	WB	Western blot

1. Introduction

1.1. Human papillomaviruses

Papillomaviruses infect epithelial cells of a variety of vertebrates including humans and may induce epithelial lesions in their respective host. Human papillomaviruses (HPVs) are non-enveloped, double-stranded DNA viruses, which infect the basal cells of the squamous epithelium of the skin and the mucosa. Since their discovery in the early 1950s, almost 200 different HPV types have been identified (Bernard *et al.* 2010, Strauss *et al.* 1949). In the 1970s, Harald zur Hausen hypothesized that HPV infections might cause cervical cancer (Gissmann & zur Hausen 1976, zur Hausen 1974, zur Hausen 1975). This hypothesis was further substantiated in the following years by detecting HPV 16 and 18 in cervical cancer. Today, HPV is recognized as an important infectious and carcinogenic agent, which plays a major role during the development of different urogenital cancers including cancers of the cervix, vulva, vagina, penis and anus as well as of head and neck cancers.

Despite the improvements in screening and vaccination, cervical cancer is still the fourth most frequent cancer in women. According to the World Health Organization (WHO) more than 270,000 women die from cervical cancer every year. In 2012, approximately 530,000 new cervical cancer cases were estimated predominantly occurring in low-income countries where the access to effective screening programs is limited. These numbers show that cervical and other HPV-associated cancer types still affect a high number of people worldwide.

To effectively reduce the number of patients dying from HPV-driven tumors, four strategies seem to be essential. First, prophylactic HPV vaccination programs need to be continued and expanded. However, as prophylactic HPV vaccination can only be effective to prevent new HPV infections, there is still a strong need for therapeutic options helping patients who are already infected. Therefore, screening for cervical and other HPV-associated cancer types needs to be improved and expanded even further to detect the disease at an early stage offering a better prognosis. Thirdly, treatment

options for later staged patients need to be optimized. Several approaches are currently tested including therapeutic vaccination (e.g. against E7 and p16) as well as the application of demethylating agents, as discussed in section 1.4.2. However, these approaches and the development of novel therapeutic strategies require a detailed understanding of the mechanisms used by HPV to infect host cells and to transform these cells into proliferating tumor cells. Therefore, as a fourth key point to target HPV-driven cancers, there is a continuous need for the development of model systems, which precisely mimic HPV infection and tumor development thereby promoting a better understanding of viral strategies.

Depending on their carcinogenic potential, HPV types are categorized as either low-risk (lr) or high-risk (hr). Generally, infections with lr-HPV types can lead to the development of genital warts (condyloma) and are rarely found in malignancies (Bodily & Laimins 2011). In contrast, infections with hr-HPV types may cause malignant transformation that potentially leads to the progression of cancer. About 99% of all cervical cancers contain genomic sequences of hr-HPV types (Ault 2006). Especially the hr-HPV types 16 and 18, which are detected in about 70% of all cervical cancers, play a predominant role. However, hr-HPV infections do not necessarily lead to the formation of cancer. The vast majority of these infections does not cause any symptoms and can mostly be cleared by the host immune system. Only a small number of infections may persist and can then progress towards cancer. The progression from persistent infections to invasive cancers includes multiple stages representing different grades of precursor lesions (intraepithelial neoplasia grade 1 to 3) and generally spans years or even decades (Carter *et al.* 2011, zur Hausen 2002).

1.1.1. HPV genome organization

The HPV genome consists of double-stranded DNA organized in an episomal structure with about 8,000 base pairs (HPV16: 7904 bp) encoding six early and two late genes (Doorbar 2005) (Figure 1). The early genes (E1, E2 and E4-E7) are mainly involved in the replication of the viral genome, which is synchronized with the DNA replication of the host cell. Furthermore, they also play important roles in the transcriptional regulation of

viral genes (E2), in viral capsid maturation and release (E4) but also deregulate cell cycle control and apoptosis pathways (E5 and mainly E6 and E7) (reviewed in (Doorbar *et al.* 2012, Moody & Laimins 2010)). The late genes L1 and L2, which are expressed in the final steps of the viral life cycle, code for the major (L1) and minor (L2) capsid proteins. Both, early and late genes are transcribed as polycistronic mRNAs from a single HPV DNA strand and are then processed by the host cellular splicing machinery (reviewed in (Graham 2010)). The expression of the early genes is regulated by the upstream regulatory region (URR), which can be divided into 5` long control region (LCR), enhancer region and promoter region. This part of the HPV genome is not transcribed into mRNA but contains binding sites for numerous host cell and viral transcription factors regulating viral early gene expression (reviewed in (Thierry 2009)). In contrast, late gene expression is controlled by the late promoter, which is located in the genomic region coding for E7. The transcriptional activity of the late promoter depends on keratinocyte differentiation (del Mar Pena & Laimins 2001). In addition to the transcriptional activity of the two promoter regions, HPV gene expression also relies on appropriate polyadenylation and alternative splicing of the polycistronic RNA, as well as on its translation into the respective protein (reviewed in (Graham 2010)). Therefore, HPV early and late gene expression is not only regulated by viral but also by host cellular factors. The role of the viral proteins during the HPV life cycle and during malignant transformation of the host cells is described in the following chapters.

1.1.2. HPV life cycle

The HPV life cycle is tightly coupled to the differentiation state of the host cell and leads to the production and the release of infectious viral particles (Figure 1). HPV virions infect undifferentiated basal and parabasal epithelial cells through traumatic micro-abrasions, which can occur during sexual intercourse (Schiller *et al.* 2010). First, the virus attaches and enters the target cell, which is mediated by receptors expressed on the surface of the host cell (Evander *et al.* 1997, Letian & Tianyu 2010). After disruption of the endosomal membrane by the viral L2 protein, the viral genome is transported into the nucleus of the host cell where it is maintained as an episome (Kamper *et al.* 2006).

This stage of infection is not associated with cytopathologic effects or detectable symptoms because expression of the viral genes is mainly repressed. Solely the early genes E1 and E2 were found to be expressed at low levels fusing the viral episomes to the host cellular chromosomes and thereby allowing the replication of the viral genome. Therefore, this state is classified as silent or latent phase of HPV infections (reviewed in (Doeberitz & Vinokurova 2009)).

The distribution of the viral genome depends on the dividing capacity of the undifferentiated cells in the basal epithelium. After mitosis both of the two daughter cells contain episomal HPV copies in their nuclei. One of these daughter cells retains its dividing capacity by remaining in the basal epithelium and thereby functions as a viral reservoir for persistent HPV infections. The other daughter cell starts to migrate and differentiate towards the superficial cell layers. This process is accompanied by elevated transcription of the early viral genes E1 and E2, as well as of the oncogenes E6 and E7 (reviewed in (Doorbar *et al.* 2012)). Thereby, replication of the viral episomes is promoted and subsequently uncoupled from the replication of the host genome leading to a substantial increase of viral episomes in the cells (reviewed in (Hebner & Laimins

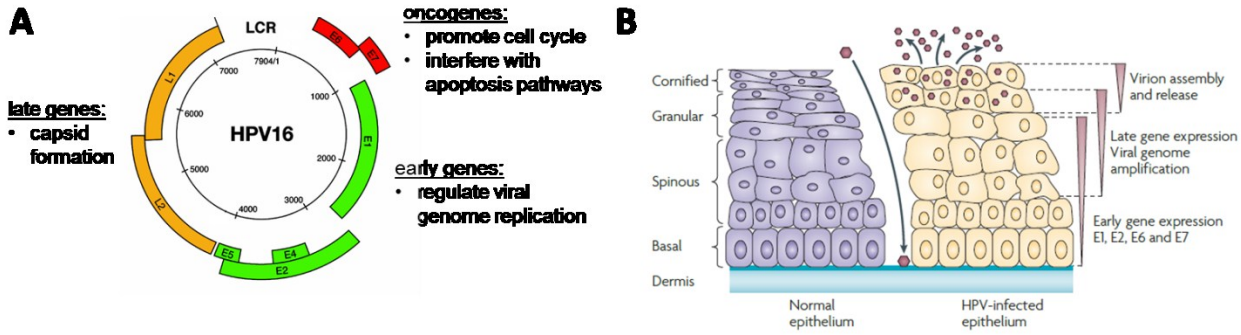

Figure 1: Schematic illustration of the HPV 16 genome and the HPV life cycle.
(A) The HPV 16 genome contains 7904 nucleotides and encodes six early genes (green) including the two oncogenes E6 and E7 (red) and two late genes (orange). The LCR regulates the expression of the early genes. (Modified from (Doorbar *et al.* 2012) **(B)** HPV (red hexagons) infects the basal cells of the squamous epithelium through micro lesions in the skin and is established as episomes. After cell division one of the infected daughter cells remains in the basal cell layer and the other infected daughter cell migrates and differentiates towards the upper cell layers. During this process HPV early gene expression is activated, the viral genome is amplified and the late genes are subsequently transcribed (as indicated by the triangles). Afterwards, the virions are assembled and finally released from dying keratinocytes in the superficial cell layer thereby completing the HPV life-cycle. (Modified from (Moody & Laimins 2010))

2006, Ibeanu 2011)).

In the final step of the viral life cycle, the viral genomes are packed into infectious viral particles, which are then released potentially infecting other host cells. This process is initiated by the increasing transcriptional activity of the HPV late promoter during the migration of the host cell through intermediate and superficial epithelial cell layers. Transcriptional activation of the late promoter leads to the expression of the late genes L1 and L2. The major capsid protein L1 self-assembles into homopentamers forming icosahedral capsids of about 50 nm in diameter (reviewed in (Buck *et al.* 2013)). L2 proteins have been shown to be located between L1 monomers in the inner surface of the virion (Lowe *et al.* 2008). The viral genome is then encapsulated and the infectious HPV particles are released from decaying keratinocytes at the epithelial surface.

The mechanisms of viral genome replication and virion release evolved by HPVs effectively prevent the recognition and targeting of the virions or of infected cells by the host immune system (reviewed in (Stubenrauch & Laimins 1999). This is mainly accomplished by minimal viral gene expression in the basal epithelial cell layers and by the prevention of host cell disruption until reaching the upper epithelial cell layer. Thereby, HPV infections can persist over long time periods without being cleared by the host immune system.

1.2. Deregulation of HPV oncogene expression mediates host cell transformation

Persistence is assumed to be a prerequisite for the progression from permissive to transforming HPV infections. However, the molecular events triggering this transition, which may only occur in distinct host cells, are not completely understood. As illustrated in Figure 2, the key event causing the shift from permissive to transforming infections seems to be the deregulated expression of the HPV oncogenes E6 and E7. These viral proteins were found to interact with numerous host cellular factors influencing a variety of molecular pathways in the cells. Generally, both oncoproteins promote cell proliferation, inhibit apoptosis pathways and are assumed to induce genomic instability

in the host cells (reviewed in (Moody & Laimins 2010)). The mechanisms, how E6 and E7 affect host cellular pathways, have intensively been studied and are described in chapter 1.3. In contrast, molecular events that potentially result in the deregulation of E6 and E7 expression are only superficially described. In the following paragraphs four major concepts are introduced that aim to explain the shift from permissive to transforming HPV infections.

In 2012, Herfs and colleagues suggested that squamous columnar junction cells are the source of cervical cancer (Herfs *et al.* 2012). This embryonic cell population, which is located at the transformation zone between endocervical columnar and ectocervical squamous epithelium, shows a distinct morphology and a unique gene expression profile. Moreover, the authors identified markers specific for this type of cells that are maintained in both squamous cell carcinomas and adenocarcinomas, further substantiating the assumption that cervical carcinogenesis primarily originates from

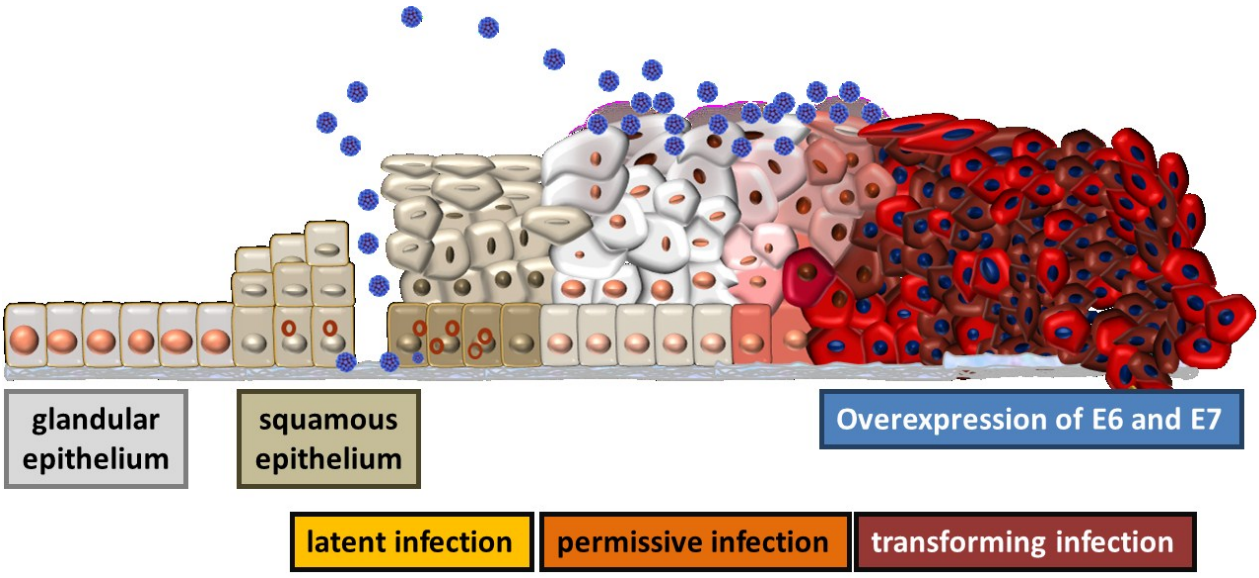

Figure 2: Pathogenesis of HPV-induced cervical lesions.
HPV (blue particles) infects the basal cells of the squamous epithelium through micro lesions in the skin. After viral uptake and transport to the nucleus the viral genome is maintained as episomes (red circles, latent infection). During S phase of the cell cycle, the viral genome is replicated and then distributed onto the daughter cells during mitosis. The viral life cycle continuous as described previously and results in the release of infectious viral particles (light grey cells, permissive infection). Especially at the squamous columnar junction zone the expression of the viral genes in the basal cells might become deregulated resulting in the overexpression of the oncogenes E6 and E7. These cells are assumed to bear an increased risk for malignant transformation and subsequent tumor progression (red cells, transforming infection). The Figure was modified according to (Doeberitz & Vinokurova 2009).

squamous columnar junction cells. Based on these observations the authors proposed that basal cells of the columnar epithelium, of the squamous epithelium as well as of the squamous columnar junction can be infected by HPV, however, only the infected squamous columnar junction cells expressing the identified marker genes harbor an elevated risk of carcinogenic progression. If the proposed model holds true, excision of the squamous columnar junction, which seems to lack the potential for regeneration, might be an option to cure early cervical lesions. Future trials, however, need to clarify whether squamous columnar junction specific genes reliably predict the likelihood of progression of infected cells and whether ablation of these cells really lowers the risk of developing cervical cancer.

In addition to the cell population infected by HPV, several other factors seem to play an important role in mediating the shift from permissive to transforming infections. At the molecular level this includes the status of the viral genome, but also epigenetic marks regulating the expression of the viral oncogenes.

Transcription of E6 and E7 is mainly controlled by the URR, which contains several transcription factor binding sites including four that allow the interaction with the viral protein E2 (Figure 3). The E2 binding sites (E2BSs) bind E2 proteins with different affinities facilitating a tight regulation of early gene expression. Interaction of E2 with the high affinity E2BS 1 activates the early promoter stimulating the production of early viral proteins including E2 itself, as well as E6 and E7 (Rapp *et al.* 1997, Steger & Corbach 1997). Rising levels of E2 then also result in interaction with the low affinity proximal E2BSs 2, 3 and 4, which represses transcription by displacing the transcription factors Sp1 and TATA-binding protein (TBP) from their respective binding sites (Stubenrauch *et al.* 1998). This feedback mechanism ensures the continuous low expression levels of the early genes and simultaneously prevents their overexpression potentially avoiding recognition by the host immune system (reviewed in (Thierry 2009)). Thereby, the HPV E2 protein functions as the master regulator of the viral life cycle (Singh *et al.* 2016).

Abrogation of this regulatory mechanism might therefore constitute an important initial step towards malignant transformation. Loss of E2 expression is frequently observed after viral integration into the host genome, which often causes disruption of the E2 ORF

(Cullen *et al.* 1991, Pett & Coleman 2007). Integration of viral genomes can be found in many cervical carcinoma cell lines and occurs frequently in advanced HPV-associated lesions (Jeon & Lambert 1995). Considerable numbers of cervical lesions associated with transforming HPV infections, however, lack integrated viral genome copies suggesting that viral genome integration might be a rather late event during carcinogenic transformation (Cullen *et al.* 1991, Wentzensen *et al.* 2004). Based on these observations other mechanisms seem to exist explaining the deregulated expression of E6 and E7 in early low-grade lesions that only contain episomal HPV copies.

One of these mechanisms proposes that altered DNA methylation patterns of CpG dinucleotides located in the E2BSs may affect the E2-mediated transcriptional regulation. Methylation at the 5` position of cytosines in the DNA functions as epigenetic

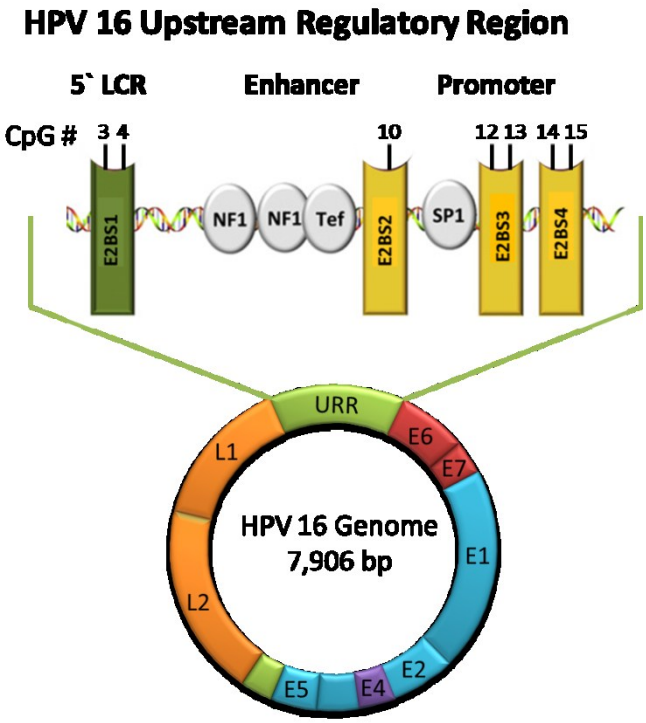

Figure 3: Schematic illustration showing the location of the URR and the E2BSs in the HPV 16 genome.
The HPV 16 URR regulates early gene transcription and can be divided into 5`LCR, enhancer and promoter region. These regions contain binding sites for different host cellular transcription factors including nuclear factor 1 (NF1), thyrotroph embryonic factor (Tef) and specificity protein 1 (Sp1). Most important for the present study are the four E2BSs allowing the interaction with the viral protein E2. The E2BSs contain several CpG dinucleotides that can be differentially methylated during HPV-mediated carcinogenesis strongly affecting the regulatory function of E2. The Figure was modified according to (Doeberitz & Vinokurova 2009).

mark influencing the transcriptional activity of the respective genomic locus. The E2BSs in the HPV URR share a consensus DNA sequence (5`-ACCG($N_4$)CGGT-3`) containing two CpG dinucleotides, which were found to be hypermethylated in HPV-associated lesions that harbor episomal viral copies as well as in HPV-related cancers that contain the viral genome integrated as a concatemer (Baker *et al.* 1987, Chaiwongkot *et al.* 2013, Romanczuk *et al.* 1990). E2BS methylation blocks the interaction with E2 proteins abrogating the E2-mediated transcriptional repression of E6 and E7 and thereby deregulating HPV oncogene expression (Kim *et al.* 2003, Thain *et al.* 1996).

In addition to elevated E2BS methylation, changes in the methylation pattern at other sites in the viral as well as in the host cellular genome seem to be involved in the transformation of HPV-infected cells. Hypermethylation of several viral genes including the late genes L1 and L2, but also E2, E5 and the URR, distinguishes low-grade lesions (cervical intraepithelial neoplasia (CIN) grade 1 and 2) from high-grade CINs and malignant tumors ((Kalantari *et al.* 2004, Mirabello *et al.* 2013, Vinokurova & von Knebel Doeberitz 2011) and reviewed in (Clarke *et al.* 2012, Johannsen & Lambert 2013)). Additionally, the transition from low- to high-grade lesions is characterized by methylation-dependent silencing of host cellular tumor suppressor genes, e.g. cell adhesion factors like cadherin 1 (CDH1) and cell adhesion molecule 1 (CADM1) (Kang *et al.* 2006, Narayan *et al.* 2003, Shivapurkar *et al.* 2007), as well as apoptotic factors including death-associated protein kinase 1 (DAPK1) ((Feng *et al.* 2005) and reviewed in (Wentzensen *et al.* 2009)).

As an additional regulatory mechanism, the expression of HPV-encoded genes can be affected by the presence of microRNAs (miRNAs) that effectively target mRNA transcripts. One of these candidates is miR-375, which was shown to interact with HPV 16 and 18 E6 and E7 transcripts, thereby triggering their subsequent degradation by endonucleases of the RNA-induced silencing complex (RISC) (Jung *et al.* 2014). Moreover, this miRNA seems to play a tumor suppressive role in HPV-associated cancer types as it also suppresses the expression of important host cellular factors including the transcription factor Sp1, telomerase reverse transcriptase (TERT) and the E6-associated protein (E6AP) ((Bierkens *et al.* 2013, Jung *et al.* 2014, Wang *et al.* 2011) and reviewed in (Yan *et al.* 2014)). Expression of the gene encoding miR-375 was found

to be repressed by hypermethylation of its promoter, which can be observed in HPV-associated preneoplastic lesions and invasive carcinomas (Wilting *et al.* 2013).

In conclusion, the introduced concepts show that the deregulated expression of E6 and E7, especially in squamocolumnar junction cells, seems to be the key event for the shift from permissive to transforming HPV infections. Additionally, hypermethylation seems to play an important role in silencing suppressive factors involved in the regulation of HPV oncogene expression. Therefore, reversing hypermethylation in HPV-transformed tumors might be a potent therapeutic strategy to restore these regulatory mechanisms. As an alternative approach, it might be effective to target host cellular pathways that have been manipulated by the HPV oncogenes. The identification of such pathways and the involved factors requires the precise understanding of E6- and E7-mediated host cellular transformation, which in turn depends on the presence of powerful model systems. The following section summarizes the most important host cellular pathways and regulatory mechanisms that are affected by the HPV oncoproteins E6 and E7.

1.3. Role of E6 and E7 during HPV-mediated carcinogenesis

The hr-HPV proteins E6 and E7 are the main viral factors that facilitate the initiation and progression of HPV-associated cancers. The enhanced expression of both oncogenes seems to be the key event for the progression from permissive HPV infections (CIN 1) to transforming high-grade lesions (CIN 2, 3 and squamous cell carcinoma). During this process E6 and E7 interact with numerous host cellular proteins resulting in the deregulation of important pathways. Thereby, E6 and E7 have an impact on all cancer hallmarks described by Hanahan and Weinberg (Hanahan & Weinberg 2000) (Figure 4). The structure and the biological activity of these two proteins, including their binding partners and affected pathways, have been extensively studied resulting in various research papers and review articles, e.g. (Klingelhutz & Roman 2012, Moody & Laimins 2010, Roman & Munger 2013). As a common feature, both oncoproteins relax cell cycle checkpoints, inhibit apoptosis and induce genomic instability upon overexpression in infected cells.

1.3.1. Hr-HPV E6 and E7 manipulate cell cycle regulation

Permanent expression of hr-HPV E6 and E7 promotes the sustained proliferation of their host cells, which is mainly mediated by the inhibition of tumor suppressive proteins that play key roles in cell cycle regulation. Hr-HPV E7 effectively binds to pocket protein family members including the retinoblastoma protein (pRB), p107 and p130 resulting in their proteasomal degradation (Berezutskaya *et al.* 1997, Boyer *et al.* 1996, Genovese *et al.* 2008, Gonzalez *et al.* 2001, Zhang *et al.* 2006). The pocket protein family members are mainly involved in cell cycle regulation by inhibiting G_1 to S-phase transition (reviewed in (Cobrinik 2005)). This function is predominantly mediated by their ability to bind to different members of the E2F transcription factor family. Upon phosphorylation of pocket proteins, E2F transcription factors are released promoting the expression of genes that stimulate cell cycle progression (Arroyo *et al.* 1993, Chellappan *et al.* 1992, Huang *et al.* 1993, Wu *et al.* 1993, Zerfass *et al.* 1995). Moreover, E2F transcription factor binding sites were found in promoters of genes regulating differentiation and apoptosis (DeGregori & Johnson 2006). To decelerate cell cycle progression the release of E2F transcription factors is prevented by the expression of $p16^{INK4a}$, which inhibits cyclin dependent kinases, such as CDK4 and CDK6 that are needed for phosphorylation of pRb. By degrading pocket proteins, hr-HPV E7 efficiently blocks $p16^{INK4a}$-mediated G_1 cell cycle arrest (Giarre *et al.* 2001). Consequently, high levels of $p16^{INK4a}$, as commonly detected in transforming HPV-associated lesions, are not able to inhibit cell cycle progression and can therefore be used as a marker for progressing HPV infections (reviewed in (von Knebel Doeberitz *et al.* 2012)).

Degradation of pocket proteins and the resulting E2F-mediated cell cycle stimulation lead to accumulation of the cell cycle regulator p53 (Demers *et al.* 1994). The tumor suppressive protein p53 regulates the cell cycle, DNA damage response as well as the initiation of apoptosis and has therefore been described as “the guardian of the genome” (Lane 1992). During the cell cycle p53 levels increase in response to DNA damage frequently resulting from replicative stress (reviewed in (Lakin & Jackson 1999, Zeman & Cimprich 2014)). As a consequence, mitosis is arrested at the G_1 or G_2 checkpoint, respectively, and the DNA damage repair machinery is activated simultaneously. If the damaged DNA can be repaired, p53 levels will decrease again allowing the cell cycle to

continue. However, permanent presence of p53 resulting from irreparable DNA damage initiates apoptosis in affected cells (reviewed in (Fridman & Lowe 2003)).

To overcome this growth inhibitory effect, hr-HPV E6 efficiently targets p53. This is mediated by the interaction between E6, p53 and the E6-associated protein (E6AP) forming a trimeric complex that results in the ubiquitination and proteasomal degradation of p53 (Huibregtse *et al.* 1993). Additionally, E6 can also bind to p53 in the absence of E6AP. Thereby, p53-mediated transcriptional regulation is blocked preventing the expression of genes involved in cell cycle arrest, DNA damage repair and apoptosis (Lechner & Laimins 1994). Moreover, the presence of hr-HPV E6 proteins indirectly influences the activity of p53 by binding histone acetyltransferases that are needed for p53 acetylation and stabilization (Patel *et al.* 1999, Zimmermann *et al.* 1999). Taken together, hr-HPV E6 and E7 work hand in hand to inactivate tumor suppressors subsequently deregulating the cell cycle and promoting the proliferation of infected cells.

1.3.2. Expression of hr-HPV E6 and E7 prevents apoptosis

Besides manipulating cell cycle control, overexpression of hr-HPV E6 and E7 also effectively inhibits apoptosis pathways. As mentioned previously, this is predominantly mediated by the ability of hr-HPV E6 to degrade p53. Moreover, hr-HPV E6 prevents apoptosis induced by tumor necrosis factors (TNFs) and by the Fas pathway ((Filippova *et al.* 2004, Filippova *et al.* 2002, Garnett *et al.* 2006) and reviewed in (Garnett & Duerksen-Hughes 2006)). However, not only hr-HPV E6, but also E7 is involved in manipulating apoptosis pathways by targeting different host cellular factors. The presence of hr-HPV E7 proteins stimulates PKB/Akt signaling, which promotes cell survival and prevents apoptosis (Pim *et al.* 2005). Furthermore, hr-HPV E7 targets the insulin-like growth factor binding protein 3 (IGFBP-3), which is overexpressed in senescent cells (Mannhardt *et al.* 2000). All in all, overexpression of hr-HPV E6 and E7 effectively delays or even completely prevents the induction of apoptosis allowing the accumulation of highly DNA-damaged cells.

1.3.3. Effects of hr-HPV oncoproteins on genomic stability

Generally, genomic instability can be defined as the inability of cells to preserve their genomic integrity during DNA replication and subsequent cell division. As most cancers show genetic or chromosomal alterations, genomic instability is assumed to be a cancer hallmark and seems to be necessary for tumor development (reviewed in (Negrini *et al.* 2010)). Genomic instability can either be observed at the nucleotide level resulting in substitutions, insertions and deletions of nucleotides, or at the chromosomal level leading to gains and losses of whole chromosomes or to chromosomal translocation (Lengauer *et al.* 1998). The first of these two forms of genomic instability seems to be predominantly caused by biallelic mutations in DNA mismatch repair genes (e.g. *hMLH1* or *hMSH2*) resulting in the accumulation of mutations mainly located in long repetitive nucleotide stretches called microsatellites. Microsatellite instability (MSI) can be detected in several cancer types predominantly colorectal cancer (CRC). Despite their high mutation rate mismatch repair-deficient cancers are mostly diploid and show normal rates of chromosomal variations (reviewed in (Boland & Goel 2010)).

In contrast, chromosomal instability is characterized by gains and losses of whole chromosomes resulting in the formation of aneuploid tumor cells. This form of genomic instability can be observed in the majority of cancers including HPV-related cancers ((Olaharski *et al.* 2006) and reviewed in (Sen 2000)). The molecular basis of chromosomal instability seems to be the alteration of genes that regulate cell cycle progression and the precise allocation of chromosomes to the daughter cells during mitosis.

As the expression of both HPV oncogenes effectively compromises DNA damage response pathways and deregulates cell cycle checkpoints, it is not surprising that chromosomal instability can be commonly observed in hr-HPV-associated cervical neoplasia and in HPV-immortalized cell lines (Hashida & Yasumoto 1991, Heselmeyer *et al.* 1996, Solinas-Toldo *et al.* 1997, White *et al.* 1994). Induction of chromosomal instability constitutes an early and central event during HPV-mediated transformation as HPV-associated lesions are already aneuploid at noninvasive stages (Bulten *et al.* 1998,

Duensing *et al.* 2000, Steinbeck 1997). In contrast, aneuploidy seems to be absent in lesions caused by lr-HPV types (Fu *et al.* 1981).

1.3.4. Hr-HPV E6 and E7 affect centrosome duplication and mitotic fidelity

Centrosomes are the main microtubule organizing organelles in the cell and therefore play an important role in the formation of spindle poles during mitosis. Generally, centrosomes consist of two centrioles (mother and daughter centriole) surrounded by pericentriolar material. Depending on the cell cycle phase cells contain either one or two centrosomes. During S phase of the cell cycle the centrosome is duplicated, which occurs concomitant to DNA replication (reviewed in (Brownlee & Rogers 2013)). Afterwards, the centrosomes migrate to opposite cell poles forming a bipolar spindle. Errors during centrosome replication potentially result in the formation of more than two spindle poles during mitosis, which can be a source for the generation of aneuploid daughter cells.

Multipolar mitoses are common in cervical cancer and have been suggested as diagnostic marker for the progression of HPV-transformed cervical lesions (Crum *et al.* 1984). Furthermore, it was found that the number of cells containing abnormal centrosomes increases with the progression of HPV-associated lesions (Skyldberg *et al.* 2001). The generation of abnormal centrosome numbers seems to be associated with the overexpression of the hr-HPV oncogenes. Duensing *et al.* showed that stable HPV 16 E6 and E7 expression promotes numerical centrosome abnormalities in normal human keratinocytes (NHKs) (Duensing *et al.* 2000). Under transient conditions the expression of HPV 16 E7 seems to play a predominant role, as the induction of abnormal centrosome numbers was observed already within 48 hours. In contrast, transient expression of HPV 16 E6 showed only minor influences on centrosome numbers (Duensing *et al.* 2000).

Abnormal centrosome numbers can be the consequence of different mechanisms, which need to be distinguished, as the affected cells are assumed to show different risks to generate viable offspring. On the one hand, numeric centrosomal aberrations might

result from cytokinesis failures and errors during mitosis. As a consequence, the accumulation of centrosomes is accompanied by nuclear abnormalities including multi-nucleation and the formation of micro-nuclei. However, the affected cells are assumed to mostly produce non-viable progeny and are therefore unlikely to contribute to the formation of chromosomally unstable cells. On the other hand, centrosome numbers can be increased by deregulated centrosome duplication control (overduplication) potentially as a consequence of the separation of DNA and centrosome replication during S phase of the cell cycle. These cells show fewer nuclear abnormalities and are more likely to generate viable, but chromosomally unstable daughter cells (reviewed in (Duensing 2005)).

The effect of HPV 16 E7 on the host cellular centrosome numbers seems to be caused by centrosome duplication errors because E7 expression was found to alter the ratio between mature and immature centrioles by increasing the proportion of functionally immature daughter centrioles (Duensing & Munger 2002). Consequently, abnormal centrosome numbers caused by HPV 16 E7 more likely originate from centrosome overduplication than from centrosome accumulation. The mechanism by which HPV 16 E7 affects centrosome duplication seems to involve its ability to degrade pocket proteins. Many factors, which coordinate centrosome duplication, are activated by E2F including cdk2/cyclin A and cdk2/cyclin E complexes (Martin *et al.* 1998, Zerfass *et al.* 1995). Therefore, hyperactivation of these factors might interfere with the tight coupling between centrosome and DNA duplication.

Taken together, expression of hr-HPV E6 and E7 very likely induces accumulation as well as overduplication of centrosomes. During mitosis these cells are prone to form more than two spindle poles potentially generating aneuploid progeny. Although most of these cells might not be viable, even moderate increases in genetic variability may contribute to the selection and subsequent outgrowth of highly proliferative subclones. This process occurs over several years or even decades and eventually leads to the formation of HPV-associated tumors.

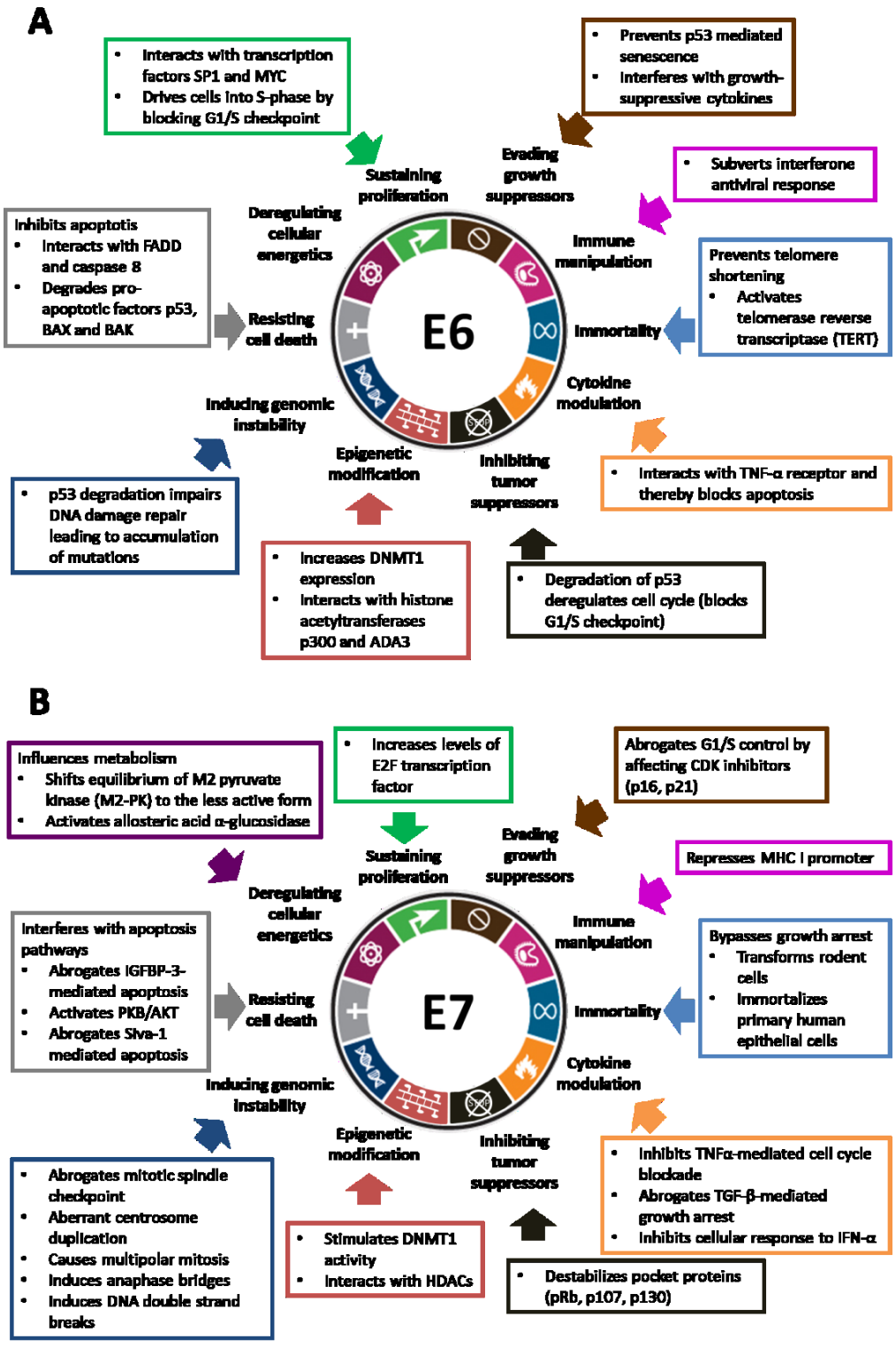

Figure 4: Deregulated expression of HPV 16 E6 and E7 affects all hallmarks of cancer.
The host cellular pathways and factors manipulated by the deregulated expression of HPV 16 **(A)** E6 and **(B)** E7 are schematically illustrated. Thereby, both HPV 16 oncoproteins affect the hallmarks of cancer described by Hanahan and Weinberg highlighting the potency of continuous HPV 16 E6 and E7 expression in the malignant transformation of infected cells. The Figure was modified based on (Hanahan & Weinberg 2000).

1.3.5. Hr-HPV E6 and E7 compromise genomic integrity

In addition to the induction of centrosome duplication errors, expression of hr-HPV E6 and E7 is associated with elevated rates of DNA damage (Duensing *et al.* 2000, Duensing & Munger 2002). Stable expression of HPV 16 E6 and E7 in NHK cells was shown to increase the number of DNA double strand breaks as detected by nuclear γ-H2AX foci (Duensing & Munger 2002). Due to the E6-mediated degradation of p53 highly DNA damaged cells may accumulate and seem to be specifically prone to chromosomal breakages. Moreover, these cells might undergo mitosis because cell cycle checkpoint control mechanisms are efficiently abrogated by both HPV oncoproteins. As a consequence, the frequency of lagging chromosomes and anaphase bridges during mitosis is elevated potentially giving rise to chromosomal changes in the resulting daughter cells. Thus, this effect seems to be another mechanism how hr-HPV E6 and E7 contribute to the induction of structural and numerical chromosome instabilities in their host cells.

1.3.6. Epigenetic alterations upon hr-HPV oncogene expression

Another important effect of hr-HPV E6 and E7 expression is the alteration of epigenetic patterns that may affect the expression of host cellular and viral genes. Hr-HPV E6 was detected to induce upregulation of DNA methyltransferase 1 (DNMT1) by suppressing its transcriptional inhibitor p53 (Au Yeung *et al.* 2010). In addition, HPV 16 E7 oncoproteins were shown to bind and subsequently enhance the activity of DNMT1 (Burgers *et al.* 2007). The DNMT-stimulating effect of both oncoproteins was further substantiated by Li *et al.* who reported the reduced expression of several DNA methyltransferases (DNMT1, DNMT3A, DNMT3B and DNMT3L) upon short-hairpin RNA knock down of HPV 16 E6 and E7 expression (Li *et al.* 2015). The authors also observed the re-activated expression of numerous tumor suppressor genes due to reduced methylation levels in their promoter regions. This study suggests that deregulated expression of hr-HPV E6 and E7 might promote hypermethylation and subsequent silencing of tumor suppressive factors, which is frequently observed during progression from low-grade HPV-associated

lesions to transforming high-grade intraepithelial neoplasia (Bierkens *et al.* 2013, Henken *et al.* 2007, Laurson *et al.* 2010, Narayan *et al.* 2003).

Overall, continuous expression of hr-HPV E6 and E7 deregulates important mechanisms in the host cells including cell cycle progression, apoptosis and gene expression. Thereby, both oncogenes establish an environment that stimulates permanent replication of infected cells. Malignant transformation seems to be further promoted by the induction of numerical and structural chromosomal instability causing high genetic variability.

1.4. Therapeutic strategies

As other cancer types, treatment of HPV-associated tumors involves three general and combinable options: surgery, radiotherapy and chemotherapy. The therapy of choice strongly depends on the diagnosed stage of the tumor. In early stages (stage 0 and I) the tumor can usually be resected either by conization, especially in cases with early stromal invasion, or by hysterectomy eliminating the risk for recurring cervical cancer. Depending on the diagnosed stage and the degree of tumor invasion in the surrounding tissue, surgery is combined with adjuvant radiotherapy or chemotherapy (reviewed in (Adams *et al.* 2014)). Most of the chemotherapeutic agents are either platinum-based substances (e.g. cisplatin or carboplatin) or taxanes (e.g. paclitaxel), which are frequently administered in combination resulting in increased response rates. Combined chemotherapy, however, results in low response rates between 25% and 35% in recurrent and metastatic tumors (Long *et al.* 2005, Moore *et al.* 2004). Furthermore, side effects can be severe as these agents are applied systemically and are not able to distinguish between tumor and normal cells. Therefore, novel therapeutic agents that target HPV-transformed cells more efficiently and more specifically are highly needed. Identification of potent substances, of relevant pathways as well as of prognostic biomarkers, in turn, depends on the development of model systems that precisely reflect the progression of HPV-associated tumors.

1.4.1. Vaccination approaches

Generally, vaccination approaches can be divided into prophylactic and therapeutic strategies. Prophylactic vaccines mainly prevent the infection with hr-HPV types, whereas patients suffering from persistent HPV infections would only benefit from therapeutic vaccination approaches. Currently, there are three prophylactic vaccines commercially available: *Cervarix*® (GlaxoSmithKline), *Gardasil*® (Merck & Co) and *Gardasil 9* (Merck & Co). *Cervarix*® is a bivalent vaccine, which contains virus like particles (VLPs) derived from HPV 16 and 18 L1 capsid proteins and therefore efficiently protects against HPV 16 and 18 infections. In addition, *Gardasil*® also prevents the infection with lr-HPV 6 and 11, which are responsible for a substantial number of genital warts. In 2014, the nine-valent vaccine *Gardasil 9* was approved by the FDA additionally protecting against HPV 31, 33, 45, 52 and 58 (Petrosky *et al.* 2015). Although, cross-protection may occur, vaccination is not assumed to prevent infections with HPV types that are not covered by the respective vaccine ((Combita *et al.* 2002) and reviewed in (Frazer 2010)). The main disadvantage of these approaches is their lack of therapeutic efficacy, as established HPV infections and especially high-grade lesions seem not to be cleared by using *Cervarix*® or *Gardasil*® ((Hildesheim *et al.* 2007) and reviewed in (Kanodia *et al.* 2008)). The lack of therapeutic efficacy might be explained by the observation that L1 capsid production decreases with the progression of HPV-associated lesions, as high-grade lesions and HPV-associated tumors tend to show a low L1 expression rate (Lee *et al.* 2008, Yoshida *et al.* 2008).

The development of therapeutic vaccines aims to overcome these limitations by initiating effective cellular immune responses (especially T cell-mediated) against HPV infected cells. Currently, several therapeutic vaccination approaches are investigated including trials based on VLPs, peptides, vectors or nucleic acids (reviewed in (Pouyanfard & Muller 2017) and (Su *et al.* 2010)). Frequently, these trials are designed to stimulate immune responses against viral antigens, mostly E6 and E7, as both are continuously expressed at high levels in HPV-associated lesions (reviewed in (Hung *et al.* 2007)). Moreover, host cellular proteins might be promising targets for vaccination. One of these candidates might be the cyclin dependent kinase inhibitor $p16^{INK4A}$, which was shown to be strongly expressed in transforming HPV infections (reviewed in (von Knebel

Doeberitz *et al.* 2012)). Therefore, $p16^{INK4A}$ is widely used as a marker for progressing HPV-associated lesions. However, targeting proteins expressed by the host cells bears the risk of autoimmunity, which needs to be excluded before entering clinical trials. Altogether, the challenges for therapeutic vaccines are high as they need to induce strong immune responses and at the same time need to overcome immunosuppression in the tumor micro-environment as well as tumor evasion strategies. Therefore, the combination of immunotherapeutic and chemotherapeutic approaches might be an attractive future strategy.

1.4.2. Demethylating agents

As hypermethylation of important viral and host genes was shown to play an important role during HPV-mediated cervical carcinogenesis, the application of demethylating agents might be a promising approach for the treatment of HPV-associated lesions (reviewed (Johannsen & Lambert 2013, Steenbergen *et al.* 2014). Especially cytidine analogs have been extensively tested in cancer therapy (reviewed in (Gowher & Jeltsch 2004). 5-aza-2'-deoxycytidine (decitabine or DAC) is one of the most prominent cytidine analogs and clinically used for the treatment of myelodysplastic syndrome (MDS) (Gore *et al.* 2006). The mechanism of action of DAC is highly dose dependent. Administered at high doses, DAC is incorporated into the DNA during replication and forms covalent adducts between DNMTs and the DNA causing cytotoxicity by inducing the formation of DNA double-strand breaks (DSBs) and subsequent apoptosis (Juttermann *et al.* 1994). At lower doses, DAC is incorporated into the DNA at much lower rates and exerts a demethylating effect by selectively inducing the proteasomal degradation of DNMT1 ((Creusot *et al.* 1982, Ghoshal *et al.* 2005, Jones & Taylor 1980) and reviewed in (Jones 1985)).

In addition to MDS, several studies investigated the effect of systemic DAC treatment on solid tumors. The patient response rate varied significantly between different types of cancer and was highly dependent on the administered dose (reviewed in (Cowan *et al.* 2010, Nie *et al.* 2014)). However, these studies did not monitor the demethylating effect of the treatment in the respective tumor cells. Therefore, the patient response rates

cannot be correlated with the demethylation of the tumor cells complicating the interpretation of the results. The effects of DAC treatment on HPV-transformed tumor cells have also been investigated in *in vitro* studies. DAC treatment repressed proliferation of HPV-transformed cell lines, which was accompanied by reduced methylation levels in the viral and host cellular genome (Kalantari *et al.* 2008, Zhang *et al.* 2015). Especially, the E2 binding sites in the HPV genome were shown to become demethylated possibly explaining the decreased E6 and E7 expression, which has been observed in the HPV 16-transformed cell lines CaSki and UM-SCC-47 (Fernandez *et al.* 2009, Zhang *et al.* 2015).

Taken together, the application of DAC might represent a promising option to treat HPV-associated lesions. There is, however, still a strong need for studies that systematically analyze the detailed effects of DAC treatment on HPV-transformed cell lines.

1.5. Rationale and aims of the project

The present thesis consists of two interconnected parts. In the first part the use of the demethylating agent DAC is systematically evaluated as a therapeutic approach to inhibit the overexpression of E6 and E7 in HPV-transformed cells and thereby to effectively prevent proliferation and colony formation of these cells. In the second part of the study a novel, cell line based model system is developed that allows the inducible expression of HPV 16 E6 and E7. Additionally, the validation of the biological relevance of the system as well as analyses to study the effects of HPV 16 oncogene expression on gene copy number variations and methylation levels are presented in this part. Figure 5 summarizes the experimental steps that were performed in each of the project parts.

Despite the progress in the development of prophylactic vaccines as well as in surgical methods, there is still a strong need for therapeutic agents especially for the treatment of late stage HPV-associated tumors. As discussed previously, hypermethylation of regulatory regions in the viral and host cell genome seems to play an important role during HPV-mediated transformation. Therefore, we hypothesized the reactivation of

these mechanisms by treating HPV-transformed cells with the demethylating substance DAC.

Based on this assumption, a panel of hr-HPV-transformed cell lines was treated with different concentrations of DAC followed by the quantification of HPV oncogene expression, proliferation and colony formation. Furthermore, the study aimed to clarify potential mechanisms activated by DAC treatment that might be involved in the regulation of HPV oncogene expression. These include demethylation of E2BSs in the HPV upstream regulatory region as well as re-expression of miR-375, which has been shown to play a tumor suppressive role in HPV-mediated cancers by directly targeting and degrading E6 and E7 transcripts.

Taken together, the first part of the present study addresses the following objectives:

- Effects of DAC treatment on HPV oncogene expression, proliferation and colony formation in HPV-transformed cell lines
- Identification of mechanisms that re-establish the regulation of HPV oncogene expression

The development of novel and more targeted therapies, as well as the identification of biomarkers predicting the progression of HPV-associated lesions require the availability of model systems that precisely reflect the biology of HPV-transformed tumors. The knowledge about the effects of HPV oncogene expression on their host cells has mainly been derived from studies in primary human keratinocytes and in established cervical cancer cell lines. However, these model systems have some disadvantages, as on the one hand primary human keratinocytes are very critical for continuous culturing and can therefore not be used to study long-term effects of HPV oncogene expression. On the other hand, established cervical cancer cell lines are already transformed into immortal tumor cells and thus do not allow to analyze early mechanisms of deregulated HPV oncogene expression. Especially the induction of chromosomal instability, potentially caused by the overexpression of HPV E6 and E7, cannot be studied in cervical carcinoma cell lines, as these cells are already chromosomally unstable.

To overcome these limitations the aim of the second part of the study was to generate an inducible HPV 16 E6 and E7 expression system, which would allow investigating the consequences of both HPV 16 oncoproteins in a time-dependent manner. For this, the well-characterized and microsatellite-unstable colon cancer cell line HCT116 was selected (Brattain *et al.* 1981). This cell line shows a nearly diploid karyotype and very low rates of chromosomal alterations (Lengauer *et al.* 1997, Thompson & Compton 2008). Therefore, HCT116 cells are considered as chromosomally stable making them specifically suitable to study HPV 16 E6- and E7-mediated effects on mitotic progression and genomic integrity. To facilitate inducible HPV 16 E6 and E7 expression in HCT116 cells the previously published HCT116-HygTK clone was used, which enables the integration of the HPV 16 E6 and E7 genes as single copies into a defined chromosomal

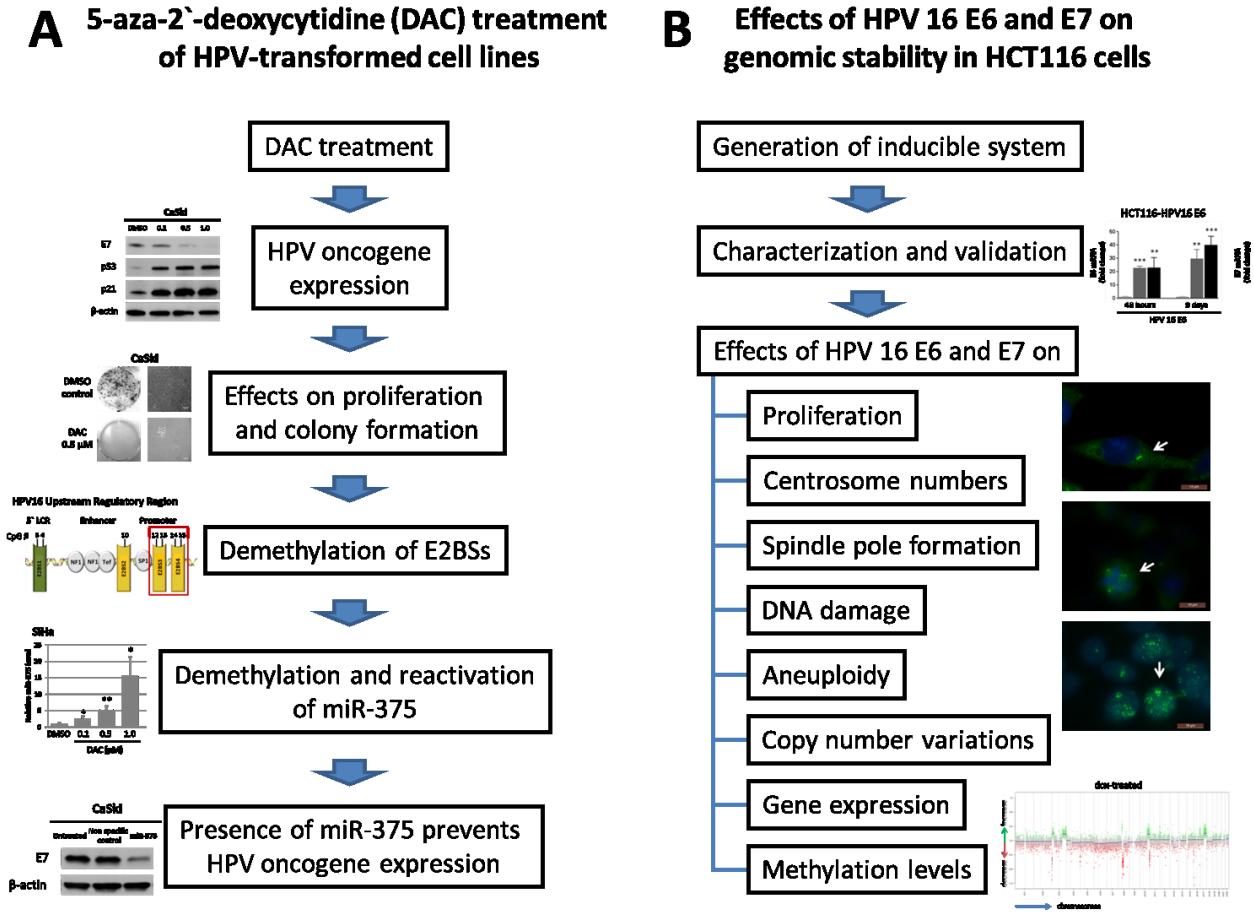

Figure 5: Overview of experimental strategy.
The figure highlights major experimental steps conducted in the present study to analyze the effects of DAC treatment on HPV-transformed cell lines **(A)** as well as the effects of inducible HPV 16 E6 and E7 expression on genomic stability in HCT116 cells **(B)**.

locus (Lee *et al.* 2013). Thereby, disruption of host cellular genes during E6 and E7 integration is avoided. After validating and characterizing the inducible system, the effects of HPV 16 oncogene expression on cell cycle progression and genomic integrity were investigated. In detail, this included the analysis of centrosome numbers in interphase cells, of spindle pole formation during mitosis, of DNA double strand break induction, of the number of aneuploid cells as well as of gene copy number variations. Additionally, alterations in host cellular gene expression and methylation levels were studied after induction of HPV 16 oncogene expression.

In summary, the second part of the thesis aims to

- generate and characterize an inducible HPV 16 E6 and E7 expression system
- validate the biological relevance of the established system by studying the effects of HPV 16 E6 and E7 on chromosomal stability and genomic integrity
- identify novel effects of E6 and E7 on gene expression and methylation patterns

By evaluating the efficiency of DAC treatment in HPV-associated cancer cell lines and by studying the effects of HPV 16 oncogene expression on host cellular mechanisms, this thesis not only addresses basic scientific questions, but also focuses on translational approaches, which might serve as the basis for future clinical trials.

2. Materials and Methods

2.1. Materials

2.1.1. Cell lines

The cervical carcinoma cell line CaSki was purchased from CLS Cell Lines Service GmbH (Pattillo *et al.* 1977). The other cervical carcinoma cell lines C4-1 (Herz *et al.* 1977), SiHa (Friedl *et al.* 1970) and SW756 (Freedman *et al.* 1982) were authenticated by multiplex human cell line authentication tests (Multiplexion). The head and neck squamous cell carcinoma (HNSCC) cell lines UM-SCC-47 and UM-SCC-104 were kindly provided by Professor Thomas E. Carey (University of Michigan) (Brenner *et al.* 2010, Tang *et al.* 2012).

HCT116 is a commonly used and well characterized colorectal cancer cell line, which was established from a single human colonic carcinoma derived from a male patient in 1981 (Brattain *et al.* 1981). Due to a mutation in the *hMLH1* gene HCT116 cells are DNA mismatch repair (MMR) deficient causing MSI. Moreover, these cells carry a mutation in codon 13 of the *ras* proto-oncogene leading to growth stimulation. HCT116 cells contain a nearly diploid set of chromosomes and show low frequencies of chromosomal alterations (Ertych *et al.* 2014, Lengauer *et al.* 1997, Thompson & Compton 2008). Therefore, this cell line is considered as chromosomally stable. The parental master cell line HCT116-HygTK was kindly provided by Dr Jennifer Lee and Dr Johannes Gebert (Lee *et al.* 2013).

2.1.2. Plasmids

The plasmid S2F-cLM2CG-FRT3 was used to clone vectors that allow doxycycline (dox)-inducible expression of HPV 16 E6 and E7 (Loew *et al.* 2006, Weidenfeld *et al.* 2009). S2F-cLM2CG-FRT3 encodes a tetracycline (tet)-controlled bidirectional promoter (P_{tet}bi) that facilitates transcription of the reporter genes firefly luciferase and mCherry (Supplementary Figure 1). The heterospecific Flp-recognition sites F3 and F are located

at the flanks of this expression cassette and were needed for subsequent recombination-mediated cassette exchange (RMCE) (Schlake & Bode 1994).

The *EcoRI*/*NotI* cleavage sites were used to excise the mCherry fragment from the S2F-cLM2CG-FRT3 vector and to replace it either by the sequence encoding HPV 16 E6 (GenBank: K02718.1, nt 83-560) or HPV 16 E7 (GenBank: K02718.1, nt 562-858). Thereby, the retroviral vectors S2F-cLM2CG-FRT3-HPV16-E6 and S2F-cLM2CG-FRT3-HPV16-E7 were generated. To clone the vector S2F-cLM2CG-FRT3-HPV16 E6-E7 for the expression of both HPV 16 oncogenes the mCherry fragment of S2F-cLM2CG-FRT3 was replaced by the HPV 16 E6 sequence as described above. Afterwards, the sequence encoding HPV 16 E7 was inserted into the *SalI*/*BamHI* restriction site of the S2F-cLM2CG-FRT3-HPV16-E6 vector replacing the firefly luciferase reporter gene. Maps of the generated vectors can be found in Supplementary Figure 1.

The vectors pVPack-GP and pVPack-VSV-G were used for retroviral assembly (Stratagene) and RMCE was mediated by the enzyme Flpo-recombinase encoded by the plasmid pCAGGS-Flpo-IRES-Puro obtained from Michael Hahn (DKFZ, Heidelberg).

2.1.3. Primer

Name	Forward (5` - 3`)	Reverse (5` - 3`)	Amplicon (bp)
Primers for RT-qPCR			
HPV 16 E6	TTG CTT TTC GGG ATT TAT GC	CAG GAC ACA GTG GCT TTT GA	204
HPV 16 E6*I	ACT GCG ACG TGA GGT GTA TTA AC	TGG AAT CTT TGC TTT TTG TCC	85
HPV 16 E7	CAG CTC AGA GGA GGA GGA TG	GCC CAT TAA CAG GTC TTC CA	166
HPV 18 E6*I	TGT ATA TTG CAA GAC AGT ATT	GCT GGA TTC AAC GGT TTC TGG	249
HPV 18 E7	CCC CAA AAT GAA ATT CCG GT	GTC GCT TAA TTG CTC GTG ACA TA	51
β-actin	ATG TGG CCG AGG ACT TTG ATT	AGT GGG GTG GCT TTT AGG ATG	107
Primers for methylation-specific qPCR			
Hsa-miR-375 gene	GGG GCG TTG TGT AGT ATT GAG TTC	GAA ACG AAA ACG AAA AAC CCG	91

β-actin gene	TGG TGA TGG AGG AGG TTT AGT AAG T	AAC CAA TAA AAC CTA CTC CTC CCT TAA	133
Primers for bisulfite-based pyrosequencing of HPV 16 E2BS 3 and 4			
Amplification primers	TTG TAA AAT TGT ATA TGG GTG TG	Bio- AAA TCC TAA AAC ATT ACA ATT CTC	180
Sequencing primer	AAT TTA TGT ATA AAA TTA AGG G		
Primers for cloning of HPV 16 E6 and E7			
HPV 16 E6 (*EcoRI* and *NotI*)	ATG AAT TCG CCA CCA TGC ACC AAA AGA GAA CTG CAA TG	ATG CGG CCG CTT ACA GCT GGG TTT CTC TAC GTG	501
HPV 16 E7 (*EcoRI* and *NotI*)	ATG AAT TCG CCA CCA TGC ATG GAG ATA CAC CTA CAT TG	ATG CGG CCG CTT ATG GTT TCT GAG AAC AGA TGG G	321
HPV 16 E7 (*SalI* and *BamHI*)	ATG TCG ACG CCA CCA TGC ATG GAG ATA CAC CTA CAT TG	ATA GGA TCC GTT ATG GTT TCT GAG AAC AGA TGG G	321
Sequencing primer for HPV 16 E6 and E7			
HPV 16 E6	ATG CAC CAA AAG AGA ACT GCA ATG	TTA CAG CTG GGT TTC TCT ACG TG	477
HPV 16 E7	ATG CAT GGA GAT ACA CCT ACA TTG C	TTA TGG TTT CTG AGA ACA GAT GG	297
Transcriptome validation			
KLF11	AGG GAG CTG TGA TGT TGG TC	TCC TCC TTC GGG AAA AGT CT	171
PKM2	ATT ATT TGA GGA ACT CCG CCG CCT	ATT CCG GGT CAC AGC AAT GAT GG	190
BLOC1S1	CCC AAT TTG CCA AGC AGA CA	CAT CCC CAA TTT CCT TGA GTG C	78
VSNL1	AAG TGA TGG AGG ACC TGG TG	GTC GCT CTT TGC AGC TTC TT	503
CKLF	TCG CTT CGC AGA ACC TAC TCA	TAT TTT CGG CTG CAC GTT ATC C	100
PLK2	CCA CCA TTC GCA CTC G	CGG CGT AGA CTT TGT TAT TT	149
CDKN1A	GTA CCA CCC AGC GGA CAA GT	CCT CAT CCC GTG TTC TCC TTT	97
TP53I3	GGC CAG GAA CAA TAT GTT AGC C	GTG GGT CAT ACT GGC CTT GTC T	173
PERP	GGC TTC ATC ATC CTG GTG AT	ACA GCA GCC AAG GCA AGG AG	110
TP53INP3	TTT CCT GTT TAC CGG CAT CTC T	TGG ACA TGA CTC AAA CTG GAG AA	77

2.1.4. Antibodies

Antibody	Source	Clone	Application (Dilution)	Company (City, Country)
β-actin	mouse mAb	C4	WB (1:20,000)	MP Biomedicals (Solon, USA)
γ-tubulin	mouse mAb	GTU-88	IF (1:100)	Sigma-Aldrich (Taufkirchen, Germany)
HPV 16 E7	mouse mAb	NM-2	WB (1:500)	Santa Cruz Biotechnology (Santa Cruz, USA)
HPV 18 E7	mouse mAb	F-7	WB (1:500)	Santa Cruz Biotechnology (Santa Cruz, USA)
Mouse IgG-Alexa488	goat pAb		IF (1:750)	Thermo Fisher Scientific (Ulm, Germany)
p21	rabbit pAb	C-19	WB (1:200)	Santa Cruz Biotechnology (Santa Cruz, USA)
p53	mouse mAb	DO-1	WB (1:500)	Santa Cruz Biotechnology (Santa Cruz, USA)
Phospho-Histone H2A.X (Ser 139)	rabbit mAb	20E3	IF (1:200)	Cell Signaling Technology (Danvers, USA)
Rabbit IgG-Alexa488	goat pAb		IF (1:750)	Thermo Fisher Scientific (Ulm, Germany)

2.1.5. Enzymes

Enzyme	Company (City, Country)
Absolute qPCR SYBR Green ROX Mix	Thermo Fisher Scientific (Ulm, Germany)
BamHI	New England Biolabs (Frankfurt, Germany)
DNase I, Amplification Grade	Life Technologies (Darmstadt, Germany)
EcoRI	New England Biolabs (Frankfurt, Germany)
HOT FIREPol DNA Polymerase	Solis Biodyne (Tartu, Estonia)
NotI	New England Biolabs (Frankfurt, Germany)
Phusion High-Fidelity DNA Polymerase	Thermo Fisher Scientific (Ulm, Germany)

(Platinum) Taq DNA Polymerase	Life Technologies (Darmstadt, Germany)
RNase A	Thermo Fisher Scientific (Ulm, Germany)
SalI	New England Biolabs (Frankfurt, Germany)
SuperScript II Reverse Transcriptase	Life Technologies (Darmstadt, Germany)
TaqMan® Universal PCR Master Mix	Thermo Fisher Scientific (Ulm, Germany)

2.1.6. Buffer

Buffer	Ingredients
Crystal violet staining solution	25% ethanol 1% formaldehyde 0.125% NaCl 0.25% crystal violet ad H_2O
TE-Buffer	10 mM Tris-HCl 1 mM EDTA
Western Blot Buffer I	300 mM Tris 20% methanol pH 10.4
Western Blot Buffer II	25 mM Tris 20% methanol pH 10.4
Western Blot Buffer III	25 mM Tris 40 mM norleucine 20% methanol pH 9.4

2.1.7. Reagents

Reagent	Company (City, Country)
5-aza-2`-deoxycytidine (Decitabine)	Sigma-Aldrich (Taufkirchen, Germany)
Bacto-agar	Fluka Chemie (Buchs, Switzerland)
BigDye® Terminator v1.1 Ready Reaction Mix	Thermo Fisher Scientific (Ulm, Germany)
BSA	Sigma-Aldrich (Taufkirchen, Germany)
Bromophenol blue	Schmid (Köngen, Germany)
Crystal Violet	Sigma-Aldrich (Taufkirchen, Germany)
DL-Norleucine	Sigma-Aldrich (Taufkirchen, Germany)
DMEM	Thermo Fisher Scientific (Ulm, Germany)
DMSO	Serva (Heidelberg, Germany)
DNA ladder	Thermo Fisher Scientific (Ulm, Germany)
dNTP Set (100 mM)	Life Technologies (Darmstadt, Germany)
Donkey serum	Sigma-Aldrich (Taufkirchen, Germany)

Doxycycline	Sigma-Aldrich (Taufkirchen, Germany)
DTT	Life Technologies (Darmstadt, Germany)
Ethanol	Sigma-Aldrich (Taufkirchen, Germany)
FBS	Thermo Fisher Scientific (Ulm, Germany)
Formaldehyde	Sigma-Aldrich (Taufkirchen, Germany)
Ganciclovir	Sigma-Aldrich (Taufkirchen, Germany)
Gentamicin	Thermo Fisher Scientific (Ulm, Germany)
Glutamine	Thermo Fisher Scientific (Ulm, Germany)
Goat serum	Sigma-Aldrich (Taufkirchen, Germany)
Hi-Di™ Formamide	Life Technologies (Darmstadt, Germany)
Hygromycin B	Sigma-Aldrich (Taufkirchen, Germany)
Isopropanol	Center of distribution, University of Heidelberg (Heidelberg, Germany)
Kodak BioMax films	Sigma-Aldrich (Taufkirchen, Germany)
Laemmli Buffer	Sigma-Aldrich (Taufkirchen, Germany)
MEM Non-Essential Amino Acids Solution (100x)	Thermo Fisher Scientific (Ulm, Germany)
β-Mercaptoethanol	Sigma-Aldrich (Taufkirchen, Germany)
Methanol	Carl Roth (Karlsruhe, Germany)
Midori Green	Biozym (Hessisch Oldendorf, Germany)
Na_2EDTA	Sigma-Aldrich (Taufkirchen, Germany)
Norleucine	Sigma-Aldrich (Taufkirchen, Germany)
NuPAGE® Sample Reducing Agent (10x)	Life Technologies (Darmstadt, Germany)
Oligo(dT) primers	Life Technologies (Darmstadt, Germany)
PBS	Thermo Fisher Scientific (Ulm, Germany)
Penicillin/streptomycin	Thermo Fisher Scientific (Ulm, Germany)
Phosphatase inhibitor	Sigma-Aldrich (Taufkirchen, Germany)
Ponceau Red	Sigma-Aldrich (Taufkirchen, Germany)
Precision Plus Protein™ Prestained Standard	Bio-Rad Laboratories (München, Germany)
Propidium iodide	Sigma-Aldrich (Taufkirchen, Germany)
Protease inhibitor	Sigma-Aldrich (Taufkirchen, Germany)
PyroMark 10x Wash Buffer	Qiagen (Hilden, Germany)
PyroMark Annealing Buffer	Qiagen (Hilden, Germany)
PyroMark Binding Buffer	Qiagen (Hilden, Germany)
PyroMark Q24 Gold Reagents	Qiagen (Hilden, Germany)
Quick Start ™ Bradford 1x Dye Reagent	Bio-Rad Laboratories (München, Germany)
Recovery ™ Cell Culture Freezing Medium	Thermo Fisher Scientific (Ulm, Germany)
Restore™ Western Blot Stripping Buffer	Thermo Fisher Scientific (Ulm, Germany)
RIPA buffer	Sigma-Aldrich (Taufkirchen, Germany)
RNaseOUT	Life Technologies (Darmstadt, Germany)
RPMI	Thermo Fisher Scientific (Ulm, Germany)
Single-stranded random hexanucleotides	Bioron (Ludwigshafen, Germany)
S.O.C medium	Life Technologies (Darmstadt, Germany)
Sodium acetate	J.T. Baker (Deventer, Netherland)

Sodium chloride (NaCl)	Sigma-Aldrich (Taufkirchen, Germany)
Sodium hydroxide (NaOH)	Carl Roth (Karlsruhe, Germany)
SYBR Green ROX Mix	Thermo Fisher Scientific (Ulm, Germany)
TBE buffer	AppliChem (Darmstadt, Germany)
Tris-base	Carl Roth (Karlsruhe, Germany)
Tris/Glycine/SDS Running buffer (10x)	Bio-Rad Laboratories (München, Germany)
Tris-HCl	Carl Roth (Karlsruhe, Germany)
Triton-X-100	Sigma-Aldrich (Taufkirchen, Germany)
Trypan blue	Sigma-Aldrich (Taufkirchen, Germany)
Trypsin-EDTA	Thermo Fisher Scientific (Ulm, Germany)
Tween-20	Sigma-Aldrich (Taufkirchen, Germany)
UltraPureTM agarose	Life Technologies (Darmstadt, Germany)
Water, DNase, RNase-FREE	MP Biomedicals (Solon, USA)

2.1.8. Kits

Kit	Company (City, Country)
Blood and Cell Culture DNA Mini Kit	Qiagen (Hilden, Germany)
CyQuant® NF Cell Proliferation Assay Kit	Thermo Fisher Scientific (Ulm, Germany)
CytoTox 96® Non-Radioactive Cytotoxicity Assay	Promega (Madison, USA)
High Pure PCR Product Purification Kit	Roche (Mannheim, Germany)
Methylamp™ DNA Modification Kit	Epigentek (Farmingdale, USA)
Novex Western Breeze Chemiluminescent Immunodetection System	Thermo Fisher Scientific (Ulm, Germany)
NucleoSpin Plasmid Kit	Machery Nagel (Düren, Germany)
PyroMark LINE-1 Kit	Qiagen (Hilden, Germany)
QIAquick Gel Extraction Kit	Qiagen (Hilden, Germany)
QIAquick® PCR Purification Kit	Qiagen (Hilden, Germany)
RNeasy Mini Kit	Qiagen (Hilden, Germany)
SuperScript® II Reverse Transcriptase Kit	Thermo Fisher Scientific (Ulm, Germany)
TaqMan® MicroRNA Assay miR-375	Thermo Fisher Scientific (Ulm, Germany)
TaqMan® MicroRNA Assay snRNA U6	Thermo Fisher Scientific (Ulm, Germany)
TaqMan® MicroRNA Reverse Transcription Kit	Thermo Fisher Scientific (Ulm, Germany)

2.1.9. Instruments

Instrument	Company (City, Country)
Cell Culture Hood (Biowizard Silverline)	Ewald Innovationstechnik GmbH (Bad Nenndorf, Germany)
Centrifuge (Heraeus Fresco 21)	Heraeus Instruments (Hanau, Germany)

Centrifuge (5810 R)	Eppendorf (Hamburg, Germany)
Centrifuge (Microcentrifuge 1-14)	Sigma Laborzentrifugen (Osterode, Germany)
ChemiDoc Imaging System	Bio-Rad Laboratories (Munich, Germany)
FACS (FACSCalibur)	Becton Dickinson (Franklin Lakes, USA)
Ice Machine	Ziegra Eismaschinen GmbH (Isernhagen, Germany)
Incubator	Heraeus Holding (Hanau, Germany)
Luminometer (Lumat LB 9507)	Berthold Technologies (Bad Wildbad, Germany)
Microscope (Leica DM5000 B)	Leica (Bensheim, Germany)
Microscope (Olympus CK40)	Olympus (Hamburg, Germany)
Microwave	Siemens (Munich, Germany)
Photometer (Ultrospec 3300)	Amersham Pharmacia (Cambridge, UK)
Pipettes (10 µL; 20 µL; 200 µL; 1000 µL)	Gilson (Limburg-Offheim, Germany)
Power supply (Power Pac 300)	Bio-Rad Laboratories (Munich, Germany)
Protein Electrophoresis System (NuPAGE)	Thermo Fisher Scientific (Ulm, Germany)
Real-Time PCR System (StepOnePlus)	Life Technologies (Darmstadt, Germany)
Scale BP 310 S	Sartorius (Göttingen, Germany)
Shaker Certomat H	Sartorius (Göttingen, Germany)
Spectrophotometer Nanodrop (ND-1000)	Thermo Fisher Scientific (Ulm, Germany)
Thermocycler (peqStar 96 universal)	VWR International GmbH (Erlangen, Germany)
Thermomixer (5436)	Eppendorf (Hamburg, Germany)
Ultracentrifuge (TLA-100.2)	Beckmann Coulter (Krefeld, Germany)
Ultrasound UW 2070	Bandelin electronics (Berlin, Germany)
Vortex (MS1 Minishaker)	IKA (Staufen, Germany)
Waterbath	Grant (Cambridge, UK)

2.2. Methods

2.2.1. Cell culture techniques

2.2.1.1. Maintenance of cell lines

C4-1, CaSki, SiHa, SW756 and HCT116 cells were cultured in DMEM (Gibco) supplemented with heat-inactivated 10% FBS (Gibco) and 1% penicillin/streptomycin (Gibco). The HNSCC cell lines UM-SCC-47 and UM-SCC-104 were grown in RPMI (Gibco) containing 10% FBS (Gibco), 1% MEM Non-Essential Amino Acids Solution

(Gibco), 1% glutamine (Gibco) and 25 µg/mL gentamicin (Gibco). All cell lines were cultured in a humidified incubator at 37 °C and 5% CO_2.

Confluent grown cells were splitted 1:10 or 1:20. For this, the growth medium was removed and the cells were washed once with pre-warmed PBS (Gibco). To detach the cells 0.05% Trypsin-EDTA (Gibco) was added and the cells were incubated at 37 °C. After cell detachment growth medium was added to inactivate the Trypsin-EDTA and the cells were collected in a falcon tube. Finally, the appropriate volume of collected cells was transferred back into the cell flask, growth medium was added and the cell flask was incubated in a humidified incubator at 37 °C and 5% CO_2 until further use.

2.2.1.2. Cryo-conservation and reculturing of cell lines

For long-term storage the cells were harvested and pelleted by centrifugation at 1,200 rpm for 5 minutes (min) and 4 °C. The cell pellet was resuspended in Recovery ™ Cell Culture Freezing Medium (Gibco) containing 10% DMSO. Afterwards, $5x10^6$ cells were transferred to cryo-vials, which were then gradually cooled to -80 °C in an isopropanol containing cell freezing box overnight. The cells were then stored in liquid nitrogen.

Reculturing was performed by thawing frozen cell vials at 37 °C and then transferring the cells to a centrifuge tube. After centrifugation at 1,200 rpm for 5 min the DMSO-containing freezing medium was removed, the pelleted cells were resuspended in pre-warmed growth medium and the suspension was transferred into T75 cell culture flasks. The cells were incubated in a humidified incubator at 37 °C and 5% CO_2 until further use.

2.2.1.3. Determination of cell number and viability

Before applying different substances the number of seeded cells was determined. For this, harvested cells were diluted with trypan blue solution in a 1:1 ratio. Trypan blue is a diazo dye, which cannot pass intact cell membranes. The substance, however,

penetrates the membrane of necrotic and apoptotic cells and is therefore used as a marker to distinguish dead from intact cells.

The cells were counted by using a hemocytometer (Neubauer improved counting chamber). The number of cells was quantified in at least four quarters of the counting chamber. Each quarter has the volume of 0.1 mm³. Thus, the mean number of cells per quarter was multiplied with 10^4 to calculate the number of cells per mL in the dilution. Finally, the result was multiplied with the dilution factor to receive the number of cells per mL in the original suspension.

$$\text{Suspension [cells/mL]} = \frac{\text{Number of cells x 10,000}}{\text{Number of counted quarters}} \text{ x dilution factor}$$

2.2.1.4. Treatment of HPV-transformed cell lines with 5-aza-2`-deoxycytidine

In order to treat CaSki, SiHa, UM-SCC-47, UM-SCC-104, C4-1 and SW756 cells with 5-aza-2`-deoxycytidine (DAC), the cells were seeded in T75 cell culture flasks and kept without treatment for 24 hours to allow adherence of the cells. Afterwards, one of the following concentrations of DAC dissolved in DMSO was added: 0.1, 0.5 or 1.0 µM. Half of the medium was changed every 24 hours and fresh DAC-containing medium was added. The treatment was continued for 72 hours and the cells were harvested afterwards.

2.2.1.5. Hygromycin B and ganciclovir treatment

Presence of the HygTK expression cassette in the generated HCT116 clones was monitored by treating the cells with hygromycin B and with ganciclovir. Therefore, the cells were seeded in a 12-well plate format and treated by adding growth medium containing 200 µg/mL hygromycin B or 40 µM ganciclovir. The medium was renewed every 24 hours and after a total treatment period of seven days the cells were fixed and stained using crystal violet as described in the respective section.

2.2.1.6. Dox treatment of inducible HCT116 cell clones

HCT116 cell clones generated for inducible expression of HPV 16 E6, E7 or E6 and E7 were treated over different time periods and with different concentrations of dox to analyse the effects of HPV 16 oncogene expression (Table 1). Therefore, the cells were seeded in 10 cm plates containing DMEM supplemented with 10% FBS, 1% penicillin/streptomycin as well as 100 or 500 ng/mL dox. The growth medium was renewed every 48 hours. After the treatment the cells were harvested and pelleted by centrifugation at 1,200 rpm for 5 min at 4 °C. Cell pellets were stored at -80 °C until further use.

To characterize the induction and silencing of the dox-sensitive promoter in a time dependent manner, dox was removed from the growth medium and HPV 16 E6 and E7 levels were quantified after different time periods. For this, the HCT116 cell clones were seeded as described previously and treated with 500 ng/mL dox for 48 hours. Afterwards, the dox-containing growth medium was removed and the cells were washed three times with dox-free growth medium and then cultured in dox-free growth medium. The cells were then harvested six hours, 24 hours and 48 hours later. The cell pellets were stored at -80 °C until they were used for E6 and E7 mRNA or protein quantification.

Table 1: List of time periods, dox concentrations and number of seeded cells used for the treatment of HCT116-HPV 16 E6 and E7 cell clones.

Duration of treatment		Dox concentrations	Number of seeded cells
48 hours		100 and 500 ng/mL	$1.5x10^6$
96 hours		500 ng/mL	$0.5x10^6$
9 days		100 and 500 ng/mL	$0.1x10^6$
Dox removal experiment			
54 hours	48 hours	500 ng/mL	$1.5x10^6$
	6 hours	no dox	
72 hours	48 hours	500 ng/mL	$0.7x10^6$
	24 hours	no dox	
96 hours	48 hours	500 ng/mL	$0.5x10^6$
	48 hours	no dox	

2.2.1.7. Crystal violet staining

Crystal violet staining supports the visualization of cell colonies and can therefore be used to monitor colony formation. After the respective treatment, the cells were washed with PBS (Gibco) and stained with crystal violet staining solution consisting of H_20, 25% ethanol (Sigma Aldrich), 1% formaldehyde (Sigma Aldrich), 0.125% NaCl (Sigma Aldrich) and 0.25% Crystal Violet (Sigma Aldrich) for 60 seconds (s). After several washing steps using PBS (Gibco), images were taken using an Olympus CK40 microscope.

2.2.1.8. Proliferation Assay

Cell proliferation of DAC-treated cell lines as well as of HCT116-HPV 16 oncogene expressing clones was quantified using the CyQuant® NF Cell Proliferation Assay Kit (Invitrogen) according to the manufacturer`s protocol. The assay employs a fluorescent dye that binds to the DNA. Thereby, cell proliferation is indirectly determined by measuring the DNA content.

To analyse the effect of HPV 16 oncogene expression on proliferation in HCT116 cells, 4000 cells were seeded per well in a 96-well plate format and treated with 500 ng/mL dox to induce HPV 16 oncogene expression as described previously. Proliferation was then quantified after six, 24, 48, 72 and 96 hours. The dox-containing growth medium was renewed every 48 hours.

The effects of DAC treatment on cell proliferation was analysed by seeding the cells into 96-well plates (1000 cells/well) and treating the cells as described previously. Afterwards, the growth medium was removed and 50 µL of dye solution (containing CyQuant NF dye reagent) was added. The cells were then incubated for 30 min at 37°C. Finally, incorporation of the fluorescence dye was measured by using a plate reader (excitation at 485 nm and emission at 542 nm).

2.2.1.9. Transfection of miR-375 in CaSki and SiHa cells

The effects of miR-375 on HPV 16 oncogene expression in CaSki and SiHa cells were investigated by transfecting miR-375 mimics. For this, the cells were seeded in six well plates and cultured at 37°C and 5% CO_2 for 48 hours. At the time of transfection the cells were approx. 70% confluent. Transfection was performed by diluting Lipofectamine 2000 (Invitrogen) in OptiMEM (Gibco) reduced serum medium in a ratio of 1:10. Next, hsa-miR-375 mimics (Sigma Aldrich) and non-specific negative controls (Mission® miRNA, Negative Control 1, Sigma Aldrich) were diluted in OptiMEM (Gibco), added to the diluted Lipofectamine 2000 in a ratio of 1:1, incubated for 5 min at room temperature and then pipetted dropwise to the medium of the cells to reach a final concentration of 100 nM for hsa-miR-375 and 25 nM for non-specific negative controls. Afterwards, the cells were incubated at 37°C and 5% CO_2 for 48 hours and then harvested, pelleted and frozen at -80 °C until they were used to quantify HPV 16 oncogene expression.

2.2.1.10. Quantification of aneuploid cells

Flow cytometry of propidium iodide (PI) stained HCT116 clones was performed to quantify the DNA content indicating the cell cycle phase. For this, dox-treated HCT116 clones were harvested using trypsin and washed with PBS. The cells were then fixed and permeabilized by adding ice-cold 70% ethanol. The cells were vortexed gently to prevent cell aggregation and incubated for one hour at -20 °C. Afterwards, the ethanol-suspended cells were centrifuged for 5 min at 300 g, the ethanol was removed and the cells were washed twice with cold PBS. To degrade RNA, 10^6 cells were resuspended in 1 mL PBS, 50 µg RNase A (Thermo Fisher) was added and the cell suspension was incubated for 45 min at 37 °C. Next, PI (Sigma Aldrich) was added to a final concentration of 10 µg/mL and the suspension was kept in the dark for 30 min at room temperature. PI stained DNA was then measured using flow cytometry (BD FACSCalibur). Histograms were prepared to assign the cells to the different cell cycle phases, thereby allowing distinguishing between subG_1, G_1, S, G_2/M and aneuploid cells. Control samples lacking either PI staining or RNase A treatment were prepared and analysed for every treatment condition.

2.2.2. Cloning and sequencing

2.2.2.1. Isolation of genomic DNA

Whole DNA was extracted by using the Blood and Cell Culture DNA Mini Kit (Qiagen) as recommended by the manufacturer`s protocol. Afterwards, the DNA concentration was measured spectrophotometrically at 260 nm using a NanoDrop 1000 Spectrophotometer.

2.2.2.2. Polymerase chain reaction (PCR)

PCR was performed to amplify DNA sequences for subsequent cloning procedures, to confirm the presence of an inserted DNA fragment and to provide enough copies for sequencing reactions.

The amplification of inserts for subsequent cloning procedures was performed utilizing Phusion High-Fidelity DNA Polymerase with proofreading capability. The reactions consisted of 4 µL template DNA (20 ng), 2.5 µL 10x buffer, 2 µL $MgCl_2$ (25 mM), 2.5 µL dNTPs (2 mM), 2.5 µL primer (forward and reverse, 5 µM), 0.125 µL Phusion DNA Polymerase (5 U/µL) and DNase- and RNase-free water to a final volume of 25 µL. After preparing the reactions on ice, PCR was performed using the following cycling conditions: initial denaturation at 95 °C for 15 min, 30-40 cycles consisting of denaturation at 95 °C for 30 s, annealing at 60 °C for 30 s and elongation at 72 °C for 30-60 s and a final elongation step at 72 °C for 2-10 min. Amplification of the HPV 16 oncogenes for the generation of S2F-cLM2CG-FRT3-HPV16 E6 and/or E7 was conducted by using primers that either carried *EcoRI* and *NotI* or *SalI* and *BamHI* restriction sites. The amplified PCR products were then purified using the High Pure PCR Product Purification Kit (Roche), following the manufacturer`s instructions.

To confirm correct expression of the inserted HPV 16 E6- and E7-coding sequences in the generated HCT116 clones, transcription was first induced by treating the clones with dox and the expressed E6 and E7 mRNA was then sequenced. Therefore, the purified RNA isolated from dox-treated HCT116 clones was transcribed into cDNA as described

in section 2.2.3.3. Reverse Transcription. Afterwards, E6 and E7 transcripts were amplified by utilizing specific primers (listed in chapter 2.1.3. Primer). The following components and concentrations were used for PCR amplification: 5 µL template cDNA (10 ng), 2.5 µL 10x PCR buffer, 0.75 µL $MgCl_2$ (50 mM), 0.5 µL dNTPs (10 mM), 1 µL primer (forward and reverse, 15 µM), 0.2 µL Platinum Taq Polymerase (5 U/µL) and DNase-, RNase-free water to a final volume of 25 µL. After preparing the amplification reaction on ice, the PCR tubes were briefly centrifuged and transferred into a PCR cycler. The program run to amplify the DNA fragments included the following steps: initial denaturation at 95 °C 5 min, 38 cycles consisting of denaturation at 95 °C for 30 s, annealing at 53 °C (E6) or 48 °C (E7) for 30 s and elongation at 72 °C for 30 s as well as final elongation at 72 °C for 7 min. Afterwards, the size of the PCR products was analysed by agarose gel electrophoresis.

2.2.2.3. Agarose gel electrophoresis

Agarose gel electrophoresis was used to assess the amplification and the size of PCR products. Phosphate residues in the DNA carry negative electric charges and therefore move towards the positively charged anode when applying an electric field during electrophoresis. The velocity of the migrating DNA sequences correlates with the size of the fragments. The separated DNA fragments can then be visualized by using DNA binding dyes (e.g. Midori Green).

1% agarose gels were prepared by dissolving 1 g of powdered agarose in 100 mL 1x TBE buffer. The solution was then boiled until the agarose was completely dissolved und cooled at room temperature to approx. 60 °C. Afterwards, Midori Green dye was added (1:25,000) and the solution was poured into a gel casting tray. A comb was inserted and after solidifying the gel was transferred into the running chamber containing 1x TBE buffer. 5 µL of the PCR product was mixed with 6x loading dye and pipetted into the pockets of the gel after removing the comb. To quantify the size of the PCR fragments the 100 bp DNA ladder (Invitrogen) was included as a reference marker. The electrophoresis was then performed for 30 min at 120 V and the DNA fragments were visualized under UV light.

2.2.2.4. Restriction digest

Restriction endonucleases were used to cut DNA at specific recognition sites. For sticky end ligation the PCR products of HPV 16 E6 and E7, as well as the vector S2F-cLM2CG-FRT3 were cleaved in a double digestion either using *EcoRI* and *NotI* or *SalI* and *BamHI*. The reactions were conducted utilizing 30 µg of vector DNA and 80 µL of purified PCR product. Next, BSA, NEBuffer compatible to the respective enzyme, double-distilled water and the restriction endonucleases (40 U/µL, NEB) were added to the DNA and the reaction was incubated for at least three hours at 37 °C. The enzymes were then heat-inactivated for 20 min at 65 °C. Afterwards, proper digestion of the vector DNA was confirmed using agarose gel electrophoresis. The vector DNA was then excised from the gel and purified using the QIAquick Gel Extraction Kit (Qiagen) following the manufacturer`s protocol.

2.2.2.5. Dephosphorylation and ligation

For the cloning of S2F-cLM2CG-FRT3-HPV16-E6 and/or E7 plasmids, dephosphorylation and ligation were carried out using the Rapid DNA Dephos & Ligation Kit (Roche) as recommended by the manufacturer`s instructions. A molar ratio of 1:5 (vector:insert) was applied. Vector self-ligation was monitored by performing the reaction in the absence of insert DNA.

2.2.2.6. Bacterial transformation

Chemocompetent *E.coli* DH5α was used for transformation of the ligation product. Briefly, 50 µL of bacteria were thawed on ice and incubated for 30 min with 2 µL of ligation mixture. The cells were then heat-shocked for 45 s at 42 °C, incubated for 2 min on ice and subsequently resuspended in 300 µL S.O.C medium. Afterwards, the mixture was incubated for one hour at 37 °C shaking at 300 rpm. In the last step, the bacteria were plated on pre-warmed LB-agar plates containing 50 µg/mL ampicillin. The plates were incubated overnight at 37 °C and then stored at 4 °C.

2.2.2.7. Colony-PCR

In order to identify *E.coli* clones carrying the correct insert, colony PCR was performed. A minimum of five single bacteria clones were picked from the agar plates after bacterial transformation. The picked clones were used as templates for subsequent colony-PCR. The PCR primers were designed to specifically amplify the HPV 16 E6 or E7 cDNA insert. PCR was conducted as described in previous sections and the size of the amplified sequence was evaluated by agarose gel electrophoresis.

2.2.2.8. Plasmid isolation from bacterial cells

After confirming that the picked bacterial colony carried the vector with the correct DNA insert, the bacterial colony was inoculated into 3-5 mL of LB-medium supplemented with 50 µg/mL ampicillin. The bacteria were grown overnight at 37 °C shaking at 200 rpm. The plasmids were then isolated from the bacteria using the NucleoSpin Plasmid Kit (Machery Nagel) according to the manufacturer`s instructions. The concentration of the plasmid DNA was quantified spectrophotometrically at 260 nm.

2.2.2.9. Purification of PCR products

PCR products that had been amplified for subsequent sequencing were purified using the QIAquick® PCR Purification Kit (Qiagen) following the manufacturer`s instructions. Briefly, 20 µL of the PCR product was mixed with 100 µL buffer PB and loaded onto a spin column provided by the kit. After centrifuging 3 min at 13,200 rpm and removing the flow through, the column bound DNA fragments were washed with 700 µL buffer PE. Again, the column was centrifuged for 3 min at 13,200 rpm and the flow through was removed. In the next step, the column was placed into a new collection tube and centrifuged for 1 min at 13,200 rpm to remove the remaining washing buffer. The column was then transferred to a 1.5 mL collection tube and 40 µL EB buffer was added to the

column. After incubating the column for 20 min at room temperature the column bound DNA fragments were eluted by centrifuging for 3 min at 13,200 rpm. The purified PCR products were stored at -20 °C until further use.

2.2.2.10. Single-stranded linear amplification using terminator dyes

To sequence the previously amplified and purified DNA fragments single-stranded linear amplification was performed using ABI PRISM® BigDye® Terminator Ready Reaction mix. The reagent contains dideoxynucleotide triphosphates (ddNTPs) to terminate elongation during PCR. Each of these terminators is labelled with a specific fluorescent dye emitting at different wavelengths. During single strand amplification ddNTPs are incorporated into the growing DNA chain with a certain probability terminating and labelling the chain corresponding to the final base (Sanger sequencing method). The following components were used for linear amplification: 4 µL of the purified PCR product, 4 µL of BigDye® Terminator v1.1 Ready Reaction Mix and 2 µL of primer (forward or reverse, 1.5 µM). The reaction was then performed for 5 min at 95 °C following 25 cycles of 10 s at 96 °C, 10 s at 53 °C for E6 and 48 °C for E7 as well as 4 min at 60 °C. In order to verify the results, both DNA strands were sequenced using either the forward or the reverse primer.

2.2.2.11. DNA precipitation

After incorporating fluorescently labelled chain-terminating ddNTPs, the single stranded DNA was purified using ethanol precipitation. For this, the amplification product was diluted in 90 µL RNase- and DNase-free H_2O and 250 µL ethanol mixed with 10 µL sodium acetate (pH 4.6) was added. By mixing the solution the DNA was precipitated. The samples were then centrifuged for 15 min at 13,000 rpm to pellet the DNA. The supernatant was gently removed and the pelleted DNA was dried at room temperature. In the next step, 250 µL of 75% ethanol was added and the samples were mixed and again centrifuged for 6 min at 13,000 rpm. After removing the supernatant and drying the pellets at room temperature, the remaining humidity was eradicated by vacuum drying

for 6 min. The DNA pellet was then dissolved in 12 µL Hi-Di™ formamide and sequenced by capillary electrophoresis.

2.2.2.12. Capillary electrophoresis

To retrieve the sequence of the fluorescently labelled DNA fragments capillary electrophoresis was performed. Therefore, the samples diluted in Hi-Di™ formamide were pipetted into 96-well plates, shortly centrifuged at 1000 rpm and loaded into the ABI PRISM® 3100 Genetic Analyser. The signals obtained by capillary electrophoresis were then converted into an electronic DNA sequence trace chromatogram and subsequently analysed using the Sequencing Analysis Software v.6.

2.2.2.13. Recombination-mediated cassette exchange

After generating three retroviral vectors for the expression of HPV 16 E6 and/or E7 (S2F-cLM2CG-FRT3-HPV16-E6 and/or E7), RMCE was performed to create HCT116-HPV 16 E6 and/or E7 clones. Briefly, $5x10^5$ HCT116-HygTK cells were seeded on 6-well plates and cultured overnight. The cells were then co-transfected with 1 µg of S2F-cLM2CG-FRT3-HPV16-E6 and/or E7 vectors (that contain HPV 16 E6 and/or E7 flanked by two Flp recombination sites, Supplementary Figure 1) and 1 µg of pCAGGS-Flpo-IRES-Puro. Transfection was carried out using FuGENE HD Transfection Reagents as recommended by the manufacturer`s instructions. Due to the exchange of the HygTK cassette, single clones could be selected and grown under ganciclovir treatment. Single clones were then picked, expanded and tested for their dox-inducible expression of HPV 16 oncogenes.

2.2.3. Quantification of gene expression

2.2.3.1. RNA purification

For the isolation of total RNA $1x10^6$ cells were harvested and washed by using PBS (Gibco). Total RNA extraction was then performed using the RNeasy Mini Kit (Qiagen) including DNaseI (Invitrogen) treatment according to the manufacturer`s instructions. In the final step, the RNA was eluted in 40 µL of RNase-free water and the concentration was measured spectrophotometrically at 260 nm using a NanoDrop 1000 Spectrophotometer.

2.2.3.2. Gene expression profiling

Whole transcriptome analyses were performed in cooperation with the Genomics and Proteomics Core Facility at the DKFZ using Illumina HumanHT-12 microarray technology. For this, HCT116-HPV 16 E6 and E7 clones were treated for 48 hours with dox as described in previous sections. Total RNA was submitted to the core facility as recommended by the guidelines of the core facility. Subsequent steps were conducted at the core facility including quality control, labelling and hybridization of the samples to the microarray as well as image acquisition. Afterwards, the raw data were evaluated and normalized. Tables containing the expression of each gene on the microarray comparing dox-treated to untreated control were prepared and used to identify differentially expressed candidate genes, which were then validated by using RT-qPCR. The submitted samples are listed in Table 2.

Table 2: List of HCT116-HPV 16 E6 and E7 clones and respective treatment conditions used for gene expression profiling.

Clone	Treatment	Concentration of dox	Biological replicates
HCT116-HPV 16 E6	48 hours	no dox	3
	48 hours	500 ng/mL	3
HCT116-HPV 16 E7	48 hours	no dox	3
	48 hours	500 ng/mL	3
HCT116-HPV 16 E6 and E7	48 hours	no dox	3
	48 hours	500 ng/mL	3
HCT116-HygTK	48 hours	no dox	3
	48 hours	500 ng/mL	3

2.2.3.3. Reverse Transcription

For reverse transcription of mRNA into cDNA SuperScript® II Reverse Transcriptase Kit (Invitrogen) was used as described in the manufacturer`s protocol. Each reaction consisted of 1 µg of total RNA, 4 µL of 5x RT buffer, 2 µL of 0.1 M dithiothreitol (DTT), 0.5 µL of 0.5 µg/µL oligo(dT) primers (Invitrogen), 0.5 µL of 0.5 µg/µL single stranded random hexanucleotides (Bioron), 1 µL of 10 mM dNTPs (Invitrogen) and 0.5 µL of SuperScript® II Reverse Transcriptase (200 U/µL), and was incubated at 37°C for 15 min, at 42°C for 60 min and at 90°C for 5 min.

Reverse transcription to quantify hsa-miR-375 expression was conducted by using TaqMan® MicroRNA Reverse Transcription Kit (Applied Biosystems) in combination with hsa-miR-375 and snRNA U6 specific stem-loop RT primers according to the TaqMan® MicroRNA Assays (Applied Biosystems) protocol. Therefore, 50 ng of total RNA were reverse transcribed. The reactions were incubated at 16 °C for 30 min, at 42°C for 30 min and at 85°C for 5 min.

2.2.3.4. Quantitative PCR

Quantitative PCR (qPCR) was performed to determine the levels of E6 and E7 mRNA expression after treating HPV-transformed cell lines with DAC as well as after inducing HCT116 cell clones with dox. For this, the Applied Biosystems StepOne™ Real-Time PCR system and the Absolute qPCR SYBR Green ROX Mix (Thermo Scientific) were used. Primers used for qPCR amplification are listed in chapter 2.1.3. Primer. Cycling conditions were 95°C for 15 min and 40 cycles of 95°C for 15 s, 60°C for 30 s and 72°C for 30 s. Melting curves were included in each run to check for amplification specificity. Actin mRNA levels were quantified as a reference control and all samples were run in triplicates. Relative mRNA expression levels were determined by performing the ΔΔCt method and the fold change was calculated as $2^{-\Delta\Delta Ct}$.

Expression of hsa-miR-375 expression was quantified using TaqMan® MicroRNA Assays (Applied Biosystems) for qPCR. The assay utilizes specific stem-loop RT primers for reverse transcription as described in the previous section. TaqMan®

Universal PCR Master Mix (Applied Biosystems) was then used for subsequent qPCR amplification. Therefore, the reaction was incubated at 95 °C for 10 min and then 40 cycles were performed with the following conditions: 95 °C for 15 s and 60 °C for 60 s. All samples were run in triplicates. Hsa-miR-375 expression was measured relative to snRNA U6 levels by performing the ΔΔCt method and the fold change was calculated as 2-ΔΔCt.

2.2.4. Protein analyses

2.2.4.1. Preparation of RIPA-lysates

RIPA-lysates were prepared for subsequent detection and quantification of proteins by performing SDS-PAGE and Western blot. First, the cells were harvested and washed by using PBS (Gibco). Afterwards, the cells were lysed by adding RIPA buffer (Sigma Aldrich) supplemented with protease and phosphatase inhibitor (Sigma Aldrich). Subsequently, the cell pellets were disrupted by sonication for 10 s and the lysates were then incubated for 30 min on ice. After centrifugation at 13,200 rpm for 15 min at 4 °C the supernatant was collected and stored at -80 °C until further use.

2.2.4.2. Bradford Assay

Bradford Assay was performed to quantify the protein concentration in RIPA lysates. For this, the cell lysates were diluted 1:20 in RNase-free water and 20 µL of the dilution were mixed with 1 mL of Quick Start ™ Bradford 1x Dye Reagent (BioRad). Next, serial dilutions of BSA standards were prepared to quantify the protein concentration in the sample. 20 µL of the serial dilutions were then mixed with 1 mL of Quick Start ™ Bradford 1x Dye Reagent (BioRad) and the protein concentration was calculated based on the absorbance at 595 nm.

2.2.4.3. SDS-polyacrylamide gel electrophoresis (SDS-PAGE)

SDS-PAGE was used to separate denatured proteins according to their electrophoretic mobility depending on the charge, the molecular weight and the conformation of the proteins.

For sample preparation, Laemmli Buffer (4x) and NuPAGE® Sample Reducing Agent (10x) were mixed with 40 µg proteins as quantified by Bradford Assay after cell lysate preparation. After incubating the mixture at 95 °C for 10 min to disrupt any protein-protein interactions, the samples were loaded onto 4-20% Mini-PROTEAN® TGX™ gels (BioRad) and run in 1x Running Buffer (BioRad) at 45 mA until the bromophenol blue reached the bottom of the gel. Precision Plus Protein™ Prestained Standard (BioRad) was used as protein marker to estimate the size of the separated proteins.

2.2.4.4. Western Blot

In order to detect proteins by binding of specific antibodies the separated proteins were blotted onto PVDF membranes. Therefore, the PVDF membrane was incubated for 10 s in 100% methanol, for 5 min in H_2O bidest. and then for 5 min in Buffer III. Simultaneously, two Whatman papers were incubated in Buffer I, three in Buffer II and five in Buffer III. The sandwich for the semi-dry blotting was prepared by stacking two Whatman paper soaked in Buffer I, three in Buffer II, the activated PVDF membrane, the SDS gel and five Whatman paper incubated in Buffer III (listed from the positive pole at the bottom to the negative pole on top of the blotting chamber). Air bubbles were removed by rolling over the sandwich with a glass pipette. The proteins were then blotted onto the membrane at 230 mA for one hour.

Protein transfer was checked by staining the membrane with Ponceau Red solution (Sigma Aldrich). Afterwards, the membrane was destained using H_2O bidest. The following steps were performed using the Novex Western Breeze Chemiluminescent Immunodetection System (Life technologies) according to the instructions of the manufacturer. Briefly, the PVDF membrane was blocked in Blocking Solution for one hour at room temperature. After washing twice with H_2O bidest. for 5 min, the membrane

was incubated in primary antibody overnight at 4°C. All primary antibodies used in this study were diluted as described in the datasheets of the manufacturers. Unbound primary antibody was removed by washing the membrane four times in Antibody Wash for 5 min. In the next step, the membrane was incubated with the secondary antibody coupled to Alkaline Phosphatase for one hour at room temperature. The membrane was again washed four times with Antibody Wash for 5 min, followed by two washing steps with H_2O bidest. for 2 min. After adding Novex AP Chemiluminescent Substrate CDP Star® (Life technologies) onto the membrane light sensitive films (Lumi-Film Chemiluminescent Detection Film, Roche Diagnostics) were used to detect PVDF membrane bound secondary antibodies. Protein expression levels were normalized to actin.

For the detection of other proteins the antibodies bound to the PVDF membrane were removed by incubating the membrane in Restore™ Western Blot Stripping Buffer (Thermo Fisher Scientific). Therefore, the PVDF membrane was washed twice in PBS to remove the chemiluminescent substrate and was then incubated for one hour in stripping buffer pre-heated to 37 °C. After washing again twice with PBS the immunodetection procedure was repeated starting with the blocking step.

2.2.4.5. Immunocytochemistry

Immunofluorescence staining of cultured cells was used to visualize and localize specific proteins in dox-induced HCT116 cell clones. Therefore, monoclonal antibodies were utilized specifically targeting γ-tubulin and phosphorylated-H2AX (γH2AX).

First, cover slips (15 mm in diameter) were placed in 10 cm cell dishes. In the next step, HCT116 cells were seeded and induced with dox for the expression of HPV 16 E6 and/or E7 as described previously. After dox treatment, the cover slips were transferred to 12-well plates (cell site up) and washed twice with PBS. Ice cold methanol was then pipetted onto the cells to fix the cells on the cover slips and to dissolve lipids from the cell membrane making it permeable to antibodies used to detect intracellular antigens. The plates were then incubated for 20 min at 4 °C before the methanol was removed

and the cover slips were washed twice with PBS. To prevent non-specific binding of the antibodies the cover slips were incubated in 2% goat serum (Sigma Aldrich) diluted in PBS for one hour at 4 °C. After blocking the cover slips were washed twice with PBS and incubated in primary antibody diluted in PBS overnight at 4 °C in a humidified chamber. The chamber was prepared using 10 cm square dishes with water-soaked filter papers covered by a layer of parafilm. The cover slips were then incubated in 50 µL drops of primary antibody solution pipetted onto the parafilm. In the next day, the cover slips were again transferred to 12-well plates and washed twice with PBS. Afterwards, the cover slips were incubated with the fluorophore-conjugated secondary antibody diluted in PBS for three hours at 37 °C. Next, the cells were washed twice with PBS and were then mounted onto microscope glass slides. The slides were analysed using a Leica DM5000 B fluorescence microscope or were stored at 4 °C until further use.

2.2.5. Detection of DNA methylation

2.2.5.1. Bisulfite conversion

Bisulfite conversion was performed to detect and subsequently analyse DNA methylation patterns. Treatment of purified DNA with sodium bisulfite deaminates unmethylated cytosine residues to uracile, whereas 5-methylacytosine remains unaffected. Afterwards, sequencing or hybridization techniques allow distinguishing between methylated and unmethylated positions in the DNA sequence. Bisulfite conversion was conducted by using the Methylamp™ DNA Modification Kit (Epigentek) as described in the manufacturer`s protocol. For this, 24 µL of isolated DNA were employed. The bisulfite-modified DNA was eluted in 30 µL of sterile water and then stored at –20 °C.

2.2.5.2. Pyrosequencing for detection of E2BS and LINE1 methylation

In order to quantify the methylation level in E2BSs 3 and 4 as well as in LINE1, bisulfite-converted DNA was first amplified using bisulfite-specific primers and then

pyrosequenced. The primers designed to cover the proximal E2BSs 3 and 4 are listed in the primers section. LINE1 methylation analysis was carried out by using PyroMark LINE1 reagents (Qiagen).

Amplification of the respective regions was performed using the following reagents: 1.25 µL 10X Qiagen PCR buffer, 15 mM $MgCl_2$, 0.25 µL 10 mM deoxynucleotide triphosphates (dNTPs), 0.125 µL of each PCR primer (25 µM), 0.1 µL (0.5 U) HotStar Taq Plus DNA Polymerase (Qiagen) and 2 µL of the bisulfite-modified DNA. The volume was then adjusted to 12.5 µL by adding ddH_2O and the PCR was under the following conditions: initial activation step at 95°C for 5 min followed by 50 cycles of denaturation at 94°C for 40 s, annealing at 50°C for 30 s, extension at 72°C for 40 s and final extension 72°C for 6 min. Correct amplification was checked by agarose gel electrophoresis.

Pyrosequencing was then performed by using PyroMark Gold Q24 reagents, the Vacuum Prep Workstation and the Q24 instrument (all Qiagen) as recommended by the manufacturer.

2.2.5.3. Methylation-specific qPCR

Methylation-specific qPCR was performed to measure the methylation level in the hsa-miR-375 promoter region. Therefore, qPCR primers were used specifically binding to the methylated and bisulfite-converted form of regions in the hsa-miR-375 promoter as published in (Wilting *et al.* 2013). QPCR was then performed as described previously to amplify this region. As a reference, bisulfite-converted and unmethylated sequences of β-actin were amplified ensuring DNA quality and efficient DNA modification.

2.2.5.4. Whole methylome analysis and evaluation of copy number variations

The methylation status of about 850,000 CpG dinucleotides as well as the presence of gene copy number variations was assessed by using Infinium® MethylationEPIC BeadChips (Illumina). Therefore, HPV 16 oncogene expression was induced in the

generated HCT116 clones by treating them for 48 hours or nine days with 500 ng/mL dox. After DNA purification and bisulfite conversion, the samples were hybridized to the array. The bisulfite conversion, the hybridization step and the generation of the raw data including respective quality checks were performed by the DKFZ Genomics and Proteomics Core Facility. The raw data was then further processed in cooperation with the Neuropathology Department using their previously established R-based analysis pipelines.

3. Results

3.1. 5-aza-2`-deoxycytidine (DAC) treatment of HPV-transformed cell lines

As hypermethylation of viral as well as host cellular genomic loci is assumed to play an important role during HPV-driven tumor formation and as treatment with the demethylating agent DAC showed promising results in myelodysplastic syndrome and in a number of solid tumors, the first aim of the present study was to systematically analyze the effects of DAC treatment on HPV oncogene expression as well as on the growth behavior of HPV-transformed cells. DAC prevents the maintenance of DNA methylation in dividing cells by being incorporated into the DNA during replication and by directly interacting with DNMT1 (Creusot *et al.* 1982, Jones 1985, Jones & Taylor 1980). Therefore, DAC treatment is assumed to globally reduce CpG methylation levels in replicating cells.

The data that are presented in the first part of this study were generated in cooperation with Maximilian Stich and resulted in the following publication (Stich *et al.* 2016).

To cover a wide range of HPV-transformed cell lines the cervical carcinoma cell lines CaSki, SiHa (both HPV 16 positive), SW756 and C4-1 (both HPV 18 positive) as well as the HPV 16-transformed head and neck squamous-cell carcinoma (HNSCC) cell lines UM-SCC-47 and UM-SCC-104 were included in this study (Table 3). The cell lines were treated for 72 hours using three different concentrations of DAC (0.1 µM, 0.5 µM and 1.0 µM). First, the effectiveness of the treatment was confirmed by quantifying CpG methylation in the retrotransposon Long Interspersed Nuclear Element 1 (LINE1) (Figure 6). LINE1 CpGs are frequently methylated and widely used as surrogate markers to assess global DNA methylation levels (Yang *et al.* 2004). In all tested cell lines the methylation level of three CpGs located in LINE1 decreased substantially confirming the effectiveness of the performed treatment. The most potent demethylating effects could be detected using 0.1 µM and 0.5 µM DAC. Increasing the DAC concentration to 1.0 µM was not found to enhance its demethylating effect, as illustrated by a U-shaped LINE1

Table 3: Characteristics of the cell lines selected for DAC treatment including HPV type, origin, chromosomal HPV integration site, E2BS methylation level and the status of the E2 gene (modified from (Stich *et al.* 2016)).

Cell line	HPV Type	Origin	Chromosomal integration site	E2BS Methylation	Status E2 Gene
CaSki	16	Cervix	>600 copies integrated in about 11 chromosomal loci (Mincheva *et al.* 1987, Yee *et al.* 1985)	High	Intact
SiHa	16	Cervix	13q21, 13q31 (Mincheva *et al.* 1987)	Low	Disrupted
UM-SCC-47	16	Lateral Tongue	3q28 (Olthof *et al.* 2015)	High	Disrupted, but E2 expression detected
UM-SCC-104	16	Floor of Mouth	17p11 (Akagi *et al.* 2014)	Low	Disrupted
C4-1	18	Cervix	8q22.1 (Gallego *et al.* 1994)	Low	Disrupted
SW756	18	Cervix	12q13 (Popescu *et al.* 1987)	Low	Disrupted

methylation profile (Figure 6). These dose-dependent characteristics of DAC treatment have been described previously and can be explained by a dual effect of the drug (reviewed in (Taby & Issa 2010)). At low doses, DNA demethylation can be detected after a low number of cell divisions, whereas at higher doses, DAC treatment shows an immediate cytotoxic effect preventing cell cycle progression. However, the cytotoxic effect of high dose DAC treatment is not assumed to be specific for HPV-transformed cells and thus only causes severe side effects by depleting regularly dividing non-tumor cells strongly limiting its clinical use. Therefore, low dose treatment causing demethylation, but not directly cytotoxicity was hypothesized to be more suitable for the treatment of HPV-transformed cells. Additionally, the level of LINE1 demethylation was found to differ between the tested cell lines, probably as a consequence of varying cell cycle lengths.

3.1.1. DAC treatment represses E6 and E7 oncogene expression

To test the hypothesis that DAC treatment reinforces regulatory mechanisms repressing HPV early gene expression, E6 and E7 mRNA expression and protein levels were analyzed. RT-qPCR quantification revealed a decrease of E6*I and E7 mRNA levels in all DAC-treated cell lines (Figure 7A). The most significant decrease was observed in CaSki, UM-SCC-47, UM-SCC-104 and SW756 cells, whereas the oncogene mRNA expression was only moderately reduced in SiHa and C4-1 cells. The lowest tested concentration of 0.1 µM DAC was sufficient to downregulate E6 and E7 mRNA expression, although the effect was more pronounced using 0.5 and 1.0 µM DAC.

Reduction of HPV E6 and E7 expression was also confirmed on the protein level as shown in Figure 7B. Due to the lack of sensitive antibodies specific for HPV 16 and 18 E6 proteins, the levels of the target proteins p53 and p21 were measured as an indirect read-out of HPV E6 protein levels. As expected, p53 and p21 levels increased in the analyzed cell lines after DAC treatment indicating a reduction of E6 protein production. In agreement with the mRNA data decreasing HPV oncoprotein levels were already detectable for samples treated with 0.1 µM DAC, however, stronger effects were again observed after increasing the DAC concentration to 0.5 and 1.0 µM. In summary, DAC treatment represses HPV oncogene expression in a wide range of HPV-transformed cell lines and causes an increase in p53 and p21 protein levels.

3.1.2. Application of DAC decelerates cell proliferation and prevents colony formation of HPV-transformed cell lines

Due to the prominent roles of p53 and p21 in the activation of cell cycle checkpoints, in the detection of DNA damage as well as in the induction of apoptosis, their joint reactivation, as a consequence of reduced E6 and E7 expression under DAC treatment, was assumed to affect proliferation and colony formation of the cells. Proliferation as well as colony formation was significantly impaired in the tested cell lines after treatment with DAC (Figure 8). In CaSki, UM-SCC-47, UM-SCC-104 and C4-1 cells treatment with 0.1 µM DAC was sufficient to substantially reduce the proliferation rate (Figure 8A).

Elevation of DAC concentration to 1.0 µM further enhanced the anti-proliferative effect, especially in SiHa and SW756 cells. As shown in Figure 8B, DAC treatment not only repressed proliferation but also efficiently inhibited colony formation of the cells. These data reveal a potent growth inhibitory effect of DAC on HPV-transformed cell lines. Furthermore, outgrowth of cells after removing DAC from the culture medium was not observed suggestive of only a low risk for the selection of DAC-resistant cell clones.

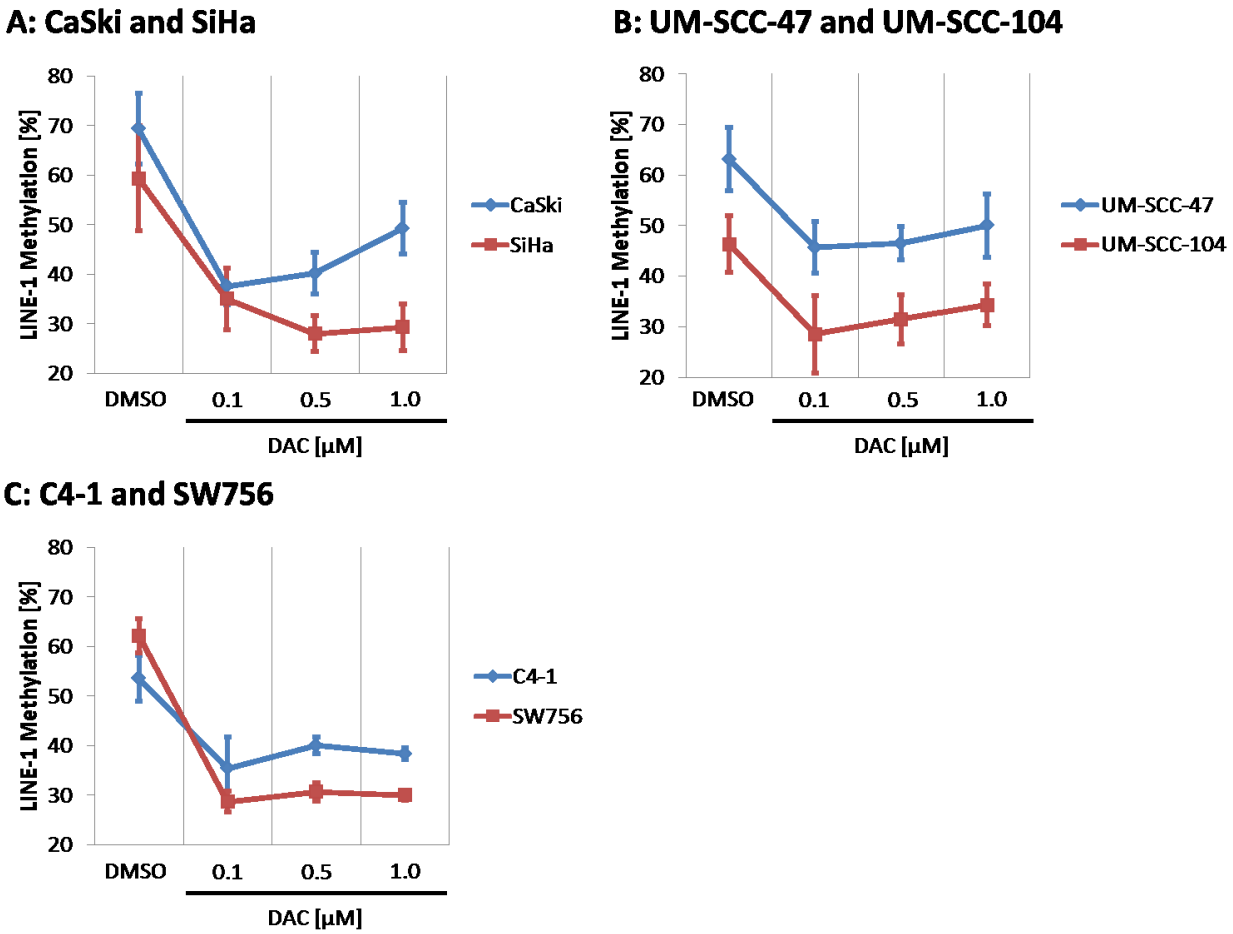

Figure 6: Decrease of LINE-1 methylation levels after DAC treatment indicates global DNA demethylation.
The diagrams show the mean methylation percentage of three CpG dinucleotides located in the LINE-1 transposable element after treating **(A)** CaSki and SiHa, **(B)** UM-SCC-47 and UM-SCC-104 as well as **(C)** C4-1 and SW756 with different concentrations of DAC ranging from 0.1 µM to 1.0 µM. LINE-1 methylation levels were determined by bisulfite conversion of isolated DNA and subsequent pyrosequencing using PyroMark LINE-1 reagents (Qiagen). (Experiment performed by Maximilian Stich (Stich *et al.* 2016)).

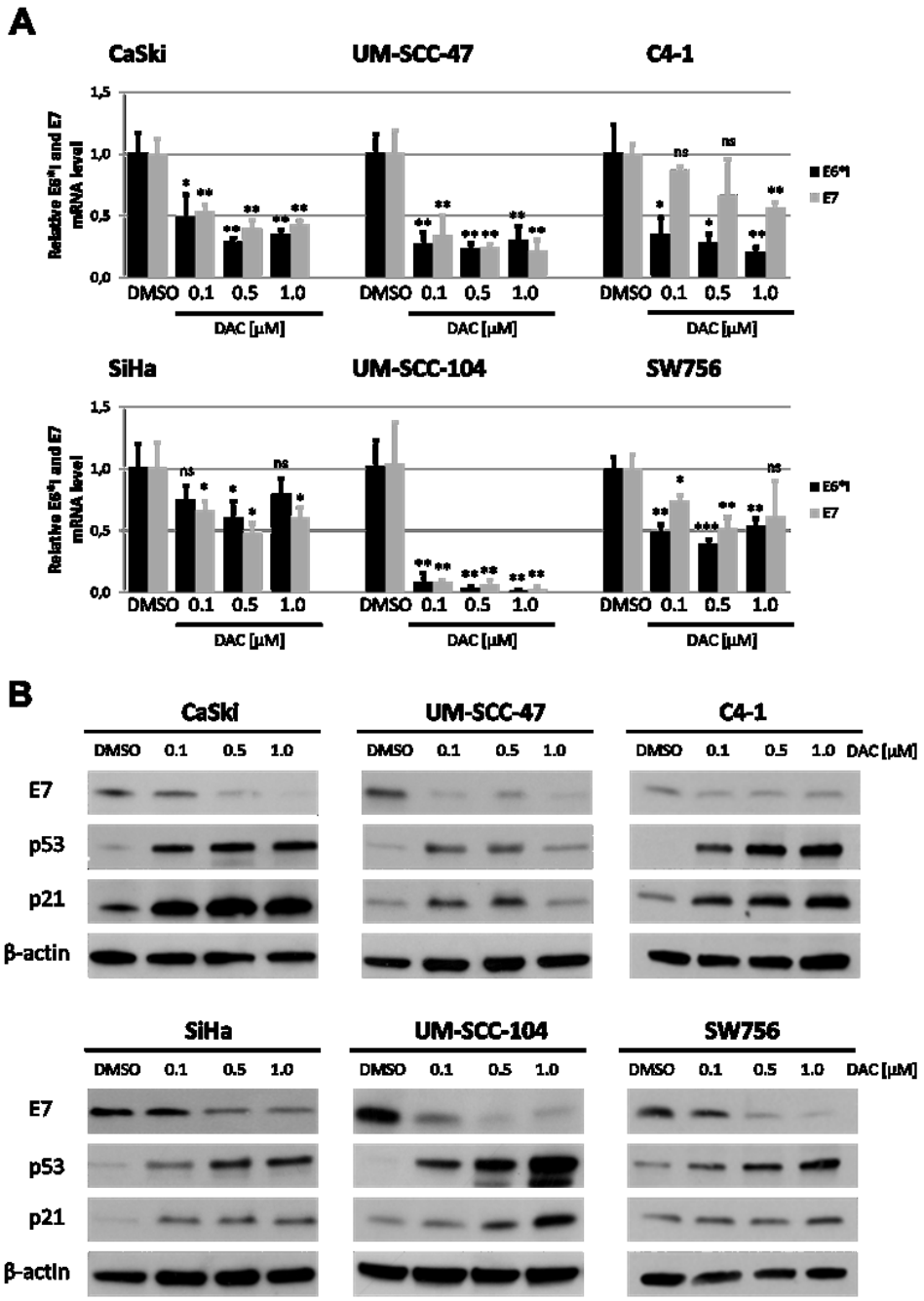

Figure 7: Effects of DAC treatment on HPV oncogene expression as well as on the downstream factors p53 and p21.

(A) HPV 16 and 18 E6*I and E7 mRNA levels were quantified using RT-qPCR in CaSki, SiHa, UM-SCC-47, UM-SCC-104, C4-1 and SW756 after DAC treatment for 72 hours. Relative mRNA expression levels were calculated by using DMSO treated cells as a reference control as well as actin levels as loading control. The presented mean values were obtained from three biological replicates and the error bars represent the according standard deviation. Student`s t-test was performed to calculate p values. *: $p<0.05$, **: $p<0.01$, ***: $p<0.001$ and ns: not significant. **(B)** HPV E7, p53 and p21 protein levels in DAC-treated HPV-transformed cell lines were quantified using Western blot analysis. β-actin was used as an internal loading control. (Experiments were performed in cooperation with Maximilian Stich (Stich *et al.* 2016))

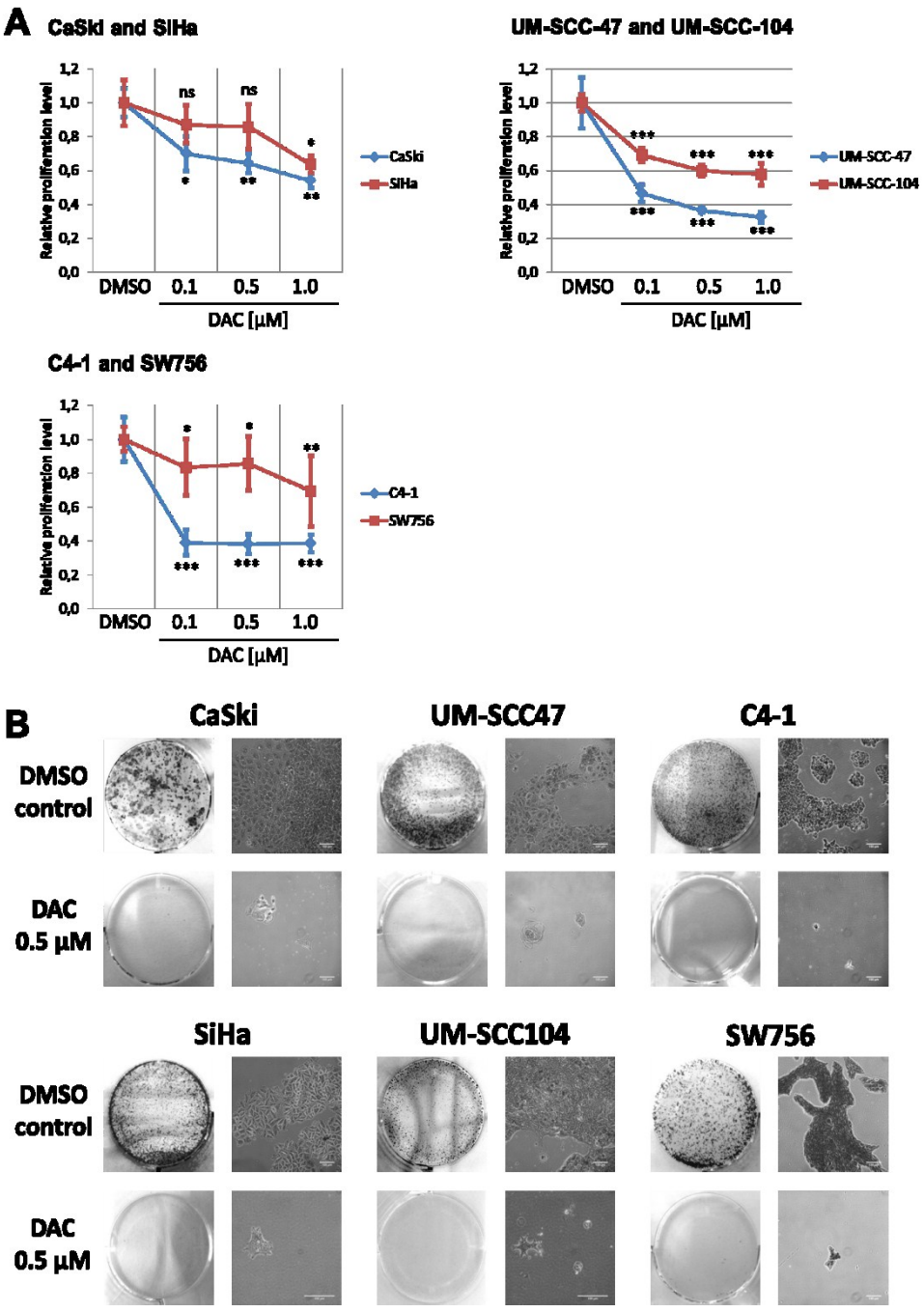

Figure 8: Proliferation and colony formation of HPV-transformed cell lines under DAC treatment.
(A) Cell proliferation was measured by quantifying the DNA content after DAC treatment for 72 hours. The diagrams show the mean proliferation level relative to DMSO-treated cells based on three biological replicates as well as the according standard deviation. The p values were calculated by performing Student`s t-test. *: $p<0.05$, **: $p<0.01$, ***: $p<0.001$ and ns: not significant. **(B)** The colony formation capacities of HPV-transformed cell lines were monitored by treating the cells with 0.5 µM DAC for 72 hours or with the solvent DMSO as indicated. The cells were then cultured without treatment for seven days and the formation of colonies was evaluated by staining with crystal violet. Representative images are shown. The scale bars reflect 100 µm. (The presented data was produced jointly with Maximilian Stich (Stich *et al.* 2016))

3.1.3. DAC treatment reduces E2BS methylation in CaSki and UM-SCC-47

Previous studies showed that HPV early gene expression is regulated by the interaction of the HPV E2 protein with four conserved E2BSs in the HPV URR (Kim *et al.* 2003, Thierry 2009). Methylation of CpGs in the E2BSs was found to prevent binding of E2 abrogating its regulatory effect and leading to transcriptional activation of the HPV early promoter (Bhattacharjee & Sengupta 2006, Leung *et al.* 2015, Vinokurova & von Knebel Doeberitz 2011). Repression of HPV oncogene transcription could therefore be the result of the DAC-mediated demethylation of the CpGs located in the E2BSs in the HPV URR (Figure 9A). To test this hypothesis methylation of E2BS 3 and 4 was quantified after DAC treatment using bisulfite conversion and subsequent pyrosequencing. Interaction of E2 with these two E2BSs has previously been demonstrated to reduce HPV oncogene transcription by displacing the transcription factors Sp1 and TBP from their respective binding sites located in direct proximity to E2BS 3 and 4 (Steger & Corbach 1997, Stubenrauch *et al.* 1998). As expected, treatment with DAC reduced the mean methylation levels of CpGs in E2BS 3 and 4 of CaSki as well as UM-SCC-47 cells (Figure 9 B and C). In contrast, methylation of E2BS 3 and 4 was not affected in SiHa and UM-SCC-104 cells as these E2BSs were not methylated in those cell lines.

Based on these data, it can be concluded that demethylation of the E2BSs during the application of DAC might reactivate the E2-mediated transcriptional regulation of E6 and E7 expression in CaSki cells, which were also shown to express E2 proteins (Fernandez *et al.* 2009). Reduced HPV oncogene expression was, however, also observed in the other cell lines that either lack expression of intact E2 due to its disruption during viral integration into the host genome or show low E2BS methylation levels (Table 3 and Figure 9). Therefore, the re-establishment of the E2-mediated transcriptional control cannot be the only mechanism silencing E6 and E7 expression observed after DAC treatment.

3.1.4. DAC-mediated activation of miR-375 reduces HPV oncogene expression

As DNA demethylation in response to DAC treatment does not only occur in the viral genome but also in the host cell genome, regulatory factors might become activated repressing HPV oncogene expression. Recently, miR-375 was found to be involved in the regulation of HPV 16 and 18 oncogene expression by directly binding and subsequently degrading E6 and E7 transcripts (Jung *et al.* 2014). Furthermore, miR-375 reduces the expression of the transcription factor Sp1, which interacts with the HPV

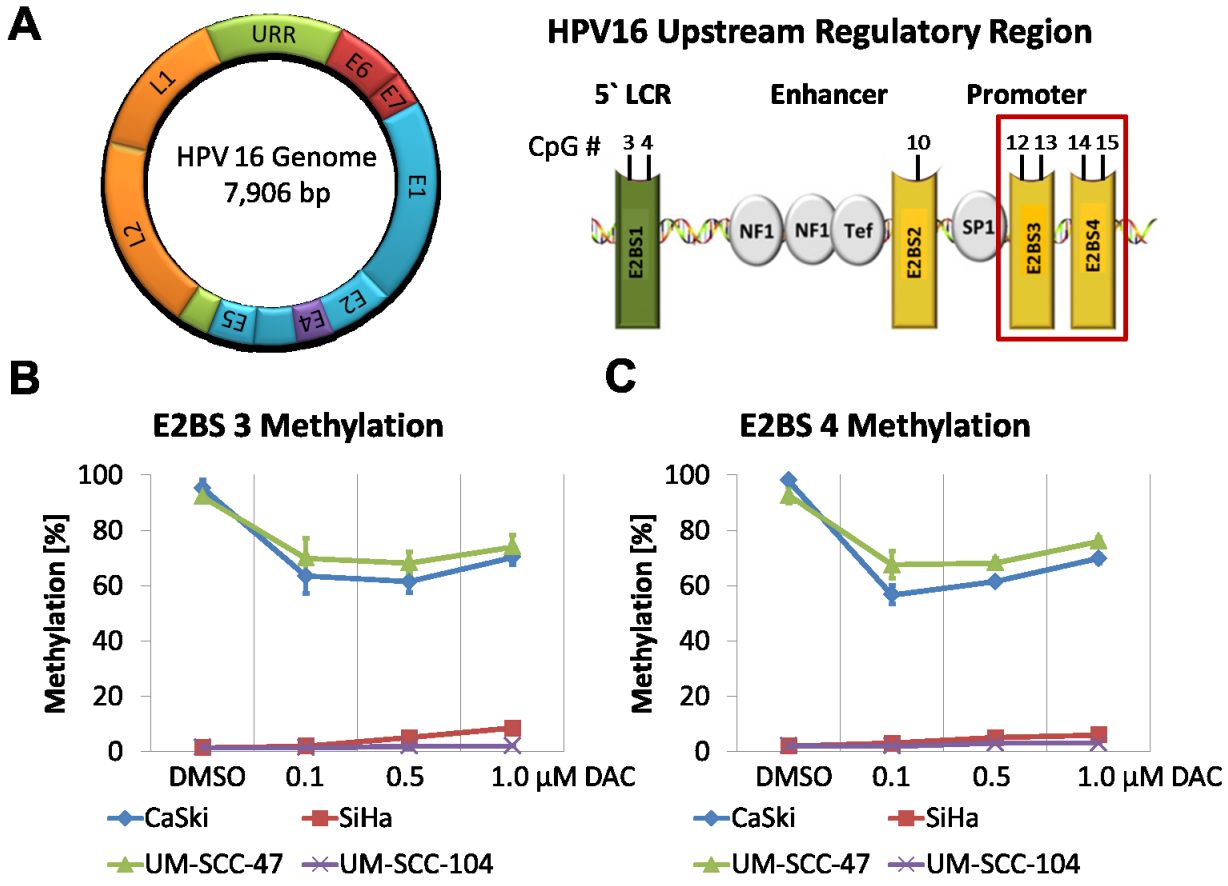

Figure 9: Quantification of E2BS 3 and 4 methylation levels in the HPV 16 URR of CaSki, SiHa, UM-SCC-47 and UM-SCC-104 cells after DAC treatment.
(A) Schematic representation of the E2BSs in the HPV 16 URR including CpG dinucleotide positions. The E2BS 3 and 4 are highlighted by the red box. Pyrosequencing was used to quantify E2BS 3 **(B)** and 4 **(C)** methylation levels in CaSki, SiHa, UM-SCC-47 and UM-SCC-104 after DAC treatment. The methylation levels are shown as mean values of the two CpGs in the respective E2BS and the error bars indicate the according standard deviation. The CpGs are located in the HPV 16 E2BS 3 at nucleotide position 37 and 43 as well as in E2BS 4 at position 52 and 58. (E2BS methylation data was produced in cooperation with Maximilian Stich (Stich *et al.* 2016))

URR and activates early gene transcription (Jung *et al.* 2014, Wang *et al.* 2011). As expression of miR-375 is dependent on the methylation level in its promoter region and as this region becomes frequently methylated during HPV-mediated cervical carcinogenesis, it could be assumed that miR-375 expression is reactivated after DAC treatment (Wilting *et al.* 2013).

To confirm the assumption the effect of DAC treatment on miR-375 promoter methylation was analyzed. Therefore, PCR primers were designed to cover six CpG dinucleotides located in the miR-375 promoter region (Figure 10A) as reported in a study published previously (Wilting *et al.* 2013). After bisulfite treatment of the isolated DNA, methylation-specific qPCR (MSP) was performed to specifically quantify methylated DNA strands. As depicted in Figure 10B, miR-375 promoter methylation was reduced after treating HPV-transformed cell lines using 0.5 µM DAC. The strongest demethylating effects were detected in SiHa and SW756 cells. The levels of miR-375 promoter demethylation slightly varied between the tested cell lines and are potentially the consequence of different growth rates. Overall, the results resemble the demethylation effects detected in LINE1.

Next, miR-375 expression was monitored by utilizing TaqMan qPCR assays. DAC treatment resulted in a substantial increase in miR-375 expression in all six analyzed cell lines as shown in Figure 11. Treatment with increasing DAC concentrations also tended to elevate miR-375 expression levels. Especially SiHa cells and the HNSCC cell lines UM-SCC-47 and UM-SCC-104 showed strong increases in miR-375 expression under DAC treatment.

To evaluate whether elevated miR-375 expression would lead to reduced E6 and E7 expression, CaSki and SiHa cells were transfected with miR-375 mimics and HPV 16 oncogene levels were quantified by RT-qPCR as well as Western blot analysis. As indicated in Figure 12 transfection of miR-375 mimics led to reduced HPV 16 E6*I and E7 mRNA levels in both cell lines compared to the levels in cells transfected with non-specific control miRNAs. Moreover, E7 protein levels decreased after transfection of miR-375 mimics. These data suggest that expression of HPV E6 and E7 is reduced by miR-375. Therefore, reactivation of miR-375 expression and subsequent degradation of

E6 and E7 mRNA transcripts provides another explanation for the reduction of E6 and E7 oncogene expression in HPV-transformed cell lines when treated with DAC.

In conclusion, DAC treatment of HPV-transformed cells appears to be a potent approach to significantly decrease HPV oncogene expression, which is assumed to contribute to the inhibition of cell growth as well as colony formation. Several mechanisms seem to play a role in the DAC-mediated reduction of E6 and E7 levels including demethylation

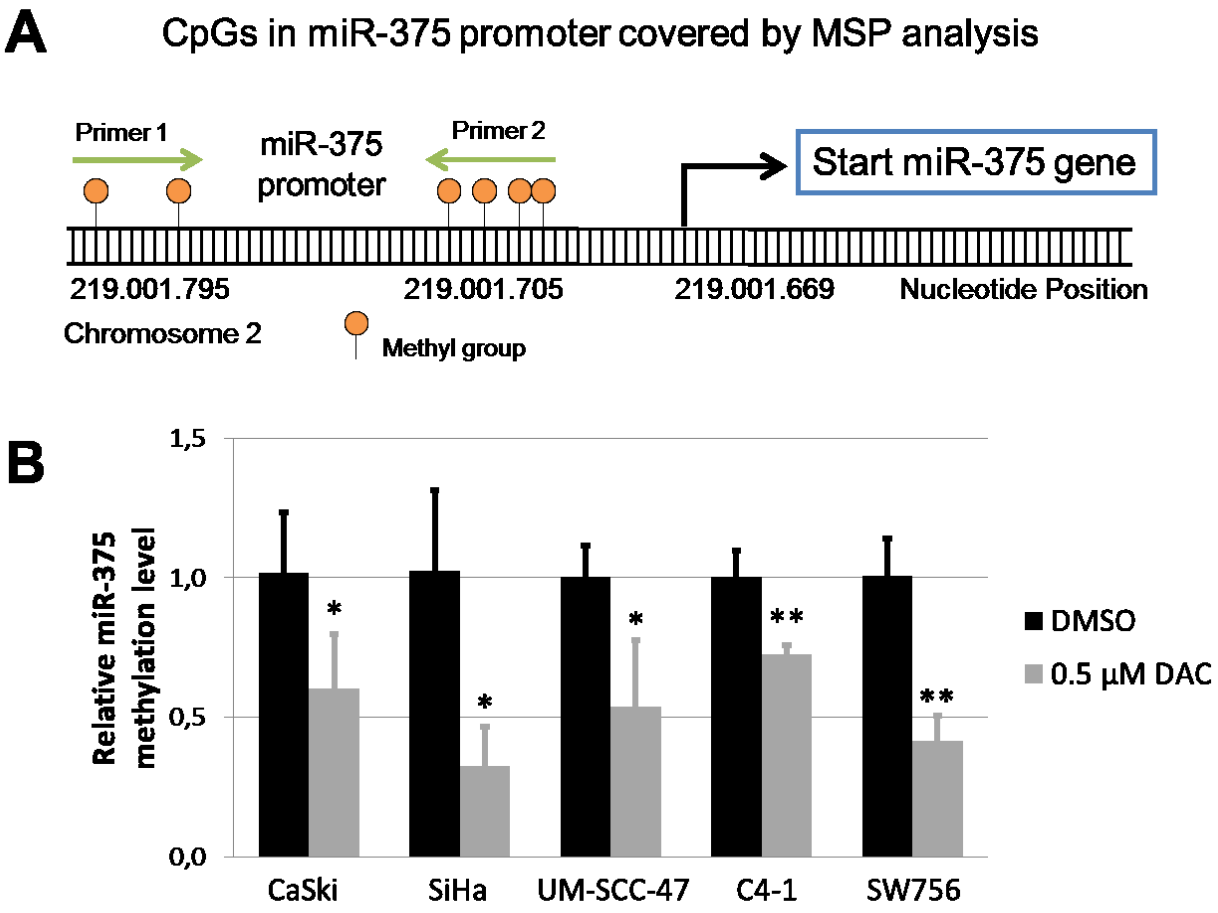

Figure 10: MiR-375 promoter methylation in DAC-treated HPV-transformed cell lines.
(A) The graphic schematically illustrates the miR-375 promoter region including six CpG dinucleotides that were covered by the primers used for the methylation-specific qPCR (MSP) assay to amplify bisulfite converted and methylated template DNA. The respective CpGs are located in close proximity to the start of the miR-375 gene (Wilting *et al.* 2013). **(B)** Relative miR-375 promoter methylation of HPV-transformed cell lines after treatment with 0.5 µM DAC. The methylation level was quantified using MSP and is shown relative to the level detected after treatment with DMSO. To verify successful bisulfite conversion and sufficient DNA quality, bisulfite converted and unmethylated β-actin sequences were amplified. The presented diagram shows the mean methylation levels from at least three independent experiments and error bars indicate the according standard deviation. P values were calculated by performing Student`s t-test. *: $p<0.05$ and **: $p<0.01$ (Stich *et al.* 2016).

of E2BSs in E2-expressing cells and reactivation of miR-375 expression. Additionally, there might be also other mechanisms involved in repressing E6 and E7 expression as well as in reducing cell proliferation, as DAC treatment globally affects the DNA methylation pattern.

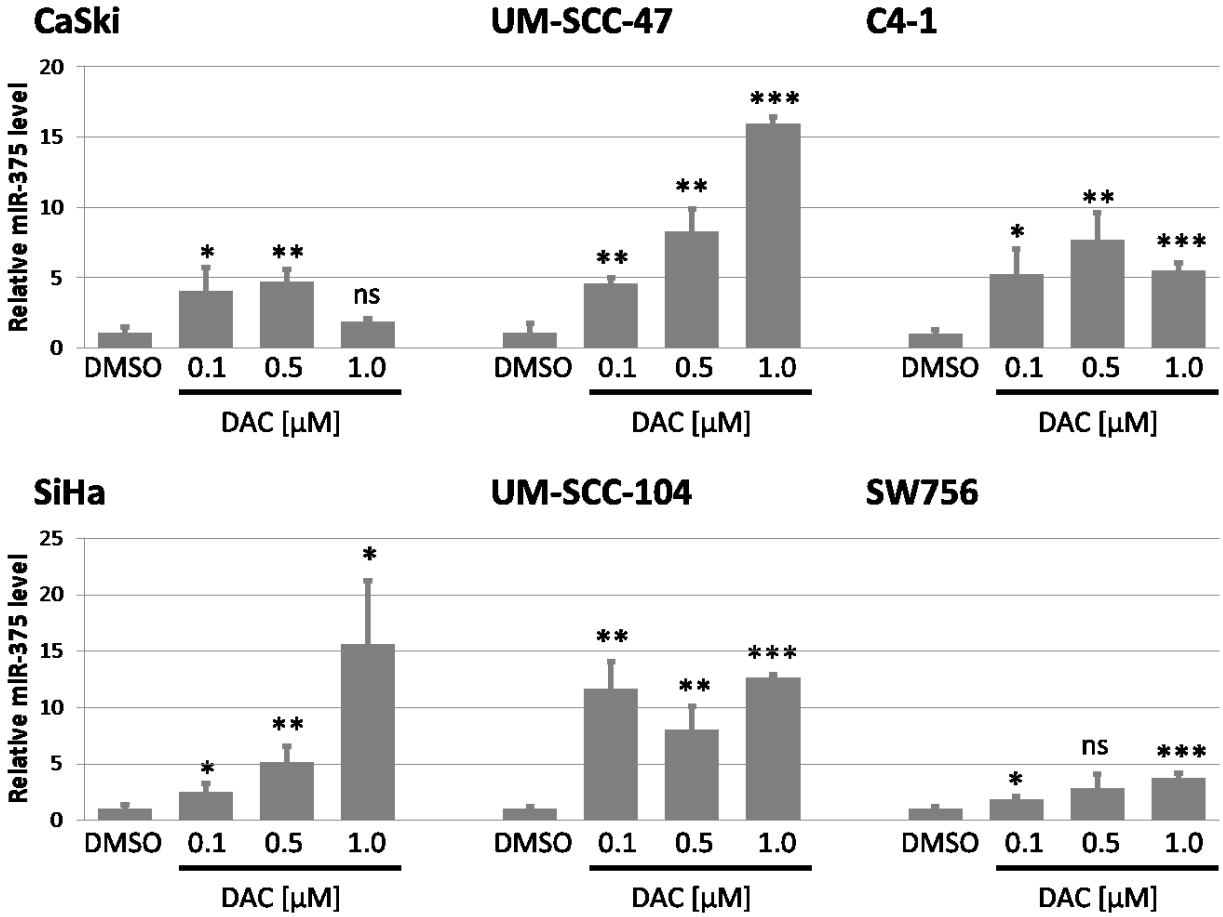

Figure 11: Expression of miR-375 in HPV-transformed cell lines after treatment with DAC.
TaqMan qPCR assays were performed to quantify the expression of miR-375 in DAC-treated HPV-transformed cell lines. The bars of the diagrams indicate miR-375 expression levels based on at least three independent replicates relative to the expression in DMSO-treated cells. The error bars represent the according standard deviation and snRNA U6 expression was quantified as internal loading control. Student`s t-test was performed to calculate p values in reference to DMSO. *: $p<0.05$, **: $p<0.01$, ***: $p<0.001$ and ns: not significant. (The presented data was generated in cooperation with Maximilian Stich (Stich *et al.* 2016))

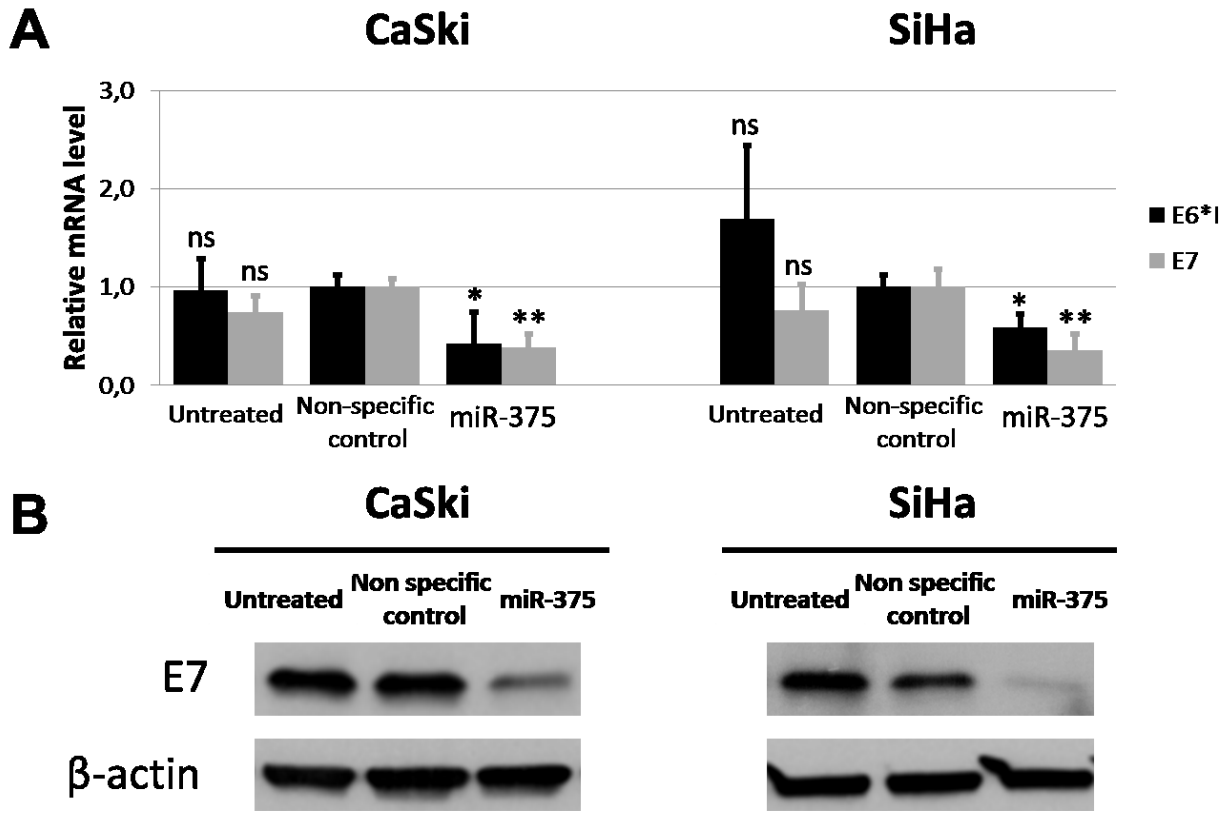

Figure 12: Expression of HPV 16 oncogenes in CaSki and SiHa cells after transfection of miR-375 mimics.

(A) RT-qPCR quantification of HPV 16 E6*I and E7 mRNA in CaSki and SiHa cells transfected either with 100 nM miR-375 mimics or 25 nM non-specific control miRNAs. The diagram shows the mean levels of HPV 16 E6*I and E7 mRNA detected 48 hours after transfection as well as the according standard deviation. The experiment was performed at least in biological duplicates. P values were calculated using Student`s t-test and non-specific control was utilized as a reference. β-actin was quantified as loading control. *: $p<0.05$, **: $p<0.01$ and ns: not significant. **(B)** Western blot was performed to detect HPV 16 E7 protein levels in CaSki and SiHa cells 48 hours after miR-375 transfection. The miRNA concentrations used for transfection were identic to (A). Actin levels were measured as internal control (Stich *et al.* 2016).

3.2. Development of novel model system to study the effects of HPV 16 oncogenes

As the identification of pathways that are manipulated by the HPV oncoproteins depends on model systems that precisely mimic the effects of E6 and E7, another aim of this study was the generation of an inducible E6 and E7 expression system in an immortalized, but chromosomally stable cell line to comprehensively study the effects of HPV 16 oncogene expression in a time-controlled manner. For this, the microsatellite-unstable colon cancer cell line HCT116 was selected (Brattain *et al.* 1981). In contrast to HPV-transformed tumor cells, immortalization of HCT116 cells is caused by MMR deficiency due to a mutation in the *hMLH1* gene. Consequently, HCT116 cells acquire and accumulate mutations, especially in microsatellites, which may lead to the inactivation of affected genes, e.g. the tumor suppressive gene encoding TGFβ receptor 2, and to the expression of truncated proteins. However, outgrowth of these cells does not require chromosomal destabilization or high rates of aneuploidy as observed in HPV-transformed tumor cells (Ertych *et al.* 2014, Lengauer *et al.* 1997, Steinbeck 1997). Therefore, inducible HPV 16 oncogene expression in HCT116 cells might represent an ideal model system to evaluate short- and long-term effects of E6 and E7 on chromosomal stability.

3.2.1. Generation of dox-inducible HCT116-HPV 16 E6 and E7 clones

In order to generate HCT116 clones for the dox-inducible expression of HPV 16 E6 and E7 either individually or in combination, HCT116-HygTK cells were used as parental master cells (Lee *et al.* 2013). These cells, which were kindly provided by Dr Johannes Gebert and Dr Jennifer Lee, constitutively express a reverse tetracycline-controlled transactivator (rtTA) (Welman *et al.* 2006). Additionally, these cells contain a hygromycin B phosphotransferase-thymidine kinase (HygTK) expression cassette integrated as a single copy resulting in resistance to hygromycin B as well as sensitivity to ganciclovir. As the HygTK expression cassette is flanked by a wild-type (F) and a mutant (F3) Flippase (Flp)-recombinase target site, expression of Flp-recombinase allows replacement of the cassette by any construct of interest. Thereby, these cell clones

allow the integration of constructs encoding the HPV 16 oncogenes as single copies into a defined chromosomal locus (Lee *et al.* 2013).

The retroviral vector S2F-cLM2CG-FRT3 (Supplementary Figure 1) was used to generate plasmids that enable dox-inducible expression of HPV 16 E6 and/or E7 (Loew *et al.* 2006, Weidenfeld *et al.* 2009). S2F-cLM2CG-FRT3 contains a tetracycline (tet)-controlled bidirectional promoter (P_{tet}bi) for concurrent regulation of the two reporter genes firefly luciferase and red fluorescent protein mCherry. This expression cassette is flanked by two heterospecific Flp-recognition sites F and F3 required for subsequent RMCE (Schlake & Bode 1994). For the generation of S2F-cLM2CG-FRT3-HPV16-E6 and S2F-cLM2CG-FRT3-HPV16-E7 the mCherry fragment in the S2F-cLM2CG-FRT3 vector was replaced by HPV 16 E6 (GenBank: K02718.1, nt 83-560) or HPV 16 E7 (GenBank: K02718.1, nt 562-858), respectively. To create the vector S2F-cLM2CG-FRT3-HPV16 E6-E7 for the expression of both HPV 16 oncogenes, the mCherry fragment of S2F-cLM2CG-FRT3 was exchanged for the HPV 16 E6 sequence, while the firefly luciferase reporter gene was substituted by the HPV 16 E7 coding sequence. Maps of the resulting vectors can be found in Supplementary Figure 1.

As a next step, the HygTK expression cassette in the HCT116-HygTK master cells was replaced by the HPV 16 oncogene-encoding sequences of the three generated vectors (Figure 13). RMCE was conducted by co-transfecting HCT116-HygTK master cells with the HPV 16 oncogene-encoding constructs and the Flp recombinase expression plasmid pCAGGS-Flpo-IRES-Puro obtained from Michael Hahn (DKFZ, Heidelberg). Replacement of the HygTK cassette resulted in the loss of both hygromycin B resistance and ganciclovir sensitivity. Thus, single clones were selected by treating the cells with ganciclovir as shown in Figure 14. Thereby, three different cell clones were established: HCT116-HPV 16 E6 and HCT116-HPV 16 E7 for the dox-inducible expression of HPV 16 E6 or E7 respectively, as well as HCT116-HPV 16 E6 and E7 for the dox-inducible expression of HPV 16 E6 and E7 in combination. In subsequent steps, the clones were characterized for their dox-inducible HPV 16 oncogene expression by RT-qPCR as well as Western blot analysis.

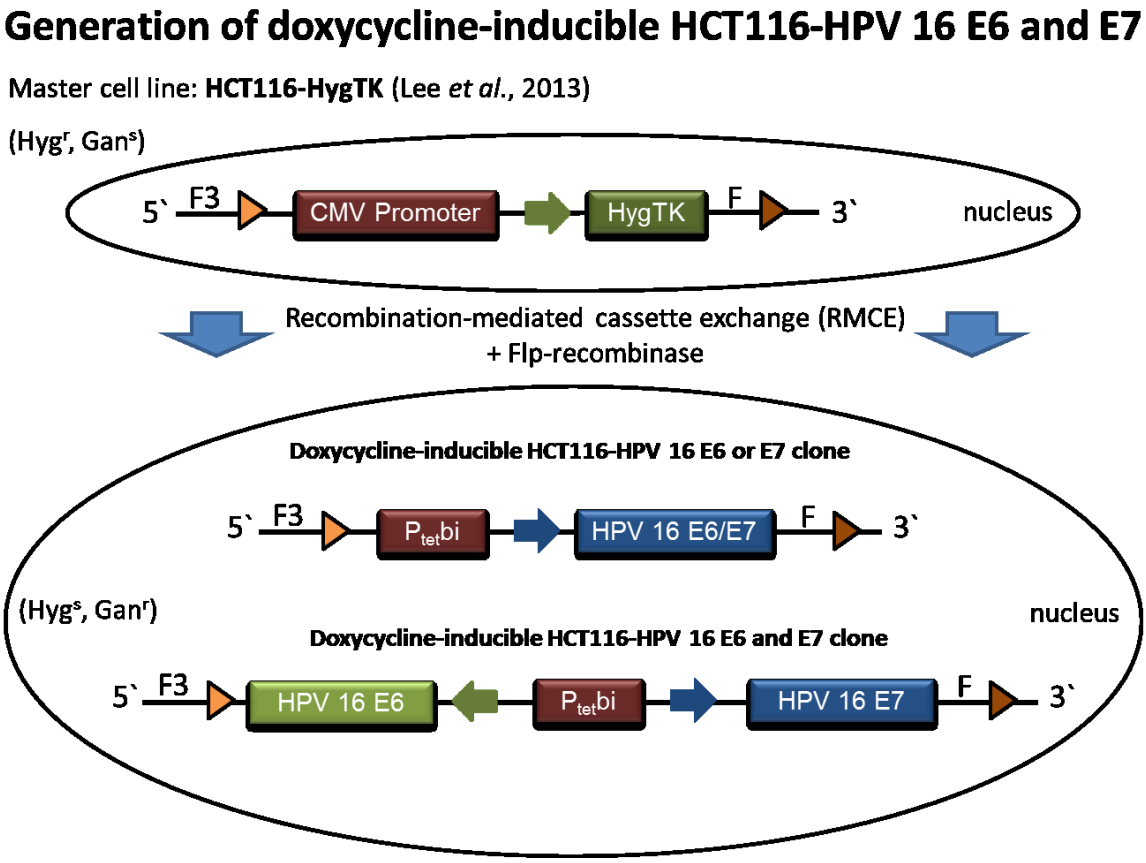

Figure 13: Generation of HCT116 clones for the dox-inducible expression of HPV 16 E6 and E7.
The master cell line HCT116-HygTK, which was obtained from (Lee *et al.* 2013) was used to generate HCT116 clones for the dox-inducible expression of HPV 16 E6 and E7. Therefore, Flp-recombinase-mediated cassette exchange was used to replace the HygTK expression cassette in the master cell line by constructs encoding HPV 16 E6 and/or E7 controlled by the bidirectional dox-inducible promoter P_{tet}bi. Thereby, three different HCT116 clones were generated for the dox-inducible expression of the HPV 16 oncogenes either individually or in combination. The clones, in which the expression cassettes were successfully replaced, were selected by treatment with ganciclovir.

3.2.2. Quantification of dox-inducible HPV 16 oncogene expression

Dox-inducible expression of the HPV 16 oncogenes in the generated HCT116 clones was analyzed on mRNA and protein level. The clones were treated with two different concentrations of dox (100 or 500 ng/mL) for 48 hours or nine days. As shown in Figure 15A, dox treatment of the HCT116-HPV 16 E6 clone resulted in 25- to 40-fold induction of HPV 16 E6 mRNA levels. Treatment of the HCT116-HPV 16 E7 clone led to an

increase in HPV 16 E7 mRNA levels of about 40 (48 hours) to almost 200-fold (nine days) compared to untreated cells. Induction of the expression of both HPV 16 oncogenes was observed after dox treatment of HCT116-HPV 16 E6 and E7 cells reaching from 91-fold (HPV 16 E6, 100 ng/mL dox for nine days) to 291-fold (HPV 16 E7, 500 ng/mL for 48 hours). As expected, HPV 16 oncogene expression tended to increase with elevated dox concentrations. The expressed HPV 16 E6 and E7 mRNA was subsequently sequenced reassuring the absence of mutations (Supplementary Figure 2).

After confirming the dox-inducible expression of HPV 16 E6 and E7 mRNA, Western blot analysis was performed to validate the translation into HPV 16 E6 and E7 proteins. Due to the lack of sensitive and selective HPV 16 E6 antibodies, p53 and p21 levels were monitored as indirect markers for the presence of HPV 16 E6 proteins. As shown in Figure 15B, p53 and p21 levels decreased in the HCT116-HPV 16 E6 clone and in the HCT116-HPV 16 E6 and E7 clone after dox treatment indicating the production of functional HPV 16 E6 proteins. Dox-dependent synthesis of HPV 16 E7 proteins was detected in the clones selected for HPV 16 E7 expression either individually or in combination with E6. In agreement with the mRNA expression data, increasing dox concentrations and prolonged treatment periods also resulted in elevated HPV 16 oncoprotein levels. Importantly, HPV 16 oncoproteins could neither be detected in the absence of dox nor in the dox-treated master cell line HCT116-HygTK indicating antibody specificity and excluding any significant leakiness of the expression system.

In the following step, activation and repression of the promoter was characterized in more detail by first adding dox and then removing it again from the growth medium. Information about how fast HPV 16 oncogene expression can be turned off after dox removal represent the basis to study whether E6- and E7-mediated effects might be reversible. For this, the generated clones were treated with dox for 48 hours. Afterwards, dox was removed from the growth medium and HPV 16 oncogene expression was quantified after six, 24, and 48 hours (Figure 16A). Consistent with previous results, dox treatment induced HPV 16 E6 and E7 mRNA and protein expression in all three clones (Figure 16B and C). After removing dox from the medium, the system was rapidly turned off as reflected by significant reduction of E6 and E7 mRNA levels already six hours

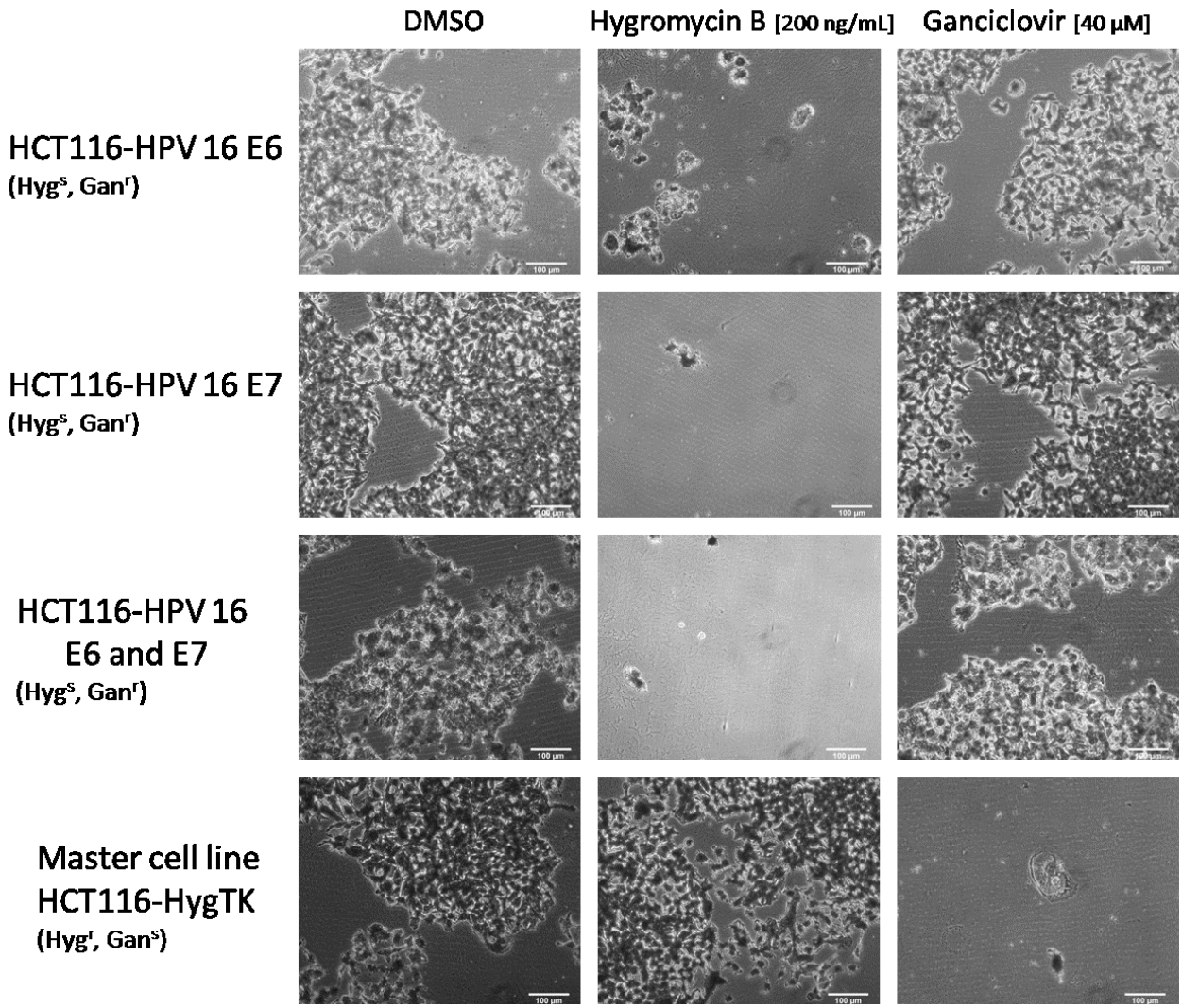

Figure 14: Treatment of HCT116 clones with hygromycin B and ganciclovir.
HCT116 clones generated for the inducible expression of HPV 16 oncogenes as well as the master cell line HCT116-HygTK were treated with DMSO (solvent control), 200 ng/mL hygromycin B or 40 µM ganciclovir to monitor the replacement of the HygTK expression cassette during the cloning process. Representative images are shown. The scale bars reflect 100 µm.

after dox removal. These results were also confirmed on protein level. As proteins possess longer half-lives than mRNA molecules and as the mRNA transcribed before dox removal is still translated into protein, the decline in HPV oncoprotein levels was slower than for HPV 16 E6 and E7 mRNA levels. However, 24 hours after dox removal no HPV 16 E6 or E7 proteins were detected by Western blot anymore.

Taken together, the generated HCT116 clones allow rapid and sustained expression of HPV 16 E6 and E7 either individually or in combination from a defined chromosomal locus after dox induction. Dox removal in return results in re-silencing of the promoter suggesting stringent HPV 16 oncogene expression only in the presence of dox. Therefore, the generated clones were used in subsequent analyses to study the effects of HPV 16 oncogene expression on proliferation, chromosomal stability, gene expression levels and DNA methylation patterns.

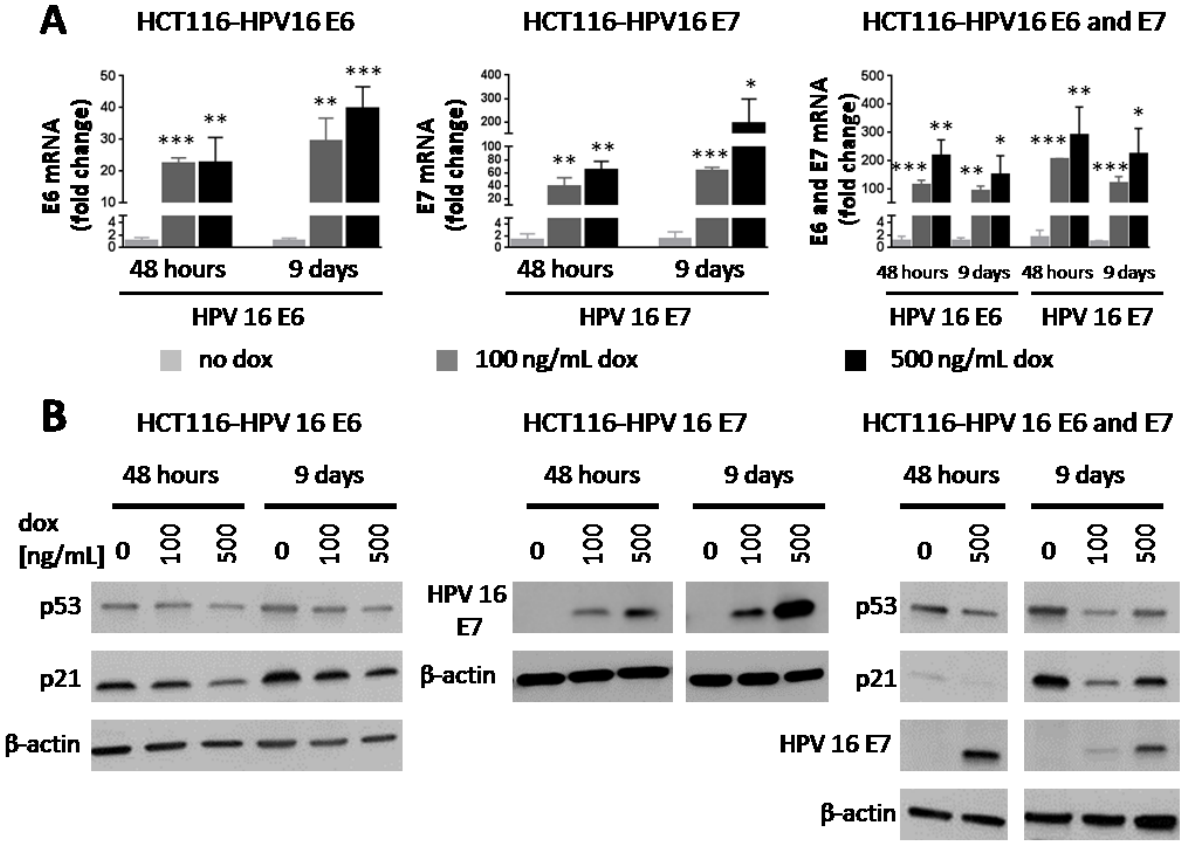

Figure 15: Quantification of inducible HPV 16 oncogene expression in HCT116-HPV 16 E6 and E7 clones.

(A) Inducible expression of HPV 16 E6 and E7 mRNA was monitored by RT-qPCR after treating the generated HCT116 clones with dox (100 or 500 ng/mL) for 48 hours or nine days. The diagrams show the mean HPV 16 E6 and E7 mRNA levels relative to those obtained in the untreated clone, respectively. The data are based on three independent treatments and the error bars represent the according standard deviation. Expression of β-actin mRNA was used as internal loading control. Student`s t-test was performed to calculate p values. *: $p<0.05$, **: $p<0.01$ and ***: $p<0.001$. **(B)** Production of HPV 16 oncoproteins was monitored by performing Western blot analysis. Due to the lack of potent HPV 16 E6 antibodies p53 and p21 protein levels were analyzed to indirectly confirm the presence of HPV 16 E6. β-actin was used as internal loading control.

3.2.3. Growth behavior of HCT116 clones after expressing HPV 16 oncogenes

In order to investigate whether induction of HPV 16 oncogene expression affects the growth behavior of the generated HCT116 clones, cell proliferation was indirectly quantified by measuring the DNA content. As shown in Figure 17, expression of HPV 16 E6 and E7 neither individually nor in combination substantially altered the proliferation of HCT116 cell clones during the measured time period ranging from six to 96 hours. After inducing the joint expression of HPV 16 E6 and E7 for 48 and 72 hours, proliferation slightly reduced compared to untreated cells. Despite being statistically significant the decrease in cell growth was only marginal and was not observed after 96 hours of HPV 16 oncogene induction anymore. To exclude that the dox concentrations used in this experiment had any effect on the proliferation of the clones, the growth behavior of the master cell clone HCT116-HygTK was also monitored. Comparing dox-treated with untreated master cells, two time points were significantly altered. However, the difference in proliferation was minor and was not detected after dox treatment for 72 and 96 hours.

Additionally, the growth behavior of the HCT116 clones after induction of HPV 16 oncogene expression was monitored microscopically using crystal violet cell staining. In agreement with the proliferation assay data, relevant differences in cell growth could not be observed after inducing the expression of HPV 16 E6 or E7 (Figure 17). These data suggest that neither dox treatment nor the induction of HPV 16 oncogene expression significantly affect the growth behavior of HCT116 clones during the analyzed time period. However, influences of the HPV 16 oncogenes on the proliferation rate after longer induction periods cannot be excluded.

3.2.4. Effects of HPV 16 E6 and E7 on chromosomal stability in HCT116 clones

As discussed in previous sections, the roles of both HPV 16 oncogenes in inducing chromosomal instability are well described for NHK cells as well as for cervical carcinoma cell lines (reviewed in (Korzeniewski *et al.* 2011)). Therefore, studying the effects of inducible HPV 16 E6 and E7 expression on chromosomal stability in the

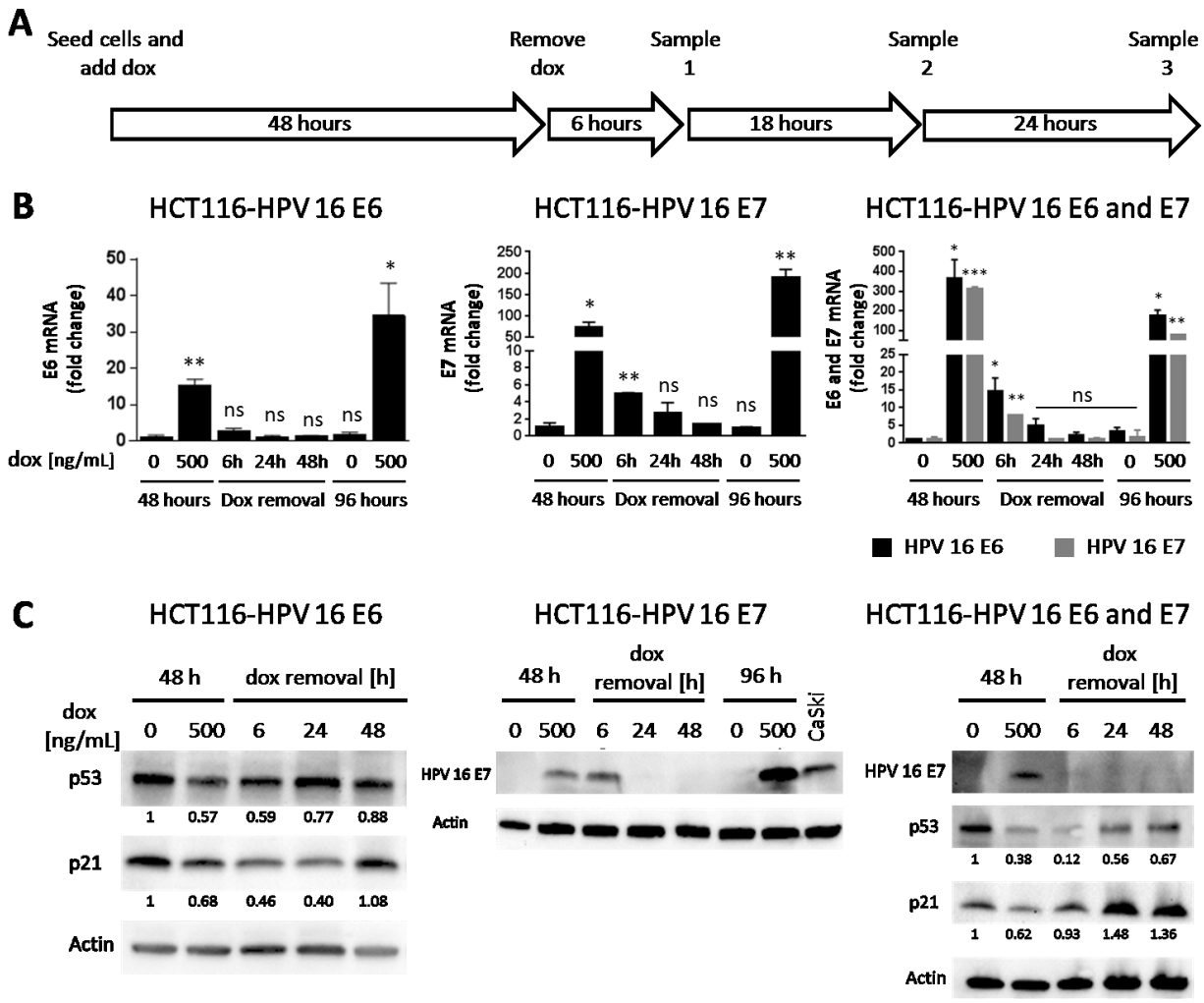

Figure 16: Characterization of inducibility of HPV 16 oncogene expression in the HCT116 clones. **(A)** The graphic illustrates the procedure of the experiment. First, HCT116 clones were seeded and HPV oncogene expression was then induced by treating the cells with 500 ng/mL dox for 48 hours. In the next step, dox was removed from the medium to prevent HPV oncogene expression. Afterwards, the cells were harvested six hours (Sample 1), 24 hours (Sample 2) and 48 hours (Sample 3) later. **(B)** Expression of HPV 16 E6 and E7 was quantified using qRT-PCR. The bars represent mean E6 and E7 mRNA levels of two independent experiments relative to the expression in untreated cells cultured for 48 hours. The according standard deviation is given by the error bars and Student`s t-test was used to determine p values. *: $p<0.05$; **: $p<0.01$; ***: $p<0.001$; ns: not significant. **(C)** Western blot was conducted to monitor the production of HPV 16 oncoproteins. Similar to Figure 15, p53 and p21 levels were used as indirect markers for the presence of HPV 16 E6. β-actin levels were detected as loading controls. The small numbers below the lanes indicate the fold changes of the densiometric quantification relative to the detected levels in not-induced cells.

generated HCT116 clones was used on the one hand to validate the biological relevance of the established model system and on the other hand to gain a more detailed picture about how and when these effects are induced.

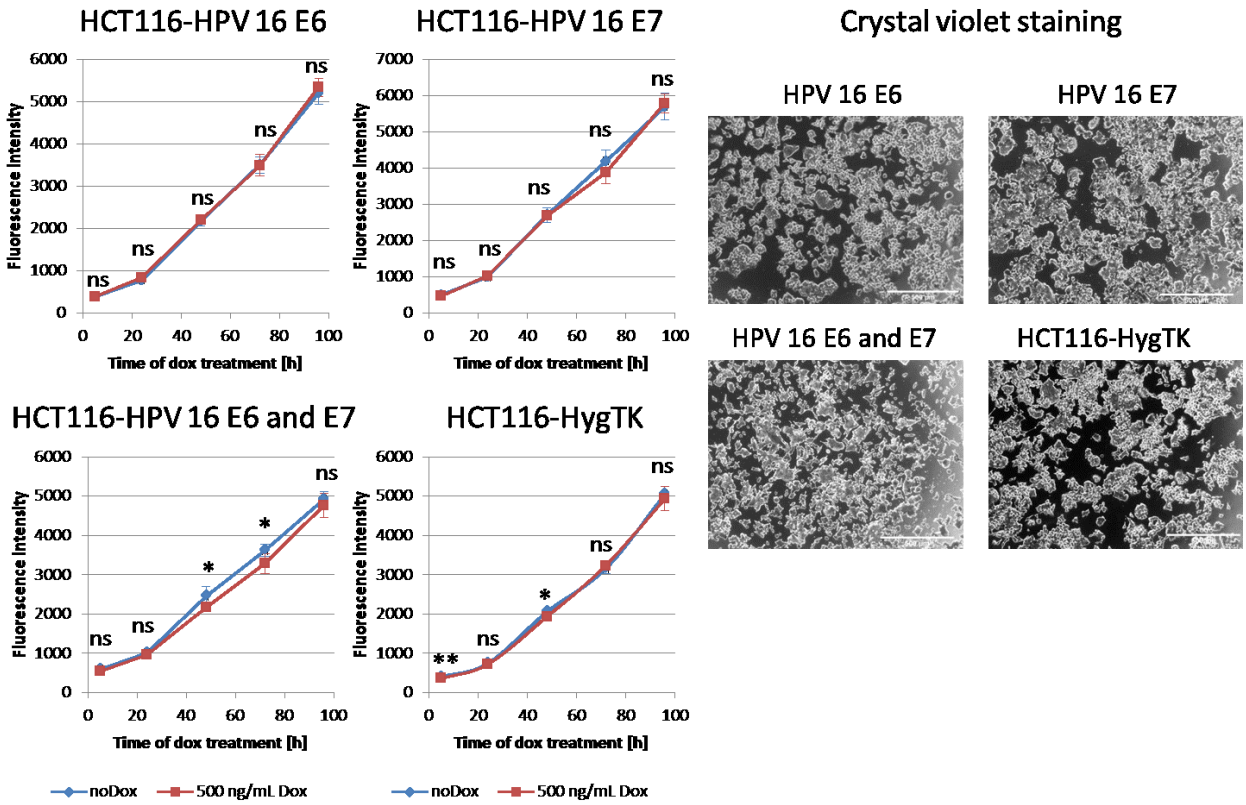

Figure 17: Proliferation of dox-inducible HCT116-HPV 16 E6 and E7 clones.
The proliferation of HPV 16 E6- and E7-expressing HCT116 clones was monitored by quantifying the DNA content. The diagrams show the mean proliferation levels of at least three independent experiments after treatment with 500 ng/mL dox for six, 24, 48, 72 and 96 hours. The according standard deviation is represented by the error bars and Student`s t-test was performed to calculate p values using untreated cells as a reference control. *: $p<0.05$, **: $p<0.01$ and ns: not significant. For the cell staining using crystal violet, the cells were treated for 96 hours with 500 ng/mL dox and then stained as described in the respective chapter in the methods section. Representative images are shown. The scale bar has a size of 500 µm.

3.2.4.1. Centrosome duplication and mitotic progression

Centrosomes are the main microtubule forming organelles in the cells and therefore play an important role in regulating bipolar mitosis and chromosomal segregation. During S phase of the cell cycle the centrosome duplicates exactly once facilitating the formation of two spindle poles during mitosis. Centrosome duplication is tightly regulated and coupled to DNA replication. However, DNA and centrosome replication are frequently deregulated in cancer cells resulting in structural and numerical centrosomal aberrations. During subsequent mitosis these cells tend to form abnormal spindle poles

that may lead to the generation of aneuploid daughter cells. Due to chromosomal damage most of the progeny cells are assumed to be unable to undergo subsequent cell divisions. Permanent mitotic errors may, however, promote high levels of genetic variations potentially increasing the risk for the generation of cells that are capable to divide and to produce viable offspring. Thereby, genomic and chromosomal instability continuously contribute to the generation and potential outgrowth of highly proliferative subclones, a common characteristic of several tumor types (reviewed in (Holland & Cleveland 2009, McGranahan *et al.* 2012)).

Previous studies showed that stable as well as transient expression of HPV 16 E6 and E7 in NHKs elevated the number of centrosomes in interphase cells leading to abnormal spindle pole formation during mitosis (Duensing *et al.* 2000). The aim of the present study was to investigate these effects in more detail by analyzing centrosome numbers and spindle pole formation after HPV 16 oncogene induction in the generated HCT116 clones. Using a dox-inducible expression system enables evaluation of centrosome numbers and spindle pole formation during a defined time period of HPV 16 E6 and E7 expression. Therefore, HPV 16 oncogene expression was induced for 48 hours and nine days reflecting about two and ten cell cycles, respectively. Afterwards, the cells were fixed and centrosomes as well as spindle poles were stained using antibodies targeting the pericentriolar marker γ-tubulin.

Induction of HPV 16 E6 expression led to a moderate increase in the proportion of interphase cells containing more than two centrosomes (Figure 18). Similar results were observed after inducing the expression of HPV 16 E7. Dox treatment of the HCT116-HPV 16 E7 clone raised the number of cells containing abnormal centrosomes from less than 2% in the untreated cell population to 5-6%. The percentage of interphase cells containing aberrant centrosomes again increased about 3-4% after expressing both HPV 16 oncogenes. As expected, increasing the concentrations of dox not only resulted in higher HPV 16 E6 and E7 expression levels, as shown in previous chapters, but also tended to elevate the percentage of cells carrying abnormal centrosome numbers. This effect was already observed after 48 hours of dox treatment. Extending the treatment period to nine days was, however, not found to further increase the level of cells containing aberrant centrosome numbers. Treatment of the parental clone HCT116-

HygTK did not cause elevated numbers of cells carrying aberrant centrosomes, thereby excluding any dox-related effects.

In the next experiment it was investigated whether the observed modest increase in cells containing aberrant centrosome numbers would also result in an increase in cells forming abnormal spindle poles during mitosis. Therefore, spindle pole formation was analyzed after inducing HPV 16 oncogene expression. As shown in Figure 19, the number of cells forming aberrant spindle poles tended to increase moderately after inducing the expression of HPV 16 oncogenes. In accordance with the evaluation of

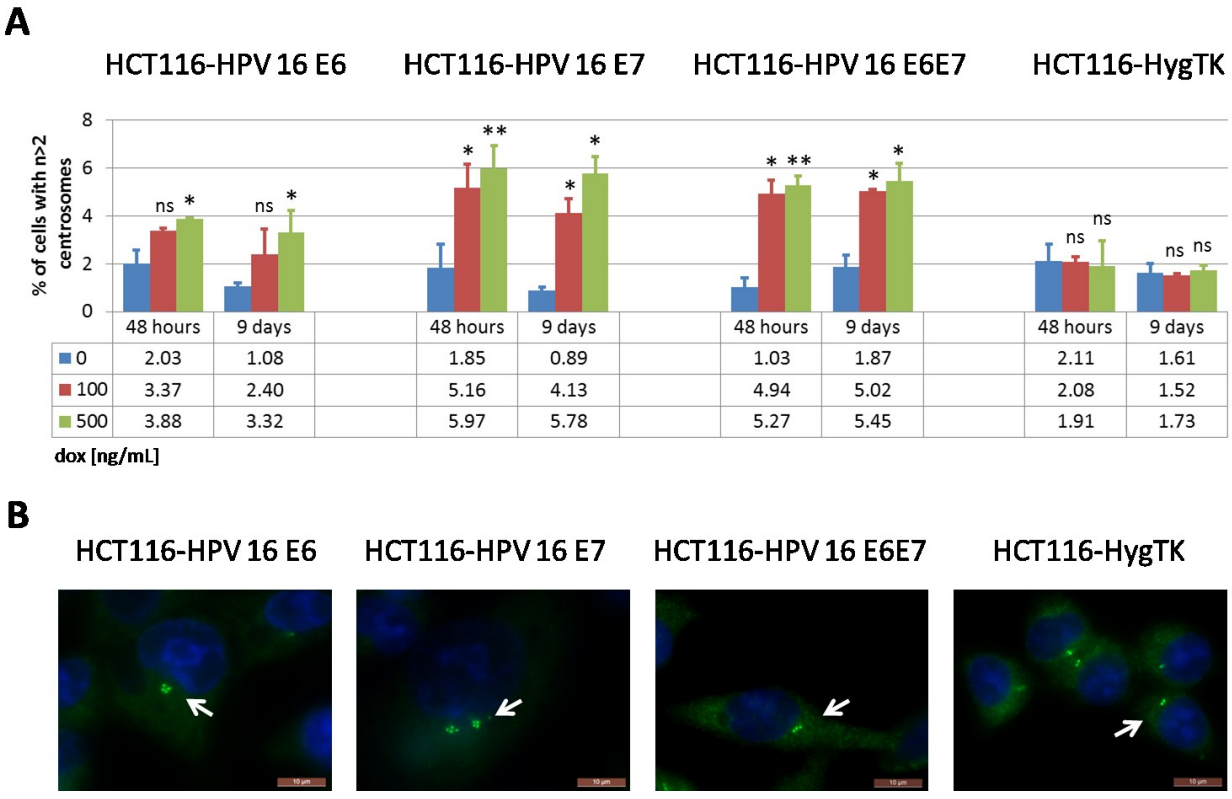

dox [ng/mL]	HCT116-HPV 16 E6		HCT116-HPV 16 E7		HCT116-HPV 16 E6E7		HCT116-HygTK	
	48 hours	9 days	48 hours	9 days	48 hours	9 days	48 hours	9 days
0	2.03	1.08	1.85	0.89	1.03	1.87	2.11	1.61
100	3.37	2.40	5.16	4.13	4.94	5.02	2.08	1.52
500	3.88	3.32	5.97	5.78	5.27	5.45	1.91	1.73

Figure 18: Quantification of abnormal centrosome numbers in HCT116 clones upon expression of HPV 16 oncogenes.
(A) Centrosomes were visualized by staining the pericentriolar marker γ-tubulin in the generated HCT116 clones induced for HPV 16 oncogene expression using either 100 or 500 ng/mL dox for 48 hours or nine days. The diagram shows the mean percentage of cells with more than two centrosomes of at least two independent experiments. The standard deviation is indicated by the error bars and Student`s t-test was performed to calculate p values using the respective untreated HCT116 clone as reference control. *: $p<0.05$, **: $p<0.01$ and ns: not significant. **(B)** The presented microscope images show examples of cells of the respective HCT116 clone containing different numbers of centrosomes after induced HPV 16 oncogene expression (as indicated by the white arrows). To visualize centrosomes the pericentriolar marker γ-tubulin was immunofluorescently labeled. The included scale bars reflect 10 µm.

centrosome numbers, this effect was already observed after 48 hours of oncogene induction and was again not further enhanced after extending the oncogene induction period to nine days. Dox treatment of the parental control cells had no significant effect on spindle pole formation.

To conclude, the level of abnormal centrosome duplication and aberrant spindle pole formation in untreated HCT116 cells is low making these cells a suitable model system to study the effects of HPV 16 oncogene expression. Induction of both oncogenes in the generated HCT116 clones moderately increases the number of cells containing abnormal centrosomes. These cells might then form aberrant spindle poles when entering mitosis as reflected by the slightly elevated number of multipolar spindles after induction of HPV 16 oncogene expression.

3.2.4.2. DNA damage in HPV 16 E6- and E7-expressing HCT116 clones

High levels of replicative stress as typically observed in proliferating tumor cells promotes the formation of DNA single- and double-strand breaks during S phase of the cell cycle (reviewed in (Hills & Diffley 2014)). Especially DSBs can significantly compromise chromosomal segregation and successful completion of mitosis. Therefore, cell cycle checkpoints have evolved to arrest cell cycle progression before entering mitosis, which allows the activation of DNA damage repair factors. Deregulated expression of the HPV 16 oncoproteins was, however, shown to impair cell cycle checkpoints as well as DNA damage response pathways in NHK cells resulting in increased levels of DNA breakages (Duensing & Munger 2002, White *et al.* 1994). To further study the effects of HPV 16 oncogene expression on DNA damage rates and to understand how fast DNA damage might occur, formation of DSBs was analyzed in HPV 16 E6- and E7-expressing HCT116 clones.

Formation of DSBs was monitored by immunofluorescent staining of histone H2AX phosphorylated at serine 139 (γH2AX). This histone component is rapidly phosphorylated after the induction of DSBs and is involved in the recruitment and activation of DNA damage response factors (Paull *et al.* 2000, Rogakou *et al.* 1998).

After inducing the expression of HPV 16 E6 the number of DNA-damaged cells, which was defined as containing more than three γH2AX foci, slightly increased from about 40% in untreated cells to 45-50% in the dox-treated cells (Figure 20). Expression of HPV 16 E7 also resulted in a moderate increase in DNA-damaged cells from 38% in untreated cells up to 50% after dox treatment. Similar effects were detected after inducing the combined expression of both HPV 16 oncogenes. In all tested HCT116 clones the increase in DSBs was already observed after 48 hours of dox treatment. Extending the treatment duration to nine days seemed to only result in slightly higher

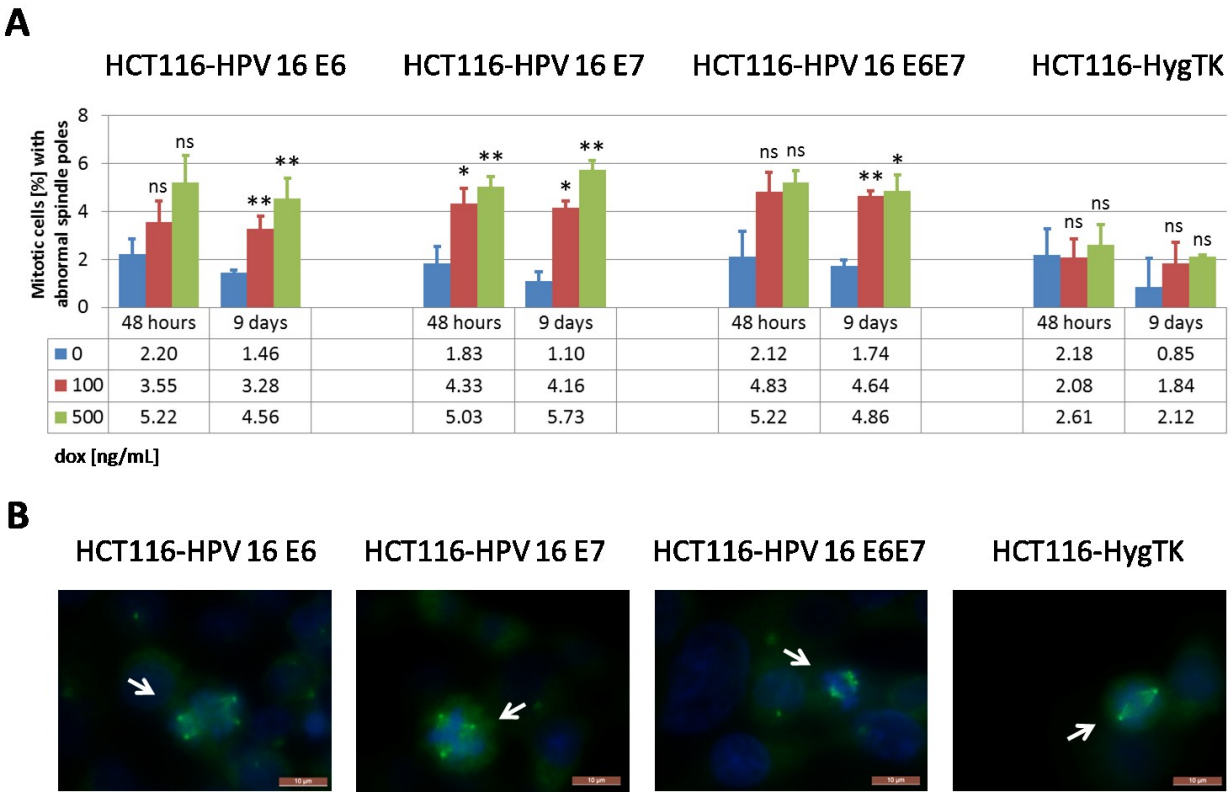

dox [ng/mL]	HCT116-HPV 16 E6		HCT116-HPV 16 E7		HCT116-HPV 16 E6E7		HCT116-HygTK	
	48 hours	9 days	48 hours	9 days	48 hours	9 days	48 hours	9 days
0	2.20	1.46	1.83	1.10	2.12	1.74	2.18	0.85
100	3.55	3.28	4.33	4.16	4.83	4.64	2.08	1.84
500	5.22	4.56	5.03	5.73	5.22	4.86	2.61	2.12

Figure 19: Analysis of spindle pole formation during mitosis in HPV 16 oncogene-expressing HCT116 clones.
(A) The formation of spindle poles during mitosis was monitored by immunofluorescent staining of γ-tubulin in HCT116-HPV 16 E6 and/or E7 clones after treatment with 100 or 500 ng/mL dox for 48 hours or nine days. The bars shown in the diagram represent the mean percentage of cell forming abnormal spindle poles based on at least biological duplicates. Cells forming either one or more than two spindles during mitosis were classified as abnormal. The error bars indicate the according standard deviation and p values were calculated by Student`s t-test using the respective untreated clone as a reference. *: $p<0.05$, **: $p<0.01$ and ns: not significant. **(B)** The images give examples for cells of the respective HCT116 clone forming multipolar, tripolar, pseudo bipolar and normal bipolar spindles during mitosis (highlighted by the white arrow). Spindle poles were visualized by immunofluorescent staining for γ-tubulin. The scale bars represent 10 µm.

levels of DNA-damaged cells. In contrast, the number of DNA-damaged cells remained unchanged when treating parental HCT116-HygTK cells excluding any dox-dependent effects on DSB formation. The presented data suggest that HPV 16 E6 but predominantly E7 might affect the formation of DSBs in HCT116 clones potentially compromising the genomic integrity of the cells.

3.2.4.3. Quantification of aneuploid cells after HPV 16 oncogene expression

Chromosomal missegregation and high levels of DNA damage during cell division promote the generation of aneuploid daughter cells. To detect those cells the DNA content of the HCT116 clones was quantified after HPV 16 oncogene induction by propidium iodide (PI) staining and subsequent flow cytometry. Thereby, the current cell cycle phase could be determined. Cells containing more chromosomal material than the cells in G_2/M phase were defined as aneuploid.

Induction of HPV 16 E6 expression for 48 hours did not affect the number of aneuploid cells. However, extending the treatment to nine days resulted in slightly elevated levels of aneuploidy (Figure 21). Stronger effects were observed after inducing the expression of HPV 16 E7 in the HCT116-HPV 16 E7 clone. Already 48 hours of E7 induction were sufficient to increase the number of aneuploid cells from 5% in untreated cells up to 10% after dox treatment. Similar effects were also detected after extending HPV 16 E7 expression to nine days. Expression of both HPV 16 oncogenes for 48 hours was, however, not found to dramatically affect aneuploidy in the HCT116-HPV 16 E6 and E7 clone, whereas extension of the E6 and E7 expression to nine days resulted in a modest but significant increase in the number of aneuploid cells. Irrespective of the dox treatment extended cultivation periods seemed to elevate the number of aneuploid cells. To exclude any dox-related effects aneuploidy was also quantified in the parental HCT116-HygTK cells identifying no significant changes.

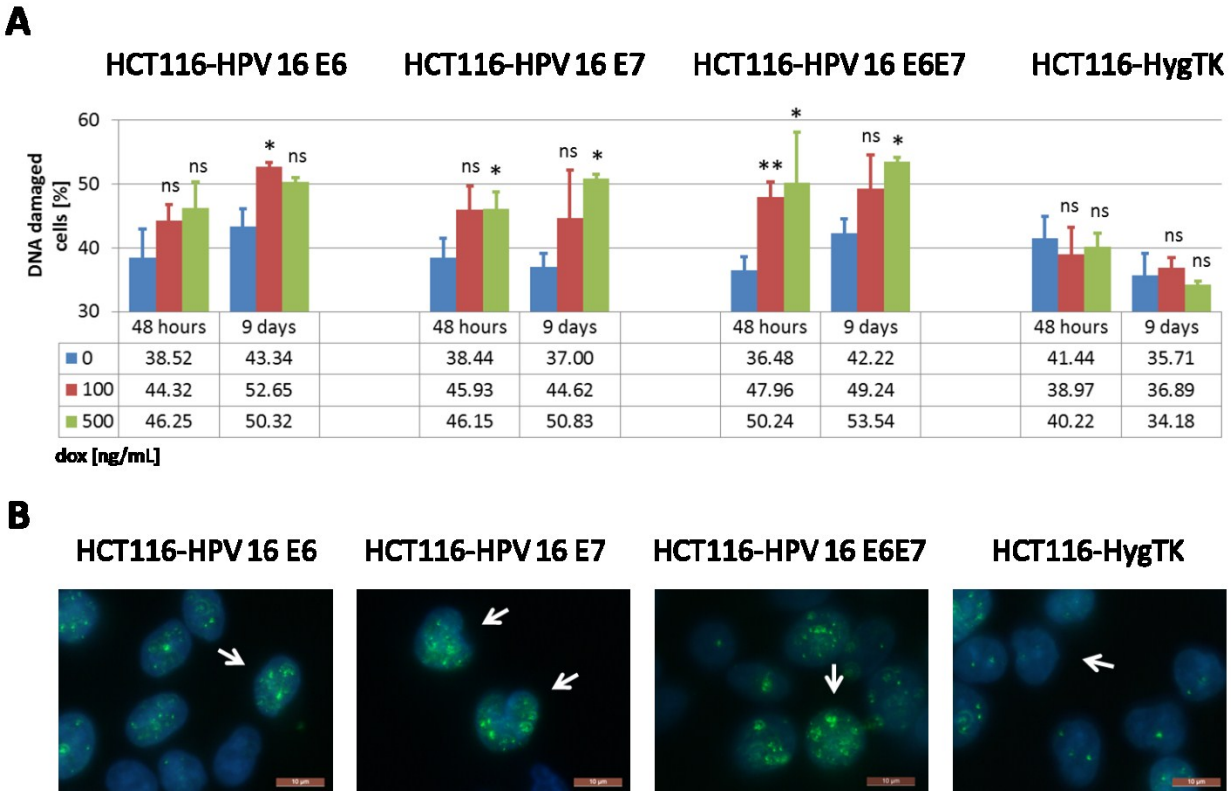

Figure 20: Analysis of DNA double-strand breaks in HPV 16 oncogene-expressing HCT116 clones. **(A)** Phosphorylation of the histone component γH2AX was used as a marker for the induction of DSBs in the generated HCT116 clones. DSBs were analyzed by counting immunofluorescently labeled γH2AX foci. Cells showing more than three foci were considered as DNA damaged. The analysis was performed after inducing HPV 16 oncogene expression for 48 hours or nine days in the indicated clones by treating the cells either with 100 or 500 ng/mL dox. The bars in the diagrams show the mean percentage of DNA damaged cells from at least two independent experiments. The standard deviation is indicated by the error bars and Student`s t-test was performed to calculate p values using untreated cells of the respective clone as reference control. *: $p<0.05$, **: $p<0.01$ and ns: not significant. **(B)** The microscope images show cells containing different levels of DNA damage (as highlighted by the white arrows). Phosphorylated γH2AX was immunofluorescently stained after induction of HPV 16 oncogene expression as described in (A). The scale bars reflect 10 µm.

Based on these data it can be concluded that the moderate increase in abnormal spindle pole formation during mitosis as well as the slight elevation in DNA damage rates after expression of HPV 16 oncogenes may promote the generation of aneuploid cells. Extended cultivation as well as prolonged oncogene induction were found to enhance this effect potentially due to the elevated number of cell cycle phases.

3.2.4.4. Genomic copy number variations after HPV 16 oncogene expression

Chromosomal missegregation during mitosis in combination with high levels of DNA damage might not only increase the number of aneuploid cells but also the frequency of genomic copy number variations (CNVs). To detect CNVs in HCT116 clones in response to HPV 16 oncogene expression, isolated and bisulfite converted DNA was hybridized to Infinium® MethylationEPIC BeadChips (Illumina), which were designed to assess the methylation status of about 850,000 CpG sites in the genome. For this purpose, the array detects methylated as well as unmethylated DNA copies, which allows quantification of the methylation level at genomic loci and also provides information about the copy number of the respective genomic region (Feber *et al.* 2014). Bisulfite treatment of the isolated DNA and subsequent hybridization to the arrays was performed at the DKFZ Genomics and Proteomics Core Facility. Raw data retrieval and subsequent processing was conducted in cooperation with colleagues from the Neuropathology Department, who had previously developed a CNV analysis pipeline that resulted in numerous publications (Sahm *et al.* 2017) (Herrlinger *et al.* 2016).

Pairwise comparison of CNV profiles between dox-treated and untreated HCT116 clones did not reveal substantial alterations that would reflect gains or losses of whole chromosomes or chromosomal arms (Figure 22). In the next step, the CNV profiles were analyzed in more detail by specifically focusing on chromosomal regions that have previously been described to be frequently gained or lost during HPV-driven cervical carcinogenesis, respectively. In HPV 16-transformed cervical carcinomas the following DNA copy number alterations have been reported: gain at chromosome 3q (rate 0.84), gain at chromosome 1q (rate 0.54), gain at chromosome 5p (rate 0.38), loss at chromosome 3p (rate 0.32) and loss at chromosome 11q (rate 0.3) (Steenbergen *et al.* 2014, Thomas *et al.* 2014). Induction of HPV 16 oncogene expression in the generated HCT116 clones could, however, not be correlated with gains or losses of any of these chromosomal arms.

The observed discrepancy might be the result of different factors complicating direct comparison between the published data and the results generated in the present study. First, specific hotspots of CNVs might only be detectable after analyzing additional biological replicates increasing the probability to identify enriched or lost chromosomal sites. Additionally, discrepancies might be the result of differences in the methods used to detect CNVs, as most of the published studies use either classical comparative genome hybridization (CGH) to karyotypically normal metaphase chromosomes or array-based CGH platforms. Finally, in the present study CNV profile analysis was performed after nine days of HPV 16 oncogene induction reflecting a rather short period of E6 and E7 expression as most cervical cancers evolve over several years or even decades.

Taken together, CNV profile analysis in HCT116 clones after induction of HPV 16 oncogene expression did not reveal any hotspots of DNA CNVs that specifically occurred in a sufficient number of cells to be detectable using Infinium® MethylationEPIC BeadChips (Illumina). The resolution for the detection of CNVs might be increased by selecting single clones after inducing HPV 16 oncogene expression for a defined time period. Thereby, cells containing identical CNVs might become enriched increasing the likelihood for their detection.

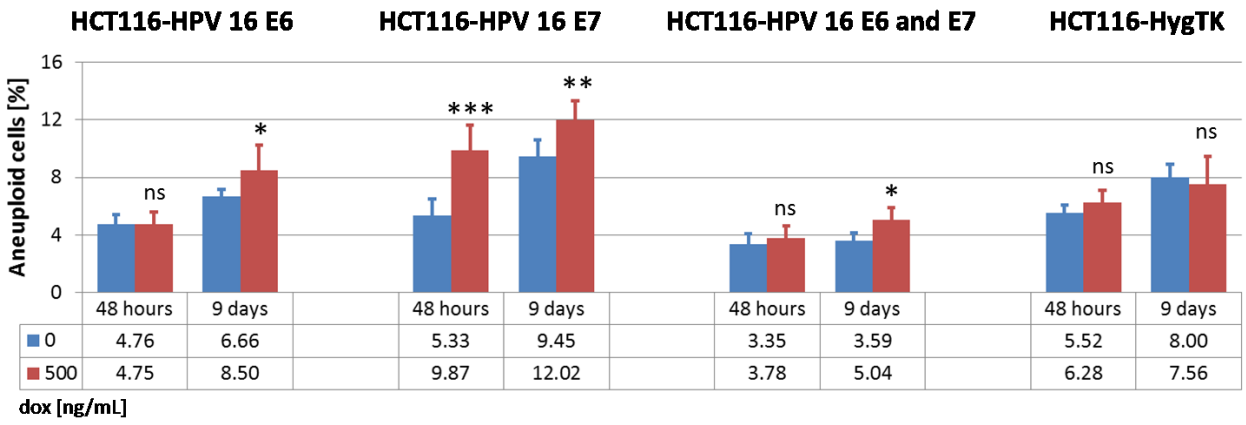

	HCT116-HPV 16 E6		HCT116-HPV 16 E7		HCT116-HPV 16 E6 and E7		HCT116-HygTK	
	48 hours	9 days	48 hours	9 days	48 hours	9 days	48 hours	9 days
0	4.76	6.66	5.33	9.45	3.35	3.59	5.52	8.00
500	4.75	8.50	9.87	12.02	3.78	5.04	6.28	7.56

Figure 21: Number of aneuploid HCT116 cells after induction of HPV 16 E6 and E7 expression.
The number of aneuploid cells was determined by performing flow cytometry of propidium iodide stained HCT116 clones after inducing HPV 16 oncogene expression for 48 hours or nine days. The results are presented as mean values based on at least five biological replicates. Error bars indicate the according standard deviation and p values were calculated by performing Student`s t-test using the respective untreated HCT116 clone as a reference control. *: $p<0.05$, **: $p<0.01$, ***: $p<0.001$ and ns: not significant.

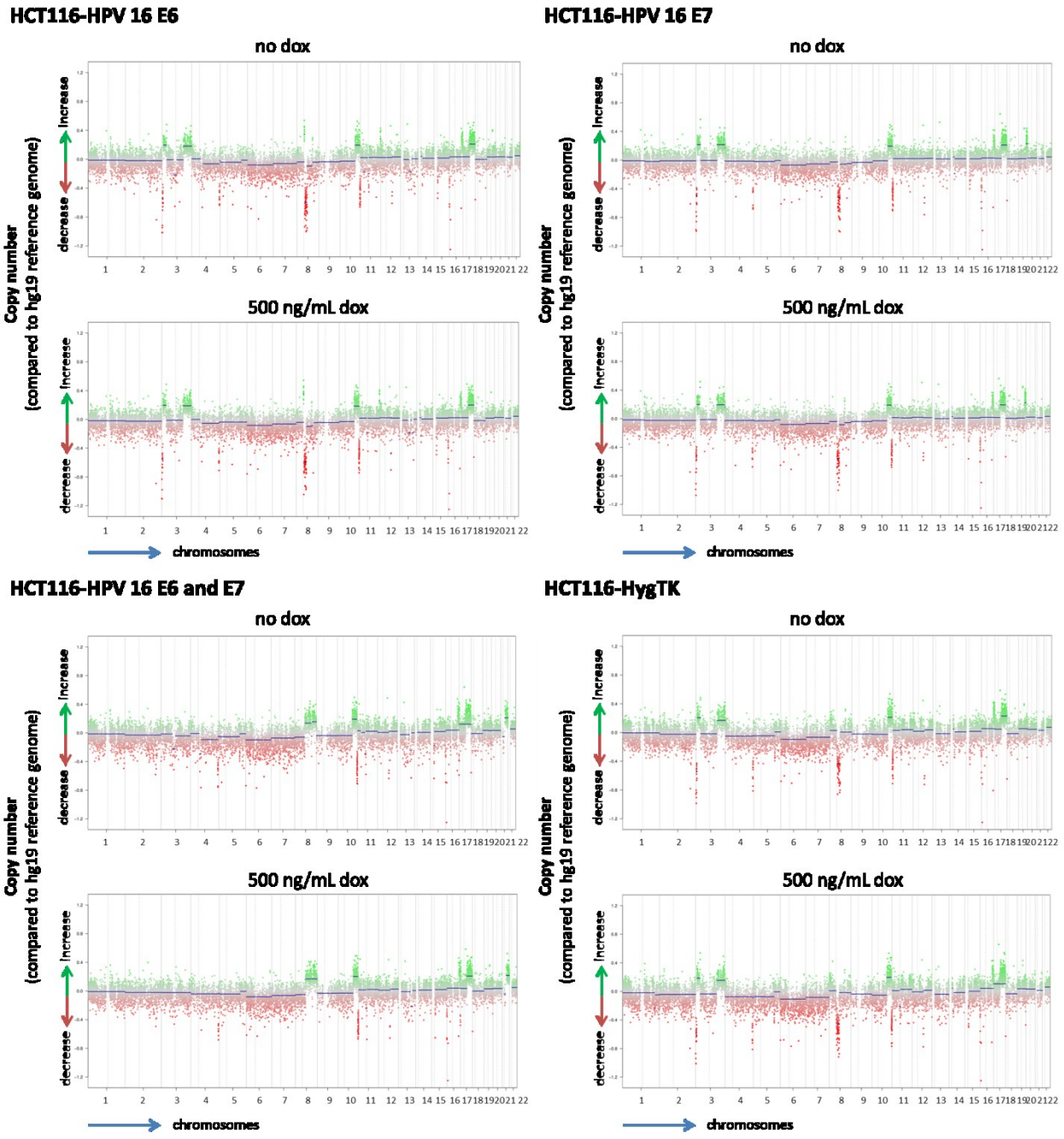

Figure 22: Copy number variation profiles of HPV 16 oncogene-expressing HCT116 clones
The effects of HPV 16 oncogene expression on copy number variations in HCT116 clones was analyzed by hybridizing bisulfite converted DNA to Infinium MethylationEPIC BeadChips (Illumina). Therefore, the respective HCT116 clone was cultured for nine days either without treatment or in the presence of 500 ng/mL dox. The conducted microarray analysis allows the quantification of copy numbers in about 850,000 genomic sites. Gains (green) and losses (red) of copies of the respective genomic sites were calculated relative to the hg19 reference genome.

3.2.5. Differential gene expression upon HPV 16 oncogene induction

In order to evaluate whether HPV 16 oncogene induction affects gene expression in HCT116 clones whole transcriptome analysis was performed using Illumina HumanHT-12 microarrays. Therefore, HPV 16 oncogene expression was induced for 48 hours and total RNA was isolated. Hybridization to the array as well as subsequent data processing was performed in cooperation with the DKFZ Genomics and Proteomics Core Facility.

Expression of the vast majority of about 31,000 tested genes remained unchanged, while a subset of genes was found to be differentially expressed following HPV 16 E6 and/or E7 induction. In particular, expression of HPV 16 E6 led to the upregulation of 512 genes, whereas 273 genes were found to be downregulated ($p<0.01$) (Benjamini & Hochberg 1995). 48 hours induction of the HCT116-HPV 16 E7 clone resulted in elevated expression levels of 161 genes and reduced expression of 63 genes. After activating both HPV 16 oncogenes 1575 genes appeared to be upregulated, whereas 1900 genes were found downregulated. Dox treatment of the parental clone HCT116-HygTK led to the upregulation of 455 genes and downregulation of 748 genes suggesting that the list of genes regulated by HPV 16 E6 and/or E7 might contain a number of false positive genes.

Therefore, the most differentially expressed candidate genes were validated by RT-qPCR. As shown in Table 4, upregulation of Kruppel-like factor 11 (KLF11) and Chemokine-like factor (CKLF) as well as downregulation of CDKN1A after induction of HPV 16 E6 expression could be confirmed. KLF11 functions as transcription factor for genes involved in the regulation of cell growth and apoptosis (Lomberk & Urrutia 2005), whereas CKLF is assumed to play a role in regulating proliferation (Tan *et al.* 2015). Reduced expression of CDKN1A, which encodes the protein p21, can be explained as a consequence of E6-mediated degradation of p53, which acts as transcription factor for CDKN1A.

In conclusion, expression of HPV 16 oncogenes seems to affect mRNA transcription of a panel of genes. Some of these candidate genes were validated by performing RT-qPCR. However, not all of the candidate genes obtained by Illumina HumanHT-12 microarray analysis could be confirmed suggesting that there might be a number of false positive

Table 4: RT-qPCR validation of differentially expressed genes identified by using Illumina HumanHT-12 microarrays upon HPV 16 oncogene expression.
To confirm the data retrieved from Illumina HumanHT-12 gene expression analysis, the mRNA levels of a panel of differentially expressed genes were measured using RT-qPCR. The table lists the fold changes of mRNA expression levels of the respective HCT116 clone comparing dox-treated [500 ng/mL] and untreated conditions after culturing for 48 hours. For direct comparison between the two assays the fold changes obtained by microarray analysis are also given. The listed fold changes represent mean values from at least three independent experiments. Student`s t-test was used to calculate p values. *: $p<0.05$, **: $p<0.01$, ***: $p<0.001$.

Gene	HCT116-							
	HPV 16 E6		HPV 16 E7		HPV 16 E6 and E7		HygTK	
	array	qPCR	array	qPCR	array	qPCR	array	qPCR
KLF11	1.53***	5.53*	1.08	1.06	2.12***	5.49**	0.99	1.08
PKM2	0.75***	0.78	0.99	0.88	0.88*	1.36	0.92	0.88
BLOC1S1	0.68**	1.13	1.01	1.51	0.99	1.77	0.91	1.19
VSNL1	0.95	1.16	0.73***	0.65	0.89	1.01	0.92	0.83
CKLF	1.23***	1.81	1.04	2.14	2.42***	4.15*	1.15***	1.00
PLK2	0.98	0.82	0.89	1.04	0.61***	1.31	0.92	0.98
CDKN1A	0.89*	0.75	0.90	1.18	0.62***	0.60*	0.95	1.01
TP53I3	0.83***	1.26	1.05	1.18	0.71***	1.02	1.07	1.15
PERP	0.94	0.94	1.10	1.16	0.72***	1.06	1.08	0.96
TP53INP1	0.99	0.74	0.96	1.19	0.77***	0.72	0.99	0.82

candidates. Therefore, the microarray data need to be interpreted carefully and should be further validated by using additional methods.

3.2.6. Effects of HPV 16 oncogenes on DNA methylation levels

As discussed in previous chapters, alterations in the methylation pattern seem to play an important role during HPV-mediated host cell transformation. These alterations not only occur in the viral, but also in the host cell genome. Several tumor suppressor genes have been shown to become transcriptionally silenced by hypermethylation during cervical carcinogenesis including E-cadherin (CDH1), Cell Adhesion Molecule 1 (CADM1) and Death-Associated Protein Kinase 1 (DAPK1) (Bierkens *et al.* 2013, Henken *et al.* 2007, Kalantari *et al.* 2014, Laurson *et al.* 2010, Narayan *et al.* 2003). Moreover, both HPV 16 oncoproteins seem to affect CpG methylation levels, as HPV 16 E6 was reported to indirectly upregulate DNMT1 transcription by targeting the

transcriptional suppressor p53 (Au Yeung *et al.* 2010). Additionally, HPV 16 E7 has been found to directly bind and activate DNMT1 (Burgers *et al.* 2007). Recently, it was also shown that shRNA knock down of HPV 16 E6 and E7 in SiHa and CaSki cells downregulates the expression of DNA methyltransferases resulting in elevated expression levels of a panel of tumor suppressor genes (Li *et al.* 2015). These findings suggest that the overexpression of the HPV 16 oncogenes might contribute to the observed increase in methylation levels during HPV-induced carcinogenesis.

The present study used Infinium® MethylationEPIC BeadChips (Illumina) to analyze the effects of HPV 16 oncogene expression on the methylation level in HCT116 clones. Thereby, CpG methylation at about 850,000 sites located in CpG islands, promoter and enhancer regions as well as in gene bodies was quantified. To investigate whether HPV 16 E6 and E7 expression would have an effect on global methylation levels, mean beta values of all CpGs located in promoter regions as well as gene bodies were calculated. In all tested HCT116 clones the mean methylation levels ranged between 46% and 48% (Figure 23). Neither 48 hours nor nine days of HPV 16 oncogene induction were found to dramatically affect the mean methylation levels suggesting that E6 as well as E7 had only minor effects on the global methylation pattern.

Despite being globally unchanged, the methylation pattern in specific genes might be substantially altered. Therefore, all genes containing at least three CpG sites in their promoter or in the gene body that showed more than 5% difference in their methylation level after HPV 16 oncogene expression were identified. After induction of HPV 16 E6 expression for 48 hours the methylation of eight genes increased whereas ten genes showed decreased methylation levels. Extending the HPV 16 E6 expression to nine days resulted in elevated CpG methylation in eleven genes and reduced methylation in 17 genes. 48 hours of HPV 16 E7 expression led to increased methylation in 39 genes and decreased levels in 77 genes, whereas induction of HPV 16 E7 for nine days only resulted in ten genes that showed elevated methylation levels and in twelve genes with lower methylation levels. After expressing both HPV 16 oncogenes raised methylation levels were identified in eleven genes after 48 hours and in 17 genes after nine days, whereas methylation was reduced in nine genes after 48 hours and in 15 genes after nine days.

Alterations in gene methylation levels mediated either by HPV 16 E6 or E7 should be detectable in the respective clone expressing E6 or E7 individually as well as in the clone expressing both oncogenes in combination. One of the candidate genes fulfilling this criterion was keratin 38. CpG methylation in the keratin 38 gene was found to increase after induction of HPV 16 E6 expression for nine days either individually or in combination with E7. Other candidates might be Olfactory Receptor Family 5 Subfamily D Member 16 (OR5D16) and Protein Kinase C Alpha Antisense RNA 1 (PRKCA-AS1). Expression of both HPV 16 oncogenes either individually or in combination resulted in elevated methylation levels in the OR5D16 gene and in reduced levels in the PRKCA-AS1 gene. Hypermethylation of the tumor suppressor genes, which have been reported during cervical carcinogenesis in previous studies, could not be detected in the present analysis. However, the analyzed data are only based on a single biological sample per treatment condition and therefore need to be further validated. Additionally, the HPV 16 E6 and E7 induction period of 48 hours or nine days might not be long enough to select

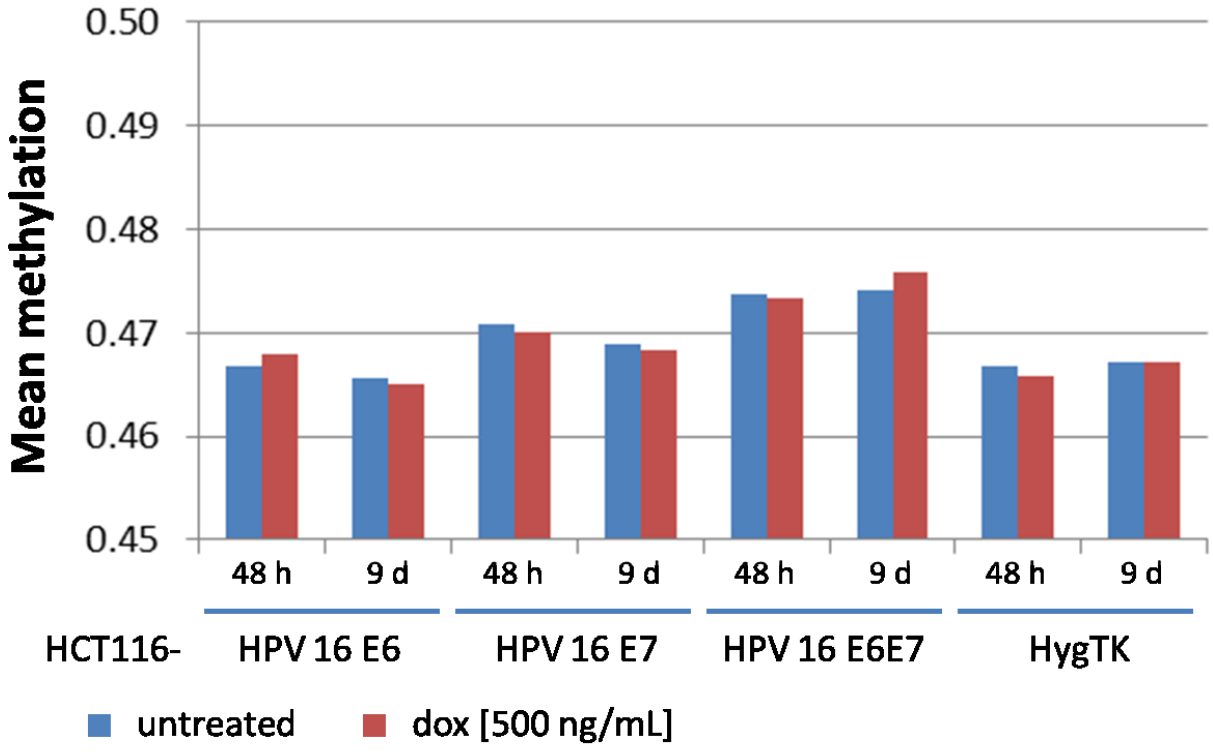

Figure 23: Mean CpG methylation of HPV 16 oncogene-expressing HCT116 clones.
The mean CpG methylation level of HPV 16 E6 and/or E7 expressing HCT116 clones was calculated using Infinium® MethylationEPIC BeadChips (Illumina) data after dox treatment [500 ng/mL] for 48 hours or nine days.

a sufficient large number of cells containing HPV 16 oncogene-specific methylation changes to be detected by the analysis.

Altogether, expression of HPV 16 oncogenes in HCT116 clones was not found to substantially affect the global methylation level. In contrast, CpG methylation of several gene promoters as well as gene bodies seemed to be altered after HPV 16 E6 and/or E7 expression. Especially keratin 38 as well as OR5D16 and PRKCA-AS1 might be candidate genes that are differentially methylated upon HPV 16 oncogene expression. Due to the lack of biological replicates the presented data need to be interpreted carefully.

4. Discussion

4.1. Role of altered DNA methylation during HPV-mediated transformation

Persistent hr-HPV infections may cause cervical and other types of tumors (zur Hausen 2002). The formation of HPV-associated tumors generally spans years or even decades and represents the final stage of multiple precancerous precursor lesions. The progression from persistent HPV infections to invasive cancer is accompanied by substantial alterations in the methylation pattern of the viral and host cellular genome (reviewed in (Johannsen & Lambert 2013, Steenbergen *et al.* 2014)). These include the gradual increase in HPV genome methylation, especially in the genes coding for the structural proteins L1 and L2 as well as for E2 and E5 (Brandsma *et al.* 2009, Fernandez *et al.* 2009, Kalantari *et al.* 2004, Mirabello *et al.* 2013). In addition, changes in the HPV URR methylation level have been observed and are assumed to play a major role during the progression of HPV-associated lesions (Bhattacharjee & Sengupta 2006, Ding *et al.* 2009, Hong *et al.* 2008). Modifications in the URR methylation pattern strongly depend on host cell differentiation as well as on the integration status of the viral genome. Due to their importance for the regulation of HPV oncogene expression, alterations in E2BS methylation during cervical carcinogenesis have been analyzed in several studies (Chaiwongkot *et al.* 2013, Kalantari *et al.* 2008, Kim *et al.* 2003, Vinokurova & von Knebel Doeberitz 2011). High levels of E2BS methylation were either detected if the viral genome was in episomal state or if it was integrated into the host genome as concatemers. In contrast, the E2BSs were found hypomethylated in lesions containing single copy HPV integrates with disrupted E2 open reading frames. These data suggest that in lesions with intact E2 gene, the E2-dependent transcriptional control of E6 and E7 is inhibited by hypermethylation either preventing E2 expression or its interaction with methylated E2BSs.

In addition to the viral genome, alterations in DNA methylation during the progression of HPV-associated lesions have been observed in host cellular genes. Hypermethylation and, as a consequence, repression of transcription have been detected in numerous

tumor suppressor genes including E-cadherin (CDH1), Cell Adhesion Molecule 1 (CADM1) and Death- Associated Protein Kinase 1 (DAPK1) (Bierkens *et al.* 2013, Kalantari *et al.* 2014, Laurson *et al.* 2010, Narayan *et al.* 2003). Moreover, the expression of several host cellular miRNAs was found to be affected by hypermethylation in their promoter regions (Jimenez-Wences *et al.* 2014). Especially, the hypermethylation-mediated silencing of the miR-375 promoter detected during the progression of HPV-infected lesions seems to play a predominant role in the deregulation of E6 and E7 expression, as this miRNA was demonstrated to directly bind and promote the degradation of HPV oncogene transcripts (Bierkens *et al.* 2013, Wang *et al.* 2011, Wilting *et al.* 2013, Yan *et al.* 2014). The tumor suppressive role of miR-375 is further pronounced by its ability to prevent the expression of several other genes including those encoding the transcription factor Sp1, which contributes to tumor development and progression, the protein CIP2A, which inhibits the degradation of the transcription factor MYC, as well as the ubiquitin-protein ligase E6AP that is involved in the E6-mediated degradation of p53 (Gartel *et al.* 2001, Jung *et al.* 2014, Junttila *et al.* 2007, Wang *et al.* 2011, Yao *et al.* 2004, Yuan *et al.* 2007).

The complexity of changing DNA methylation levels during the progression of HPV-associated lesions is further highlighted by recent studies, which show that the expression of E6 and E7 is not only affected by altered DNA methylation levels, but both HPV oncoproteins itself also manipulate the DNA methylation machinery. HPV 16 E6 was demonstrated to induce the expression of DNMT1 by degrading its transcriptional repressor p53, and HPV 16 E7 was reported to directly bind and activate DNMT1 (Au Yeung *et al.* 2010, Burgers *et al.* 2007). In addition, short-hairpin RNA-mediated knock-down of E6 and E7 expression was found to reduce the levels of DNA methyltransferases in SiHa and CaSki cells. Thereby, DNA methylation levels decreased leading to elevated expression of a panel of tumor suppressor genes and to inhibited proliferation (Li *et al.* 2015). In summary, the published data indicate that the alterations in the DNA methylation pattern during the progression of HPV-associated lesions are complex and crucial for the deregulation of HPV oncogene expression. Especially hypermethylation of CpGs in the E2BSs, as well as in tumor suppressor genes seems to play a predominant role during the formation of HPV-driven tumors. Therefore, the

application of demethylating substances might represent an attractive strategy to interfere with increasing DNA methylation levels, thereby re-establishing the regulatory functions of the E2BSs and of affected tumor suppressor genes.

4.2. Treatment of HPV-transformed cell lines with the demethylating agent DAC

Demethylating agents have been extensively used for the treatment of hematopoietic malignancies (Sorm & Vesely 1968). The most potent group of demethylating substances is the group of cytidine analogs, which are incorporated into the DNA during replication irreversibly binding to DNMT1. In addition, these substances induce the proteasomal degradation of DNMT1 thereby mediating global DNA demethylation in replicating cells (Creusot *et al.* 1982, Jones 1985, Jones & Taylor 1980). One of the most prominent members is DAC, whose demethylating effects have been thoroughly studied resulting in the FDA approval for the treatment of myelodysplastic syndrome (Kantarjian *et al.* 2006, Tefferi & Vardiman 2009). In addition to hematological diseases, the effects of DAC treatment on solid tumors have been investigated in several clinical trials (reviewed in (Cowan *et al.* 2010, Nie *et al.* 2014)). In these studies the response to DAC treatment strongly relied on the tumor type, however, the level of DNA demethylation in the tumor cells was not directly measured. Numerous reports have demonstrated that the level of DAC-mediated DNA demethylation highly depends on its administered dose (Issa *et al.* 2004, Tsai *et al.* 2012). High concentrations of DAC have been observed to cause cytotoxicity without inducing DNA demethylation (Juttermann *et al.* 1994). As a consequence, the administration of lower doses seems to be more promising for clinical application especially when DNA demethylation is expected to provide tumor specific effects.

In the present study, the effects of DAC treatment were systematically analyzed in a panel of HPV-transformed cell lines. To consider its dose dependent mechanism of action, different DAC concentrations were tested ranging from 0.1 µM to 1.0 µM. DNA demethylation was examined by monitoring LINE-1 methylation levels, which decreased

in all of the analyzed cell lines. Especially in CaSki cells, increasing the concentration of DAC to 1.0 µM did not further enhance the demethylating effect resulting in the previously discussed characteristic U-shaped LINE-1 methylation profile.

After confirming DNA demethylation, the effects of DAC treatment on the expression of E6 and E7 in the HPV-transformed cell lines were investigated. Transcription of E6 and E7 decreased in all of the analyzed cell lines. The most significant effects were detected in CaSki, UM-SCC-47 and UM-SCC-104 cells, whereas moderate decreases of E6 and E7 expression were observed in SiHa cells. Western blot analysis, however, revealed substantial reductions in E7 protein levels in all cell lines including SiHa cells. Repression of HPV 16 E6 and E7 expression in CaSki and UM-SCC-47 cells after DAC treatment have also been described in other publications (Fernandez *et al.* 2009, Zhang *et al.* 2015). In one of these reports as well as in a study published by Kalantari *et al.*, DAC treatment was, however, not found to significantly affect the expression levels of HPV 16 oncogenes in SiHa cells (Kalantari *et al.* 2008).

In addition to the inhibition of HPV oncogene expression, DAC treatment caused significant increases in p53 and p21 levels in the cell lines. Enhanced presence of p53 and p21 can be explained by decreases in HPV E6 levels after DAC treatment. As both, p53 and p21, are potent cell cycle inhibitors, reduced cell proliferation was expected and also detected by quantifying the DNA content as well as the colony formation capacity of the cells. The inhibition of proliferation might, however, be caused by multiple interconnected mechanisms. In addition to the elevation of p53 and p21 levels, reduction of HPV oncogene expression affects several other factors, which regulate cell cycle progression. In particular, reactivation of pocket proteins (pRb, p107 and p130), potentially as a consequence of repressed HPV E7 production, decelerates the cell cycle by binding E2F transcription factors. Moreover, DAC treatment inhibits proliferation independent of the presence of HPV by forming covalent bonds with DNMT1. These bonds are cytotoxic because gene transcription and DNA replication are prevented (Juttermann *et al.* 1994). Furthermore, global DNA demethylation might inhibit cell division by activating the expression of numerous tumor suppressor genes and by inducing cell differentiation (Baylin 2005, Jones & Taylor 1980). Taken together, several mechanisms are involved in the DAC-mediated inhibition of cell proliferation. These can

be distinguished in mechanisms that are either dependent or independent of DNA demethylation. The effects caused by reduced DNA methylation levels can, in turn, be grouped into those specific for HPV-transformed cells or those independent of HPV infections. Due to the HPV specificity of some of these mechanisms, it can be hypothesized that especially patients suffering from HPV-associated lesions might benefit from DAC therapy.

4.3. DAC-dependent mechanisms that inhibit HPV oncogene expression

The present study aimed to investigate DAC-dependent mechanisms that lead to the inhibition of HPV oncogene expression. As introduced previously, one of the potential mechanisms regulating E6 and E7 transcription is the alteration of E2BS methylation levels, which affects the binding of E2 and thereby the transcriptional activity of the HPV URR. Therefore, the methylation levels of the E2BS 3 and 4 were quantified after DAC treatment. These two E2BSs were selected for the analysis because the interaction of E2 with these has been reported to silence the transcriptional activity of the HPV early promoter by preventing the interaction of the transcription factors Sp1 and TBP with their respective binding sites located in close proximity to E2BS 3 and 4 (Steger & Corbach 1997, Stubenrauch *et al.* 1998). Hypermethylation of E2BS 3 and 4 sites has, in turn, been demonstrated to prevent the E2-mediated repression of URR transcription (Chaiwongkot *et al.* 2013, Kim *et al.* 2003, Thain *et al.* 1996).

As expected, DAC treatment decreased the methylation levels of CpGs located in the E2BS 3 and 4 in CaSki and UM-SCC-47 cells. These cell lines have previously been shown to express E2, further substantiating the hypothesis that the E2-mediated transcriptional regulation of E6 and E7 expression is reactivated after DAC treatment (Akagi *et al.* 2014, Olthof *et al.* 2015, Zhang *et al.* 2015). Demethylation of E2BS 3 and 4 was, however, not detected in SiHa and UM-SCC-104 cells, as the E2BSs in these cell lines are not methylated. Moreover, SiHa and UM-SCC-104 cells lack intact E2 gene copies and consequently do not express functional E2 proteins (Akagi *et al.* 2014, Olthof

et al. 2015). Therefore, additional mechanisms exist explaining the decrease in HPV oncogene expression in E2-disrupted cells after DAC treatment.

One of these additional mechanisms seems to be the reactivated expression of miR-375. Transcription of miR-375 has been demonstrated to depend on the methylation level of CpGs located in its promoter region (Wilting *et al.* 2013). Elevated methylation, as observed during HPV-driven transformation of the host cells, has been found to silence the transcription of miR-375 precursors (Bierkens *et al.* 2013, Wang *et al.* 2011). Reduced miR-375 expression directly affects HPV oncogene levels because this miRNA has been demonstrated to bind to E6 and E7 transcripts promoting their degradation (Jung *et al.* 2014). To further investigate the role of miR-375 in the regulation of HPV oncogene expression, the methylation level of six CpGs in the miR-375 promoter was analyzed. DAC treatment caused significant demethylation of this region in the analyzed cell lines. Subsequent quantification of miR-375 expression revealed a substantial increase after DAC treatment. To finally demonstrate the functional relevance of reactivated miR-375 transcription in repressing HPV oncogene expression, miR-375 was transfected into CaSki and SiHa cells. As a consequence, E6 and E7 expression was found to decrease in both cell lines, thereby underlining the role of this miRNA in the regulation of HPV oncogene expression levels.

In conclusion, DAC treatment effectively represses proliferation and colony formation of HPV-transformed cell lines. This effect is mediated by several mechanisms, which predominantly depend on global DNA demethylation (at least in the tested dose ranges). In addition, it can be hypothesized that HPV-infected cells are specifically sensitive to the treatment with DAC, as reduced E2BS methylation in the presence of E2 proteins as well as demethylation-mediated reactivation of miR-375 strongly inhibit the expression of HPV oncogenes. Therefore, the application of DAC as demethylating therapy might be a promising approach for the treatment of HPV-associated lesions. The systematic analysis of this substance in clinical trials is, thus, highly needed. The data presented in the current study might represent the basis legitimating those future clinical trials as well as subsequent analyses investigating, for example, immunological pathways including antigen expression and presentation, which have previously been reported to be

affected by the application of DAC (Mora-Garcia Mde *et al.* 2006, Nie *et al.* 2001, Weber *et al.* 1994).

4.4. Generation of a model system for the inducible HPV 16 oncogene expression

Deregulated expression of the HPV oncogenes E6 and E7 is the key event for the progression from permissive to transforming HPV infections. As discussed previously, overexpression of both oncogenes abrogates cell cycle checkpoints, interferes with apoptosis pathways and induces chromosomal instability in proliferating cells (reviewed in (Klingelhutz & Roman 2012, Moody & Laimins 2010, Roman & Munger 2013)). For this reason, several approaches have been tested to target E6 and E7 in HPV-infected cells. Especially trials using antisense RNAs directed against E6 and E7 transcripts showed promising results *in vitro*, but could not be transferred into the clinics (Alvarez-Salas & DiPaolo 2007, Gu *et al.* 2007). As direct targeting of E6 and E7 seems to have limited success, the inhibition of HPV oncogene expression or the interference with the effects mediated by E6 and E7 expression might be more promising. Approaches aiming to repress HPV oncogene expression have been introduced and discussed in the previous chapters. The development of effective treatment options for patients suffering from HPV-driven tumors, however, also relies on the precise understanding of the biological effects resulting from E6 and E7 overexpression.

The role of the oncogenes during the formation of HPV-associated tumors has been extensively studied in normal human keratinocytes as well as in HPV-transformed cell lines. These model systems, however, show a number of limitations that complicate the investigation of HPV oncogene-dependent effects especially during the transformation of the host cells. Primary human keratinocytes are very critical for continuous culturing and can therefore not be used to study medium- and long-term effects of HPV oncogene expression. In contrast, established cervical cancer cell lines are already HPV-transformed and can easily be cultured over long time periods. These cell lines, however, do not allow investigating the mechanisms that initiated the formation of tumor

cells. Therefore, the present study aimed to overcome some of these limitations by generating an inducible HPV 16 E6 and E7 expression system.

The human colon cancer cell line HCT116 was selected as a model system because the development of these tumor cells can be distinguished from HPV-mediated immortalization. HCT116 cells are MMR deficient due to a mutation in the *hMLH1* gene (Boland & Goel 2010, Parsons *et al.* 1993). Consequently, these cells accumulate frameshift mutations, especially in microsatellites, during DNA replication. As microsatellites can be found in several tumor suppressor genes including *TGFBR2* and *hMSH3*, these genes are frequently mutated in microsatellite-unstable tumors. Despite showing a high mutation rate, HCT116 cells are characterized by low numbers of chromosomal variations, which is also reflected by their stable and almost diploid karyotype (Brattain *et al.* 1981, Ertych *et al.* 2014). In contrast, chromosomal instability and aneuploidy seem to play a fundamental role during the development of HPV-driven tumors, as both can already be detected in early HPV-associated lesions (Hashida & Yasumoto 1991, Solinas-Toldo *et al.* 1997, Steinbeck 1997). The formation of HPV-transformed cells depends on the expression of the oncogenes E6 and E7, which target a variety of host cellular factors, in particular p53 and the retinoblastoma protein family members. Inhibition of the respective signaling pathways not only relaxes cell cycle checkpoints, but also promotes the completion of abnormal mitosis (Duensing *et al.* 2000, Duensing & Munger 2002, Moody & Laimins 2010). Consequently, HPV-transformed cells show high rates of numerical and structural chromosomal alterations (Heselmeyer *et al.* 1996, Steenbergen *et al.* 2014, Thomas *et al.* 2014). The tumor suppressor genes p53 and the retinoblastoma family members are not mutated in HCT116 cells (Liu & Bodmer 2006). In conclusion, immortalization of HCT116 cells is characterized by a mutator phenotype, whereas HPV-driven transformation requires chromosomal instability.

For the generation of HCT116 cells allowing the dox-inducible expression of HPV 16 E6 and E7, the master cell line HCT116-HygTK was used. These cells have been established previously and were kindly provided by Dr Jennifer Lee and Dr Johannes Gebert (Lee *et al.* 2013). HCT116-HygTK cells continuously express the reverse tetracycline-controlled transactivator (rtTA). The HygTK expression cassette of these

cells is flanked by Flp-recombination sites. By expressing Flp recombinase this locus was re-targeted to insert constructs allowing the dox-inducible expression of HPV 16 E6 and E7 either individually or in combination. For that reason, the performed strategy allowed to integrate single copies of the HPV 16 oncogenes into a defined chromosomal locus, thereby excluding mutational effects resulting of the random integration of multiple E6 and E7 sequences. Moreover, this integration strategy is assumed to only have a minimal risk for epigenetic silencing of the inserted construct because the expression of the HygTK cassette was found to remain active in the parental cell clone over long cultivation periods (discussed in the dissertation submitted by Dr. Jennifer Lee).

The dox-inducible expression of the HPV 16 oncogenes was subsequently confirmed by systematically treating the generated clones using different concentrations of dox over varying time periods. As expected, elevated doses of dox as well as prolonged treatment led to increasing HPV 16 E6 and E7 expression levels. This effect was observed on mRNA and on protein level. Presence of HPV 16 oncoproteins was not detected in the absence of dox excluding any significant leakiness of the system. Due to the lack of specific antibodies, the presence of HPV 16 E6 was monitored indirectly by measuring p53 and p21 levels, which were found to decrease after induction of HPV 16 E6 expression. As the HPV 16 E6-mediated degradation of p53 occurs on the protein level and as transcription of p53 is not known to be affected by HPV 16 E6, slight expression of p53 was still detectable and also expected after HPV 16 E6 induction.

Deactivation of the dox-dependent promoter was then studied by removing dox from the growth medium. In all of the HCT116 clones HPV 16 E6 and E7 transcript levels decreased significantly already six hours after dox-removal. Due to their prolonged half-lives, HPV 16 oncoprotein levels declined more slowly than mRNA levels and could not be detected 24 hours after removing dox. These data indicate the immediate deactivation of the dox-inducible promoter in the absence of dox.

In conclusion, the generated model system enables the rapid and sustained induction of HPV 16 E6 and E7 expression either individually or in combination from a defined chromosomal locus in HCT116 cells. In contrast to other model systems, which have been used to study HPV infections, the presented inducible system has several

advantages. First, short- and long-term effects of HPV 16 oncogene expression can easily be investigated by adding dox to the growth medium. As HPV 16 oncogene expression can be deactivated by removing dox, the system might, additionally, be used to distinguish between effects that depend on continuous presence of E6 and E7 and those that are irreversibly initiated by the oncoproteins. Finally, inducible expression of the HPV 16 oncogenes in HCT116 cells might be specifically advantageous to systematically analyze the consequences of both oncoproteins on the chromosomal stability of the cells. Therefore, several experiments were performed to investigate whether HPV 16 oncogene induction compromises chromosomal integrity in HCT116 cells, which would, in turn, also confirm the biological functionality of E6 and E7 in this system.

4.5. Effects of HPV 16 oncogenes on chromosomal stability in HCT116 cells

After generating an inducible HPV 16 E6 and E7 expression system, the next objective of the project was to validate its biological relevance as well as to use the system for the discovery of yet undescribed effects of the HPV 16 oncogenes. First, proliferation of the generated HCT116 clones was analyzed showing no substantial differences between dox-induced and untreated cells during 96 hours induction period. Thus, short-term expression of the HPV 16 oncogenes seems not sufficient to significantly affect the proliferation of already immortalized HCT116 cells. The induction phase of 96 hours, however, reflects a rather short time period and can be interpreted as a starting point for more detailed analyses of the growth behavior. As alterations in the proliferation rate were also not detected in the parental HCT116-HygTK cells, these data indicate the absence of significant dox-related growth modulatory effects.

Due to the chromosomal stability of HCT116 cells and due to the E6- and E7-dependent induction of genomic instability in NHK cells, the biological functionality and relevance of the generated system could be evaluated by investigating the consequences of HPV 16 oncogene expression on chromosomal stability and genomic integrity in HCT116 cells.

Transient and stable expression of HPV 16 E6 and E7 in NHK cells were shown to increase the number of interphase cells containing abnormal centrosomes (Duensing *et al.* 2000). Aberrant centrosome numbers are assumed to result from the uncoupling of DNA replication form centrosome duplication during S phase of the cell cycle. Especially the E7-mediated degradation of the pocket proteins pRb, p107 and p130 seems to contribute to this effect because the expression of several factors, which coordinate centrosome duplication, is regulated by the transcription factor E2F (Martin *et al.* 1998, Zerfass *et al.* 1995). As centrosomes separate in prophase forming the spindle poles during mitosis, it is not surprising that aberrant numbers of centrosomes strongly increase the risk for the occurrence of multipolar spindles. In fact, elevated rates of abnormal spindle pole formation have been observed after expressing HPV 16 E6 and E7 in NHK cells (Duensing *et al.* 2000). In addition, presence of HPV 16 E6 compromises DNA integrity due to the degradation of p53, which plays an important role in the activation of the DNA damage repair machinery (Duensing & Munger 2002). The combination of aberrant mitosis and destabilized DNA is assumed to increase the risk for the generation of aneuploid daughter cells. Although most of these daughter cells are presumably not viable, the genomic variability in the cell population might be substantially elevated, thereby increasing the probability for the outgrowth of potent subclones, which, in turn, can be considered as a source for genomic instability.

The effects of HPV 16 oncogene expression on chromosomal stability in HCT116 cells were analyzed by quantifying centrosome numbers in interphase cells, by monitoring spindle pole formation during mitosis and by measuring the presence of DNA double-strand breaks. In addition, the number of aneuploid cells was determined and the occurrence of gene copy number variations was evaluated potentially reflecting hotspots of chromosomal instability.

After inducing HPV 16 oncogene expression in the generated HCT116 clones, the number of interphase cells containing abnormal centrosomes as well as the number of aberrant spindle poles during mitosis moderately increased. In accordance with published data, this effect seems to be specifically pronounced in the E7-expressing clones (Duensing *et al.* 2000). Elevated centrosome and spindle pole numbers were already detected after 48 hours of dox treatment and remained relatively constant, as no

further increases were noticed after nine days of dox treatment. Induction of HPV 16 E6 expression also slightly elevated centrosome numbers and spindle pole formation in the respective HCT116 clones. The effects were, however, not as apparent as after induction of HPV 16 E7 expression.

In addition to centrosome and spindle pole numbers, we also detected a modest elevation of DNA double-strand breaks after inducing HPV 16 E6 and E7 expression in HCT116 cells as indicated by γH2AX foci. As discussed previously, expression of HPV 16 E6 interferes with DNA damage repair pathways by reducing the levels of p53, whereas HPV 16 E7 is assumed to promote DNA breakages by degrading pRb, which effectively prevents cell cycle arrest upon DNA damage induction (Harrington 1998). Expression of both oncogenes in combination led to slightly higher numbers of DNA double-strand breaks compared to the individual induction of either E6 or E7, potentially indicating the presence of cooperative effects.

Chromosomal missegregation, caused by multipolar mitosis, in combination with impaired genomic integrity, reflected by high numbers of DNA double-strand breaks, promotes the generation of aneuploid daughter cells. As expected, aneuploidy increased after induction of HPV 16 E6 and E7 expression revealed by FACS-based cell cycle analyses. Again, stronger effects were detected in the HPV 16 E7-expressing cells compared to those expressing HPV 16 E6. Extended cultivation periods of the cells as well as prolonged HPV 16 oncogene expression resulted in elevated numbers of aneuploid cells. Although most of the cells undergoing abnormal mitosis might not be viable, this observation suggests that a subset of these cells potentially survives and subsequently divides, thereby increasing the percentage of aneuploid cells in the population over time.

To study alterations in the genome of HPV 16 oncogene-expressing HCT116 cells in more detail, gene copy number variations were quantified using Infinium® MethylationEPIC BeadChips (Illumina). These microarrays were designed to assess the methylation status of more than 850,000 CpGs in the human genome by detecting methylated as well as unmethylated DNA copies of the respective CpG containing locus. Thereby, the method not only facilitates the quantification of methylation levels, but also

provides data about the number of copies of specific loci. To identify hotspots of copy number variations, HPV 16 E6 and E7 expression was induced for nine days reflecting approximately ten cell division cycles. Induction of HPV 16 oncogene expression was not found to cause significant gains or losses of whole chromosomes or chromosomal arms in a sufficient number of cells to be detected by the analysis. Thus, DNA copy number alterations, which have been published in HPV 16-transformed cervical carcinoma cells, could not be detected and therefore not directly be correlated to the presence of the HPV 16 oncoproteins.

There are a number of factors, which may explain this discrepancy and that need to be kept in mind when interpreting the presented data. First, the copy number variation data were generated from a single biological replicate per treatment condition. Therefore, these preliminary data may provide first insights, but do not allow statistical interpretations. The complexity of the analysis is further increased, due to the absence of information about the time-span of HPV 16 oncogene induction that would be optimal to identify CNV hotspots. Ten cell division cycles might, thus, not be enough to generate a sufficient number of cells containing the same alteration to be detected by the array. To further enrich the number of cells with identical CNVs, it might be necessary to select and expand single clones after the induction of HPV 16 oncogene expression. Following this strategy would, however, require the analysis of a sufficient number of clones to identify common CNVs and to estimate their rate of occurrence. Therefore, this approach would be comparably budget- and time-consuming. The comparison of CNV data between different studies is further complicated due to the different methods that have been used for the analysis. The majority of the publications performed either classical comparative genome hybridization (CGH) to karyotypically normal metaphase chromosomes or array CGH.

In conclusion, the presented gene copy number variation analysis constitutes a primary and preliminary experiment. Additional biological replicates and potentially the inclusion of generated subclones allowing a profound statistical analysis are highly needed.

4.6. Gene expression and DNA methylation upon HPV 16 oncogene induction

The final aim of the present study was the identification of yet undiscovered effects of the HPV 16 oncogenes. Due to the simplicity of HPV 16 E6 and E7 activation and deactivation in the generated HCT116 clones, these cells represent an ideal model system to analyze direct consequences of E6 and E7 expression in a time dependent manner. In order to obtain a complete picture of E6- and E7-mediated effects in the cells, global gene expression and methylation analyses were performed. Although E6 and E7 are not known to directly affect gene expression, both inhibit factors, like p53 or pRb, which in turn regulate the transcription of down-stream genes. Therefore, E6 and E7 are assumed to have a more indirect effect on the gene expression pattern of the cells.

Here, we used Illumina HumanHT-12 microarrays to identify differentially expressed genes after 48 hours of HPV 16 oncogene expression. Afterwards, the most promising candidate genes were further validated by performing RT-qPCR. As expected, one of the transcriptionally silenced genes in the HPV 16 E6, but not HPV 16 E7, expressing clones was CDKN1A, which codes for the cyclin-dependent kinase inhibitor p21. Expression of p21 is directly dependent on p53 and, thus, HPV 16 E6-mediated degradation of p53 was anticipated to inhibit the expression of CDKN1A, thereby again, highlighting the biological functionality of the HPV oncoproteins and the significance of the performed analysis. In addition to the downregulation of CDKN1A, gene expression analysis as well as RT-qPCR validation revealed the upregulation of KLF11 and CKLF after the induction of HPV 16 E6 expression. Up to now, these two proteins have neither been extensively studied, nor linked to the presence or progression of HPV infections. KLF11 has been reported to regulate the expression of genes that play a role in the control of cell growth and apoptosis (Lomberk & Urrutia 2005). CKLF has also been suggested to contribute to the control of cell proliferation (Tan *et al.* 2015). However, the function and biological relevance of the HPV 16 E6-mediated upregulation of these two factors during HPV infection or during the progression of HPV-associated lesions needs to be further evaluated by more comprehensive investigations. To translate the results

from mRNA to protein level, Western blot quantification of KLF11 and CKLF protein levels after induction of HPV 16 E6 expression could be performed. Furthermore, it needs to be analyzed whether HPV 16 E6 directly affects the expression of these genes, or whether the effects are mediated indirectly, potentially as a consequence of the reduction of p53 levels.

In addition to global gene expression analysis, alterations in the methylation pattern of gene promoter, CpG islands and enhancer regions were determined in response to HPV 16 oncogene expression. As summarized in the Introduction, the transformation of HPV-infected cells frequently involves changes in the CpG methylation levels in specific host cellular and viral genes. During HPV-driven cervical carcinogenesis, increasing methylation levels have especially been observed in tumor suppressor genes including E-cadherin (CDH1), Cell Adhesion Molecule 1 (CADM1) and Death-Associated Protein Kinase 1 (DAPK1) (Bierkens *et al.* 2013, Henken *et al.* 2007, Kalantari *et al.* 2014, Laurson *et al.* 2010, Narayan *et al.* 2003). Thereby, the regulation of transcriptional activity of these genes is disturbed promoting the transformation of the host cell and the progression of HPV-associated lesions. Alterations of methylation patterns during cervical carcinogenesis might be caused by different mechanisms. First, changes in the cellular differentiation status are usually accompanied by substantial alterations in the DNA methylation level (Khavari *et al.* 2010). Transformation of HPV-infected cells and overexpression of the oncogenes E6 and E7 prevents differentiation of the cells, thereby, efficiently avoiding cell cycle exit. As differentiation seems to be linked to reduced methylation levels in specific gene panels, HPV-transformed cells have been found to become hypermethylated in numerous sites (Fernandez *et al.* 2009). Recent publications suggest that the deregulated HPV oncogene expression, which constitutes a key event during HPV-mediated transformation of the host cells, plays an important role in this process by manipulating the DNA methylation machinery. HPV 16 E6 has been demonstrated to activate DNMT1 expression by degrading its transcriptional suppressor p53, whereas HPV 16 E7 has been reported to directly interact with DNMT1 enhancing its activity (Au Yeung *et al.* 2010, Burgers *et al.* 2007). The assumption that both oncoproteins deregulate the expression and the activity of DNA methyltransferases has further been substantiated by the study of Li *et al*. The authors demonstrated that

the knock down of HPV 16 E6 and E7 expression in SiHa and CaSki cells causes a reduction in DNA methyltransferase levels, thereby decreasing CpG methylation levels and promoting the expression of several tumor suppressor genes (Li *et al.* 2015).

Based on these findings, we hypothesized that induction of HPV 16 oncogene expression might affect the CpG methylation levels in HCT116 cells. To determine the methylation status of as many CpG dinucleotides as possible, hybridization of bisulfite-converted DNA to Infinium® MethylationEPIC BeadChips (Illumina) was performed. This state-of-the-art technique allows the quantification of CpG methylation levels in about 850,000 sites in the human genome in parallel. Due to the previously performed analysis of gene copy number variations, the information about CpG methylation levels was already available and therefore, only needed to be bioinformatically processed and interpreted. Changes in the genome-wide CpG methylation level were neither detected after 48 hours nor after nine days of HPV oncogene induction. In contrast, alterations in the methylation pattern of several genes were identified including keratin 38, OR5D16 and PRKCA-AS1. However, the biological relevance of the differential methylation in these genes in response to HPV 16 E6 and E7 expression needs to be evaluated, as none of these candidates has yet been linked to the progression of HPV infections. Alterations in the methylation level of tumor suppressor genes that have been reported to become hypermethylated during HPV-associated cervical carcinogenesis in previous publications, was not observed in the current study. This discrepancy might have several interconnected reasons. First, the described hypermethylation of tumor suppressor genes might not only be mediated by the overexpression of the HPV oncogenes, but also by other mechanisms, especially differentiation-related processes. Furthermore, HPV-driven transformation of the host cells is assumed to span a long time period. Therefore, nine days of HPV oncogene expression represent a reasonable starting point for the analysis of short-term effects, but might not be sufficient to identify long-term changes in gene methylation patterns. Finally, it is important to point out that these data represent a preliminary experiment to acquire first insights into global methylation changes. As indicated previously, the presented data are based on single biological samples per treatment condition, therefore, complicating the statistical interpretation.

To conclude, the present analysis did not reveal substantial alterations in the global methylation level after nine days of HPV 16 oncogene expression. Thus, the HPV 16 E6 and E7 induction period might not be long enough to induce differential methylation in a sufficient number of cells to be detected by the analysis. Nevertheless, differential CpG methylation was observed in a small subset of genes potentially indicating the ability of HPV 16 E6 and E7 to affect the methylation level of specific genes. However, these findings need to be validated by analyzing additional biological replicates. Altogether, the performed methylation analysis represents a sound basis for more comprehensive trials, which are important long-term aims of this project.

4.7. Outlook

The present study combines two essential aspects characteristic for translational research. One of these aspects is the systematic testing of previously selected candidate substances in preclinical settings. Here, the demethylating agent DAC has been identified as a promising candidate for the treatment of HPV-related tumors because previous studies had indicated the importance of hypermethylation during the progression of HPV-associated lesions. Therefore, investigating the efficacy of DAC treatment can be interpreted as logical consequence of previous findings and also constitutes a necessary step towards a more comprehensive evaluation of the substance *in vivo* and in clinical trials. The second aspect involves determined research that aims to identify novel candidate genes, mechanisms and pathways that might represent potential drug targets. This aspect strongly depends on the presence of powerful model systems that precisely mimic the *in vivo* situation and also allow to address important scientific questions. In the current study, we have introduced an inducible HPV 16 E6 and E7 expression system, which represents a unique experimental platform to study the effects of both HPV 16 oncoproteins in a time-controlled manner.

Due to the promising results of the DAC treatment and the successful validation of the inducible HPV 16 oncogene expression system, both parts of this study constitute a

starting point for future analyses. These may include the investigation of additional pathways, which are assumed to be influenced by the treatment with demethylating agents. Especially immune regulatory mechanisms seem to be affected, as DAC treatment has been reported to alter endogenous tumor antigen expression and presentation (Mora-Garcia Mde *et al.* 2006, Nie *et al.* 2001, Weber *et al.* 1994). By enhancing the expression of tumor antigens, DAC treatment might improve the recognition and subsequent elimination of tumor cells by immune effector cells. As these effects are difficult to study in cell culture experiments *in vitro*, the next step of the project would comprise the systematic testing *in vivo*, for example, by conducting animal studies. However, as the application of DAC has already been approved by the FDA for the treatment of myelodysplastic syndrome, it seems to be more efficient to directly evaluate its effects on HPV-associated tumors in clinical trials.

The generation and validation of the inducible HPV 16 E6 and E7 expression system as well as the investigation of the consequences of HPV 16 oncogene expression on chromosomal stability, gene expression and CpG methylation levels also led to a number of open questions. First, the detailed mechanism of the E7-mediated uncoupling of centrosome duplication from DNA replication is still not completely understood. As the deregulation of this mechanism is assumed to substantially contribute to the induction of chromosomal instability, future experiments might use the established model system to elucidate this mechanism in further detail. These may include the immunocytological staining of γ-tubulin in combination with the Centrosomal protein 170 (CEP170) after induction of HPV 16 oncogene expression. As CEP170 is specifically localized at mature mother centrioles, its immunostaining in combination with γ-tubulin allows to discriminate mother from daughter centrioles. As a consequence, centrosome accumulation, which is characterized by multiple mother and daughter centrioles, could be clearly distinguished from centrosome overduplication, which requires the increased number of daughter centrioles in the presence of a single mother centriole (Guarguaglini *et al.* 2005).

In addition, the ability of the HPV 16 oncogenes to induce gene copy number variations awaits further investigation. Prolonged HPV induction and subsequent outgrowth of single clones might significantly advance the validity of the analysis, thereby elevating the probability to identify hotspots of chromosomal alterations. The data generated from

these experimental trials could also be used for genome-wide DNA methylation analyses potentially improving the understanding of HPV oncogene-mediated epigenetic modifications.

Overall, the generation and the validation of a novel, inducible HPV 16 E6 and E7 expression system have paved the way for subsequent studies, which may further investigate the consequences of HPV 16 oncogene expression. Thereby, the present thesis not only contributes to a better understanding of the role of E6 and E7 during HPV-mediated transformation of infected cells, but might also represent the basis for future approaches to target the effects of HPV oncogene expression in the clinics.

5. References

Adams A K, Wise-Draper T M & Wells S I (2014) Human papillomavirus induced transformation in cervical and head and neck cancers. *Cancers (Basel)* **6:** 1793-1820

Akagi K, Li J, Broutian T R, Padilla-Nash H, Xiao W, Jiang B, Rocco J W, Teknos T N, Kumar B, Wangsa D, He D, Ried T, Symer D E & Gillison M L (2014) Genome-wide analysis of HPV integration in human cancers reveals recurrent, focal genomic instability. *Genome Research* **24:** 185-199

Alvarez-Salas L M & DiPaolo J A (2007) Molecular approaches to cervical cancer therapy. *Curr Drug Discov Technol* **4:** 208-219

Arroyo M, Bagchi S & Raychaudhuri P (1993) Association of the human papillomavirus type 16 E7 protein with the S-phase-specific E2F-cyclin A complex. *Molecular and Cellular Biology* **13:** 6537-6546

Au Yeung C L, Tsang W P, Tsang T Y, Co N N, Yau P L & Kwok T T (2010) HPV-16 E6 upregulation of DNMT1 through repression of tumor suppressor p53. *Oncol Rep* **24:** 1599-1604

Ault K A (2006) Epidemiology and natural history of human papillomavirus infections in the female genital tract. *Infect Dis Obstet Gynecol* **2006 Suppl:** 40470

Baker C C, Phelps W C, Lindgren V, Braun M J, Gonda M A & Howley P M (1987) Structural and transcriptional analysis of human papillomavirus type 16 sequences in cervical carcinoma cell lines. *Journal of Virology* **61:** 962-971

Baylin S B (2005) DNA methylation and gene silencing in cancer. *Nat Clin Pract Oncol* **2 Suppl 1:** S4-11

Benjamini Y & Hochberg Y (1995) Controlling the False Discovery Rate - a Practical and Powerful Approach to Multiple Testing. *Journal of the Royal Statistical Society Series B-Methodological* **57:** 289-300

Berezutskaya E, Yu B, Morozov A, Raychaudhuri P & Bagchi S (1997) Differential regulation of the pocket domains of the retinoblastoma family proteins by the HPV16 E7 oncoprotein. *Cell Growth Differ* **8:** 1277-1286

Bernard H U, Burk R D, Chen Z, van Doorslaer K, zur Hausen H & de Villiers E M (2010) Classification of papillomaviruses (PVs) based on 189 PV types and proposal of taxonomic amendments. *Virology* **401:** 70-79

Bhattacharjee B & Sengupta S (2006) CpG methylation of HPV 16 LCR at E2 binding site proximal to P97 is associated with cervical cancer in presence of intact E2. *Virology* **354:** 280-285

Bierkens M, Hesselink A T, Meijer C J, Heideman D A, Wisman G B, van der Zee A G, Snijders P J & Steenbergen R D (2013) CADM1 and MAL promoter methylation levels in hrHPV-positive cervical scrapes increase proportional to degree and

duration of underlying cervical disease. *International Journal of Cancer* **133:** 1293-1299

Bierkens M, Krijgsman O, Wilting S M, Bosch L, Jaspers A, Meijer G A, Meijer C J, Snijders P J, Ylstra B & Steenbergen R D (2013) Focal aberrations indicate EYA2 and hsa-miR-375 as oncogene and tumor suppressor in cervical carcinogenesis. *Genes, Chromosomes and Cancer* **52:** 56-68

Bodily J & Laimins L A (2011) Persistence of human papillomavirus infection: keys to malignant progression. *Trends in Microbiology* **19:** 33-39

Boland C R & Goel A (2010) Microsatellite instability in colorectal cancer. *Gastroenterology* **138:** 2073-2087 e2073

Boyer S N, Wazer D E & Band V (1996) E7 protein of human papilloma virus-16 induces degradation of retinoblastoma protein through the ubiquitin-proteasome pathway. *Cancer Research* **56:** 4620-4624

Brandsma J L, Sun Y, Lizardi P M, Tuck D P, Zelterman D, Haines G K, 3rd, Martel M, Harigopal M, Schofield K & Neapolitano M (2009) Distinct human papillomavirus type 16 methylomes in cervical cells at different stages of premalignancy. *Virology* **389:** 100-107

Brattain M G, Fine W D, Khaled F M, Thompson J & Brattain D E (1981) Heterogeneity of malignant cells from a human colonic carcinoma. *Cancer Research* **41:** 1751-1756

Brenner J C, Graham M P, Kumar B, Saunders L M, Kupfer R, Lyons R H, Bradford C R & Carey T E (2010) Genotyping of 73 UM-SCC head and neck squamous cell carcinoma cell lines. *Head Neck* **32:** 417-426

Brownlee C W & Rogers G C (2013) Show me your license, please: deregulation of centriole duplication mechanisms that promote amplification. *Cellular and Molecular Life Sciences* **70:** 1021-1034

Buck C B, Day P M & Trus B L (2013) The papillomavirus major capsid protein L1. *Virology* **445:** 169-174

Bulten J, Poddighe P J, Robben J C, Gemmink J H, de Wilde P C & Hanselaar A G (1998) Interphase cytogenetic analysis of cervical intraepithelial neoplasia. *American Journal of Pathology* **152:** 495-503

Burgers W A, Blanchon L, Pradhan S, de Launoit Y, Kouzarides T & Fuks F (2007) Viral oncoproteins target the DNA methyltransferases. *Oncogene* **26:** 1650-1655

Carter J R, Ding Z & Rose B R (2011) HPV infection and cervical disease: a review. *Aust N Z J Obstet Gynaecol* **51:** 103-108

Chaiwongkot A, Vinokurova S, Pientong C, Ekalaksananan T, Kongyingyoes B, Kleebkaow P, Chumworathayi B, Patarapadungkit N, Reuschenbach M & von Knebel Doeberitz M (2013) Differential methylation of E2 binding sites in episomal and integrated HPV 16 genomes in preinvasive and invasive cervical lesions. *International Journal of Cancer* **132:** 2087-2094

Chellappan S, Kraus V B, Kroger B, Munger K, Howley P M, Phelps W C & Nevins J R (1992) Adenovirus E1A, simian virus 40 tumor antigen, and human papillomavirus E7 protein share the capacity to disrupt the interaction between transcription factor E2F and the retinoblastoma gene product. *Proceedings of the National Academy of Sciences, USA* **89:** 4549-4553

Clarke M A, Wentzensen N, Mirabello L, Ghosh A, Wacholder S, Harari A, Lorincz A, Schiffman M & Burk R D (2012) Human papillomavirus DNA methylation as a potential biomarker for cervical cancer. *Cancer Epidemiol Biomarkers Prev* **21:** 2125-2137

Cobrinik D (2005) Pocket proteins and cell cycle control. *Oncogene* **24:** 2796-2809

Combita A L, Touze A, Bousarghin L, Christensen N D & Coursaget P (2002) Identification of two cross-neutralizing linear epitopes within the L1 major capsid protein of human papillomaviruses. *Journal of Virology* **76:** 6480-6486

Cowan L A, Talwar S & Yang A S (2010) Will DNA methylation inhibitors work in solid tumors? A review of the clinical experience with azacitidine and decitabine in solid tumors. *Epigenomics* **2:** 71-86

Creusot F, Acs G & Christman J K (1982) Inhibition of DNA methyltransferase and induction of Friend erythroleukemia cell differentiation by 5-azacytidine and 5-aza-2'-deoxycytidine. *The Journal of Biological Chemistry* **257:** 2041-2048

Crum C P, Ikenberg H, Richart R M & Gissman L (1984) Human papillomavirus type 16 and early cervical neoplasia. *N Engl J Med* **310:** 880-883

Cullen A P, Reid R, Campion M & Lorincz A T (1991) Analysis of the physical state of different human papillomavirus DNAs in intraepithelial and invasive cervical neoplasm. *Journal of Virology* **65:** 606-612

DeGregori J & Johnson D G (2006) Distinct and Overlapping Roles for E2F Family Members in Transcription, Proliferation and Apoptosis. *Curr Mol Med* **6:** 739-748

del Mar Pena L M & Laimins L A (2001) Differentiation-dependent chromatin rearrangement coincides with activation of human papillomavirus type 31 late gene expression. *Journal of Virology* **75:** 10005-10013

Demers G W, Halbert C L & Galloway D A (1994) Elevated wild-type p53 protein levels in human epithelial cell lines immortalized by the human papillomavirus type 16 E7 gene. *Virology* **198:** 169-174

Ding D C, Chiang M H, Lai H C, Hsiung C A, Hsieh C Y & Chu T Y (2009) Methylation of the long control region of HPV16 is related to the severity of cervical neoplasia. *Eur J Obstet Gynecol Reprod Biol* **147:** 215-220

Doeberitz M & Vinokurova S (2009) Host factors in HPV-related carcinogenesis: cellular mechanisms controlling HPV infections. *Archives of Medical Research* **40:** 435-442

Doorbar J (2005) The papillomavirus life cycle. *Journal of Clinical Virology* **32 Suppl 1:** S7-15

Doorbar J, Quint W, Banks L, Bravo I G, Stoler M, Broker T R & Stanley M A (2012) The biology and life-cycle of human papillomaviruses. *Vaccine* **30 Suppl 5:** F55-70

Duensing S (2005) A tentative classification of centrosome abnormalities in cancer. *Cell Biol Int* **29:** 352-359

Duensing S, Lee L Y, Duensing A, Basile J, Piboonniyom S, Gonzalez S, Crum C P & Munger K (2000) The human papillomavirus type 16 E6 and E7 oncoproteins cooperate to induce mitotic defects and genomic instability by uncoupling centrosome duplication from the cell division cycle. *Proceedings of the National Academy of Sciences, USA* **97:** 10002-10007

Duensing S & Munger K (2002) The human papillomavirus type 16 E6 and E7 oncoproteins independently induce numerical and structural chromosome instability. *Cancer Research* **62:** 7075-7082

Duensing S & Munger K (2002) Human papillomaviruses and centrosome duplication errors: modeling the origins of genomic instability. *Oncogene* **21:** 6241-6248

Ertych N, Stolz A, Stenzinger A, Weichert W, Kaulfuss S, Burfeind P, Aigner A, Wordeman L & Bastians H (2014) Increased microtubule assembly rates influence chromosomal instability in colorectal cancer cells. *Nat Cell Biol* **16:** 779-791

Evander M, Frazer I H, Payne E, Qi Y M, Hengst K & McMillan N A (1997) Identification of the alpha6 integrin as a candidate receptor for papillomaviruses. *Journal of Virology* **71:** 2449-2456

Feber A, Guilhamon P, Lechner M, Fenton T, Wilson G A, Thirlwell C, Morris T J, Flanagan A M, Teschendorff A E, Kelly J D & Beck S (2014) Using high-density DNA methylation arrays to profile copy number alterations. *Genome Biol* **15:** R30

Feng Q, Balasubramanian A, Hawes S E, Toure P, Sow P S, Dem A, Dembele B, Critchlow C W, Xi L, Lu H, McIntosh M W, Young A M & Kiviat N B (2005) Detection of hypermethylated genes in women with and without cervical neoplasia. *J Natl Cancer Inst* **97:** 273-282

Fernandez A F, Rosales C, Lopez-Nieva P, Grana O, Ballestar E, Ropero S, Espada J, Melo S A, Lujambio A, Fraga M F, Pino I, Javierre B, Carmona F J, Acquadro F, Steenbergen R D, Snijders P J, Meijer C J, Pineau P, Dejean A, Lloveras B, Capella G, Quer J, Buti M, Esteban J I, Allende H, Rodriguez-Frias F, Castellsague X, Minarovits J, Ponce J, Capello D, Gaidano G, Cigudosa J C, Gomez-Lopez G, Pisano D G, Valencia A, Piris M A, Bosch F X, Cahir-McFarland E, Kieff E & Esteller M (2009) The dynamic DNA methylomes of double-stranded DNA viruses associated with human cancer. *Genome Research* **19:** 438-451

Filippova M, Parkhurst L & Duerksen-Hughes P J (2004) The human papillomavirus 16 E6 protein binds to Fas-associated death domain and protects cells from Fas-triggered apoptosis. *The Journal of Biological Chemistry* **279:** 25729-25744

Filippova M, Song H, Connolly J L, Dermody T S & Duerksen-Hughes P J (2002) The human papillomavirus 16 E6 protein binds to tumor necrosis factor (TNF) R1 and

protects cells from TNF-induced apoptosis. *The Journal of Biological Chemistry* **277:** 21730-21739

Frazer I H (2010) Measuring serum antibody to human papillomavirus following infection or vaccination. *Gynecologic Oncology* **118:** S8-11

Freedman R S, Bowen J M, Leibovitz A, Pathak S, Siciliano M J, Gallager H S & Giovanella B C (1982) Characterization of a cell line (SW756) derived from a human squamous carcinoma of the uterine cervix. *In Vitro* **18:** 719-726

Fridman J S & Lowe S W (2003) Control of apoptosis by p53. *Oncogene* **22:** 9030-9040

Friedl F, Kimura I, Osato T & Ito Y (1970) Studies on a new human cell line (SiHa) derived from carcinoma of uterus. I. Its establishment and morphology. *Proc Soc Exp Biol Med* **135:** 543-545

Fu Y S, Reagan J W & Richart R M (1981) Definition of precursors. *Gynecologic Oncology* **12:** S220-231

Gallego M I, Zimonjic D B, Popescu N C, DiPaolo J A & Lazo P A (1994) Integration site of human papillomavirus type-18 DNA in chromosome band 8q22.1 of C4-I cervical carcinoma: DNase I hypersensitivity and methylation of cellular flanking sequences. *Genes, Chromosomes and Cancer* **9:** 28-32

Garnett T O & Duerksen-Hughes P J (2006) Modulation of apoptosis by human papillomavirus (HPV) oncoproteins. *Arch Virol* **151:** 2321-2335

Garnett T O, Filippova M & Duerksen-Hughes P J (2006) Accelerated degradation of FADD and procaspase 8 in cells expressing human papilloma virus 16 E6 impairs TRAIL-mediated apoptosis. *Cell Death and Differentiation* **13:** 1915-1926

Gartel A L, Ye X, Goufman E, Shianov P, Hay N, Najmabadi F & Tyner A L (2001) Myc represses the p21(WAF1/CIP1) promoter and interacts with Sp1/Sp3. *Proceedings of the National Academy of Sciences, USA* **98:** 4510-4515

Genovese N J, Banerjee N S, Broker T R & Chow L T (2008) Casein kinase II motif-dependent phosphorylation of human papillomavirus E7 protein promotes p130 degradation and S-phase induction in differentiated human keratinocytes. *Journal of Virology* **82:** 4862-4873

Ghoshal K, Datta J, Majumder S, Bai S, Kutay H, Motiwala T & Jacob S T (2005) 5-Aza-deoxycytidine induces selective degradation of DNA methyltransferase 1 by a proteasomal pathway that requires the KEN box, bromo-adjacent homology domain, and nuclear localization signal. *Molecular and Cellular Biology* **25:** 4727-4741

Giarre M, Caldeira S, Malanchi I, Ciccolini F, Leao M J & Tommasino M (2001) Induction of pRb degradation by the human papillomavirus type 16 E7 protein is essential to efficiently overcome p16INK4a-imposed G1 cell cycle Arrest. *Journal of Virology* **75:** 4705-4712

Gissmann L & zur Hausen H (1976) Human papilloma virus DNA: physical mapping and genetic heterogeneity. *Proceedings of the National Academy of Sciences, USA* **73:** 1310-1313

Gonzalez S L, Stremlau M, He X, Basile J R & Munger K (2001) Degradation of the retinoblastoma tumor suppressor by the human papillomavirus type 16 E7 oncoprotein is important for functional inactivation and is separable from proteasomal degradation of E7. *Journal of Virology* **75:** 7583-7591

Gore S D, Jones C & Kirkpatrick P (2006) Decitabine. *Nat Rev Drug Discov* **5:** 891-892

Gowher H & Jeltsch A (2004) Mechanism of inhibition of DNA methyltransferases by cytidine analogs in cancer therapy. *Cancer Biology & Therapy* **3:** 1062-1068

Graham S V (2010) Human papillomavirus: gene expression, regulation and prospects for novel diagnostic methods and antiviral therapies. *Future Microbiol* **5:** 1493-1506

Gu W, Putral L N, Irving A & McMillan N A (2007) The development and future of oligonucleotide-based therapies for cervical cancer. *Curr Opin Mol Ther* **9:** 126-131

Guarguaglini G, Duncan P I, Stierhof Y D, Holmstrom T, Duensing S & Nigg E A (2005) The forkhead-associated domain protein Cep170 interacts with Polo-like kinase 1 and serves as a marker for mature centrioles. *Molecular Biology of the Cell* **16:** 1095-1107

Hanahan D & Weinberg R A (2000) The hallmarks of cancer. *Cell* **100:** 57-70

Hashida T & Yasumoto S (1991) Induction of chromosome abnormalities in mouse and human epidermal keratinocytes by the human papillomavirus type 16 E7 oncogene. *Journal of General Virology* **72 (Pt 7):** 1569-1577

Hebner C M & Laimins L A (2006) Human papillomaviruses: basic mechanisms of pathogenesis and oncogenicity. *Reviews in Medical Virology* **16:** 83-97

Henken F E, Wilting S M, Overmeer R M, van Rietschoten J G, Nygren A O, Errami A, Schouten J P, Meijer C J, Snijders P J & Steenbergen R D (2007) Sequential gene promoter methylation during HPV-induced cervical carcinogenesis. *Br J Cancer* **97:** 1457-1464

Herfs M, Yamamoto Y, Laury A, Wang X, Nucci M R, McLaughlin-Drubin M E, Munger K, Feldman S, McKeon F D, Xian W & Crum C P (2012) A discrete population of squamocolumnar junction cells implicated in the pathogenesis of cervical cancer. *Proceedings of the National Academy of Sciences, USA* **109:** 10516-10521

Herrlinger U, Jones D T, Glas M, Hattingen E, Gramatzki D, Stuplich M, Felsberg J, Bahr O, Gielen G H, Simon M, Wiewrodt D, Schabet M, Hovestadt V, Capper D, Steinbach J P, von Deimling A, Lichter P, Pfister S M, Weller M & Reifenberger G (2016) Gliomatosis cerebri: no evidence for a separate brain tumor entity. *Acta Neuropathol* **131:** 309-319

Herz F, Miller O J, Miller D A, Auersperg N & Koss L G (1977) Chromosome analysis and alkaline phosphatase of C41, a cell line of human cervical origin distinct from HeLa. *Cancer Research* **37:** 3209-3213

Heselmeyer K, Schrock E, du Manoir S, Blegen H, Shah K, Steinbeck R, Auer G & Ried T (1996) Gain of chromosome 3q defines the transition from severe dysplasia to

invasive carcinoma of the uterine cervix. *Proceedings of the National Academy of Sciences, USA* **93:** 479-484

Hildesheim A, Herrero R, Wacholder S, Rodriguez A C, Solomon D, Bratti M C, Schiller J T, Gonzalez P, Dubin G, Porras C, Jimenez S E & Lowy D R (2007) Effect of human papillomavirus 16/18 L1 viruslike particle vaccine among young women with preexisting infection: a randomized trial. *JAMA* **298:** 743-753

Hills S A & Diffley J F (2014) DNA replication and oncogene-induced replicative stress. *Curr Biol* **24:** R435-444

Holland A J & Cleveland D W (2009) Boveri revisited: chromosomal instability, aneuploidy and tumorigenesis. *Nature Reviews: Molecular Cell Biology* **10:** 478-487

Hong D, Ye F, Lu W, Hu Y, Wan X, Chen Y & Xie X (2008) Methylation status of the long control region of HPV 16 in clinical cervical specimens. *Mol Med Rep* **1:** 555-560

Huang P S, Patrick D R, Edwards G, Goodhart P J, Huber H E, Miles L, Garsky V M, Oliff A & Heimbrook D C (1993) Protein domains governing interactions between E2F, the retinoblastoma gene product, and human papillomavirus type 16 E7 protein. *Molecular and Cellular Biology* **13:** 953-960

Huibregtse J M, Scheffner M & Howley P M (1993) Localization of the E6-AP regions that direct human papillomavirus E6 binding, association with p53, and ubiquitination of associated proteins. *Molecular and Cellular Biology* **13:** 4918-4927

Hung C F, Monie A, Alvarez R D & Wu T C (2007) DNA vaccines for cervical cancer: from bench to bedside. *Experimental & Molecular Medicine* **39:** 679-689

Ibeanu O A (2011) Molecular pathogenesis of cervical cancer. *Cancer Biology & Therapy* **11:** 295-306

Issa J P, Garcia-Manero G, Giles F J, Mannari R, Thomas D, Faderl S, Bayar E, Lyons J, Rosenfeld C S, Cortes J & Kantarjian H M (2004) Phase 1 study of low-dose prolonged exposure schedules of the hypomethylating agent 5-aza-2'-deoxycytidine (decitabine) in hematopoietic malignancies. *Blood* **103:** 1635-1640

Jeon S & Lambert P F (1995) Integration of human papillomavirus type 16 DNA into the human genome leads to increased stability of E6 and E7 mRNAs: implications for cervical carcinogenesis. *Proceedings of the National Academy of Sciences, USA* **92:** 1654-1658

Jimenez-Wences H, Peralta-Zaragoza O & Fernandez-Tilapa G (2014) Human papilloma virus, DNA methylation and microRNA expression in cervical cancer (Review). *Oncol Rep* **31:** 2467-2476

Johannsen E & Lambert P F (2013) Epigenetics of human papillomaviruses. *Virology* **445:** 205-212

Jones P A (1985) Effects of 5-azacytidine and its 2'-deoxyderivative on cell differentiation and DNA methylation. *Pharmacol Ther* **28:** 17-27

Jones P A & Taylor S M (1980) Cellular differentiation, cytidine analogs and DNA methylation. *Cell* **20:** 85-93

Jung H M, Phillips B L & Chan E K (2014) miR-375 activates p21 and suppresses telomerase activity by coordinately regulating HPV E6/E7, E6AP, CIP2A, and 14-3-3zeta. *Mol Cancer* **13:** 80

Junttila M R, Puustinen P, Niemela M, Ahola R, Arnold H, Bottzauw T, Ala-aho R, Nielsen C, Ivaska J, Taya Y, Lu S L, Lin S, Chan E K, Wang X J, Grenman R, Kast J, Kallunki T, Sears R, Kahari V M & Westermarck J (2007) CIP2A inhibits PP2A in human malignancies. *Cell* **130:** 51-62

Juttermann R, Li E & Jaenisch R (1994) Toxicity of 5-aza-2'-deoxycytidine to mammalian cells is mediated primarily by covalent trapping of DNA methyltransferase rather than DNA demethylation. *Proceedings of the National Academy of Sciences, USA* **91:** 11797-11801

Kalantari M, Calleja-Macias I E, Tewari D, Hagmar B, Lie K, Barrera-Saldana H A, Wiley D J & Bernard H U (2004) Conserved methylation patterns of human papillomavirus type 16 DNA in asymptomatic infection and cervical neoplasia. *Journal of Virology* **78:** 12762-12772

Kalantari M, Lee D, Calleja-Macias I E, Lambert P F & Bernard H U (2008) Effects of cellular differentiation, chromosomal integration and 5-aza-2'-deoxycytidine treatment on human papillomavirus-16 DNA methylation in cultured cell lines. *Virology* **374:** 292-303

Kalantari M, Osann K, Calleja-Macias I E, Kim S, Yan B, Jordan S, Chase D M, Tewari K S & Bernard H U (2014) Methylation of human papillomavirus 16, 18, 31, and 45 L2 and L1 genes and the cellular DAPK gene: Considerations for use as biomarkers of the progression of cervical neoplasia. *Virology* **448:** 314-321

Kamper N, Day P M, Nowak T, Selinka H C, Florin L, Bolscher J, Hilbig L, Schiller J T & Sapp M (2006) A membrane-destabilizing peptide in capsid protein L2 is required for egress of papillomavirus genomes from endosomes. *Journal of Virology* **80:** 759-768

Kang S, Kim J W, Kang G H, Lee S, Park N H, Song Y S, Park S Y, Kang S B & Lee H P (2006) Comparison of DNA hypermethylation patterns in different types of uterine cancer: cervical squamous cell carcinoma, cervical adenocarcinoma and endometrial adenocarcinoma. *International Journal of Cancer* **118:** 2168-2171

Kanodia S, Da Silva D M & Kast W M (2008) Recent advances in strategies for immunotherapy of human papillomavirus-induced lesions. *International Journal of Cancer* **122:** 247-259

Kantarjian H, Issa J P, Rosenfeld C S, Bennett J M, Albitar M, DiPersio J, Klimek V, Slack J, de Castro C, Ravandi F, Helmer R, 3rd, Shen L, Nimer S D, Leavitt R, Raza A & Saba H (2006) Decitabine improves patient outcomes in myelodysplastic syndromes: results of a phase III randomized study. *Cancer* **106:** 1794-1803

Khavari D A, Sen G L & Rinn J L (2010) DNA methylation and epigenetic control of cellular differentiation. *Cell Cycle* **9:** 3880-3883

Kim K, Garner-Hamrick P A, Fisher C, Lee D & Lambert P F (2003) Methylation patterns of papillomavirus DNA, its influence on E2 function, and implications in viral infection. *Journal of Virology* **77:** 12450-12459

Klingelhutz A J & Roman A (2012) Cellular transformation by human papillomaviruses: lessons learned by comparing high- and low-risk viruses. *Virology* **424:** 77-98

Korzeniewski N, Spardy N, Duensing A & Duensing S (2011) Genomic instability and cancer: lessons learned from human papillomaviruses. *Cancer Letters* **305:** 113-122

Lakin N D & Jackson S P (1999) Regulation of p53 in response to DNA damage. *Oncogene* **18:** 7644-7655

Lane D P (1992) Cancer. p53, guardian of the genome. *Nature* **358:** 15-16

Laurson J, Khan S, Chung R, Cross K & Raj K (2010) Epigenetic repression of E-cadherin by human papillomavirus 16 E7 protein. *Carcinogenesis* **31:** 918-926

Lechner M S & Laimins L A (1994) Inhibition of p53 DNA binding by human papillomavirus E6 proteins. *Journal of Virology* **68:** 4262-4273

Lee H, Lee K J, Jung C K, Hong J H, Lee Y S, Choi Y J, Lee K Y & Park G (2008) Expression of HPV L1 capsid protein in cervical specimens with HPV infection. *Diagn Cytopathol* **36:** 864-867

Lee J, Ballikaya S, Schonig K, Ball C R, Glimm H, Kopitz J & Gebert J (2013) Transforming growth factor beta receptor 2 (TGFBR2) changes sialylation in the microsatellite unstable (MSI) Colorectal cancer cell line HCT116. *PLoS One* **8:** e57074

Lengauer C, Kinzler K W & Vogelstein B (1997) Genetic instability in colorectal cancers. *Nature* **386:** 623-627

Lengauer C, Kinzler K W & Vogelstein B (1998) Genetic instabilities in human cancers. *Nature* **396:** 643-649

Letian T & Tianyu Z (2010) Cellular receptor binding and entry of human papillomavirus. *Virology Journal* **7:** 2

Leung T W, Liu S S, Leung R C, Chu M M, Cheung A N & Ngan H Y (2015) HPV 16 E2 binding sites 1 and 2 become more methylated than E2 binding site 4 during cervical carcinogenesis. *J Med Virol* **87:** 1022-1033

Li L, Xu C, Long J, Shen D, Zhou W, Zhou Q, Yang J & Jiang M (2015) E6 and E7 gene silencing results in decreased methylation of tumor suppressor genes and induces phenotype transformation of human cervical carcinoma cell lines. *Oncotarget* **6:** 23930-23943

Liu Y & Bodmer W F (2006) Analysis of P53 mutations and their expression in 56 colorectal cancer cell lines. *Proceedings of the National Academy of Sciences, USA* **103:** 976-981

Loew R, Vigna E, Lindemann D, Naldini L & Bujard H (2006) Retroviral vectors containing Tet-controlled bidirectional transcription units for simultaneous regulation of two gene activities. *J Mol Genet Med* **2:** 107-118

Lomberk G & Urrutia R (2005) The family feud: turning off Sp1 by Sp1-like KLF proteins. *Biochem J* **392:** 1-11

Long H J, 3rd, Bundy B N, Grendys E C, Jr., Benda J A, McMeekin D S, Sorosky J, Miller D S, Eaton L A & Fiorica J V (2005) Randomized phase III trial of cisplatin with or without topotecan in carcinoma of the uterine cervix: a Gynecologic Oncology Group Study. *J Clin Oncol* **23:** 4626-4633

Lowe J, Panda D, Rose S, Jensen T, Hughes W A, Tso F Y & Angeletti P C (2008) Evolutionary and structural analyses of alpha-papillomavirus capsid proteins yields novel insights into L2 structure and interaction with L1. *Virology Journal* **5:** 150

Mannhardt B, Weinzimer S A, Wagner M, Fiedler M, Cohen P, Jansen-Durr P & Zwerschke W (2000) Human papillomavirus type 16 E7 oncoprotein binds and inactivates growth-inhibitory insulin-like growth factor binding protein 3. *Molecular and Cellular Biology* **20:** 6483-6495

Martin L G, Demers G W & Galloway D A (1998) Disruption of the G1/S transition in human papillomavirus type 16 E7-expressing human cells is associated with altered regulation of cyclin E. *Journal of Virology* **72:** 975-985

McGranahan N, Burrell R A, Endesfelder D, Novelli M R & Swanton C (2012) Cancer chromosomal instability: therapeutic and diagnostic challenges. *EMBO Rep* **13:** 528-538

Mincheva A, Gissmann L & zur Hausen H (1987) Chromosomal integration sites of human papillomavirus DNA in three cervical cancer cell lines mapped by in situ hybridization. *Med Microbiol Immunol* **176:** 245-256

Mirabello L, Schiffman M, Ghosh A, Rodriguez A C, Vasiljevic N, Wentzensen N, Herrero R, Hildesheim A, Wacholder S, Scibior-Bentkowska D, Burk R D & Lorincz A T (2013) Elevated methylation of HPV16 DNA is associated with the development of high grade cervical intraepithelial neoplasia. *International Journal of Cancer* **132:** 1412-1422

Moody C A & Laimins L A (2010) Human papillomavirus oncoproteins: pathways to transformation. *Nature Reviews: Cancer* **10:** 550-560

Moore D H, Blessing J A, McQuellon R P, Thaler H T, Cella D, Benda J, Miller D S, Olt G, King S, Boggess J F & Rocereto T F (2004) Phase III study of cisplatin with or without paclitaxel in stage IVB, recurrent, or persistent squamous cell carcinoma of the cervix: a gynecologic oncology group study. *J Clin Oncol* **22:** 3113-3119

Mora-Garcia Mde L, Duenas-Gonzalez A, Hernandez-Montes J, De la Cruz-Hernandez E, Perez-Cardenas E, Weiss-Steider B, Santiago-Osorio E, Ortiz-Navarrete V F, Rosales V H, Cantu D, Lizano-Soberon M, Rojo-Aguilar M P & Monroy-Garcia A (2006) Up-regulation of HLA class-I antigen expression and antigen-specific CTL

response in cervical cancer cells by the demethylating agent hydralazine and the histone deacetylase inhibitor valproic acid. *J Transl Med* **4:** 55

Narayan G, Arias-Pulido H, Koul S, Vargas H, Zhang F F, Villella J, Schneider A, Terry M B, Mansukhani M & Murty V V (2003) Frequent promoter methylation of CDH1, DAPK, RARB, and HIC1 genes in carcinoma of cervix uteri: its relationship to clinical outcome. *Mol Cancer* **2:** 24

Negrini S, Gorgoulis V G & Halazonetis T D (2010) Genomic instability--an evolving hallmark of cancer. *Nature Reviews: Molecular Cell Biology* **11:** 220-228

Nie J, Liu L, Li X & Han W (2014) Decitabine, a new star in epigenetic therapy: the clinical application and biological mechanism in solid tumors. *Cancer Letters* **354:** 12-20

Nie Y, Yang G, Song Y, Zhao X, So C, Liao J, Wang L D & Yang C S (2001) DNA hypermethylation is a mechanism for loss of expression of the HLA class I genes in human esophageal squamous cell carcinomas. *Carcinogenesis* **22:** 1615-1623

Olaharski A J, Sotelo R, Solorza-Luna G, Gonsebatt M E, Guzman P, Mohar A & Eastmond D A (2006) Tetraploidy and chromosomal instability are early events during cervical carcinogenesis. *Carcinogenesis* **27:** 337-343

Olthof N C, Huebbers C U, Kolligs J, Henfling M, Ramaekers F C, Cornet I, van Lent-Albrechts J A, Stegmann A P, Silling S, Wieland U, Carey T E, Walline H M, Gollin S M, Hoffmann T K, de Winter J, Kremer B, Klussmann J P & Speel E J (2015) Viral load, gene expression and mapping of viral integration sites in HPV16-associated HNSCC cell lines. *International Journal of Cancer* **136:** E207-218

Parsons R, Li G M, Longley M J, Fang W H, Papadopoulos N, Jen J, de la Chapelle A, Kinzler K W, Vogelstein B & Modrich P (1993) Hypermutability and mismatch repair deficiency in RER+ tumor cells. *Cell* **75:** 1227-1236

Patel D, Huang S M, Baglia L A & McCance D J (1999) The E6 protein of human papillomavirus type 16 binds to and inhibits co-activation by CBP and p300. *EMBO Journal* **18:** 5061-5072

Pattillo R A, Hussa R O, Story M T, Ruckert A C, Shalaby M R & Mattingly R F (1977) Tumor antigen and human chorionic gonadotropin in CaSki cells: a new epidermoid cervical cancer cell line. *Science* **196:** 1456-1458

Paull T T, Rogakou E P, Yamazaki V, Kirchgessner C U, Gellert M & Bonner W M (2000) A critical role for histone H2AX in recruitment of repair factors to nuclear foci after DNA damage. *Curr Biol* **10:** 886-895

Petrosky E, Bocchini J A, Jr., Hariri S, Chesson H, Curtis C R, Saraiya M, Unger E R & Markowitz L E (2015) Use of 9-valent human papillomavirus (HPV) vaccine: updated HPV vaccination recommendations of the advisory committee on immunization practices. *MMWR Morb Mortal Wkly Rep* **64:** 300-304

Pett M & Coleman N (2007) Integration of high-risk human papillomavirus: a key event in cervical carcinogenesis? *J Pathol* **212:** 356-367

Pim D, Massimi P, Dilworth S M & Banks L (2005) Activation of the protein kinase B pathway by the HPV-16 E7 oncoprotein occurs through a mechanism involving interaction with PP2A. *Oncogene* **24:** 7830-7838

Popescu N C, Amsbaugh S C & DiPaolo J A (1987) Human papillomavirus type 18 DNA is integrated at a single chromosome site in cervical carcinoma cell line SW756. *Journal of Virology* **61:** 1682-1685

Pouyanfard S & Muller M (2017) Human papillomavirus first and second generation vaccines-current status and future directions. *Biol Chem* **398:** 871-889

Rapp B, Pawellek A, Kraetzer F, Schaefer M, May C, Purdie K, Grassmann K & Iftner T (1997) Cell-type-specific separate regulation of the E6 and E7 promoters of human papillomavirus type 6a by the viral transcription factor E2. *Journal of Virology* **71:** 6956-6966

Rogakou E P, Pilch D R, Orr A H, Ivanova V S & Bonner W M (1998) DNA double-stranded breaks induce histone H2AX phosphorylation on serine 139. *The Journal of Biological Chemistry* **273:** 5858-5868

Roman A & Munger K (2013) The papillomavirus E7 proteins. *Virology* **445:** 138-168

Romanczuk H, Thierry F & Howley P M (1990) Mutational analysis of cis elements involved in E2 modulation of human papillomavirus type 16 P97 and type 18 P105 promoters. *Journal of Virology* **64:** 2849-2859

Sahm F, Korshunov A, Schrimpf D, Stichel D, Jones D T, Capper D, Koelsche C, Reuss D, Kratz A, Huang K, Wefers A K, Schick M, Bewerunge-Hudler M, Mittelbronn M, Platten M, Hanggi D, Jeibmann A, Unterberg A, Herold-Mende C, Pfister S M, Brandner S, Wick W & von Deimling A (2017) Gain of 12p encompassing CCND2 is associated with gemistocytic histology in IDH mutant astrocytomas. *Acta Neuropathol* **133:** 325-327

Schiller J T, Day P M & Kines R C (2010) Current understanding of the mechanism of HPV infection. *Gynecologic Oncology* **118:** S12-17

Schlake T & Bode J (1994) Use of mutated FLP recognition target (FRT) sites for the exchange of expression cassettes at defined chromosomal loci. *Biochemistry* **33:** 12746-12751

Sen S (2000) Aneuploidy and cancer. *Curr Opin Oncol* **12:** 82-88

Shivapurkar N, Sherman M E, Stastny V, Echebiri C, Rader J S, Nayar R, Bonfiglio T A, Gazdar A F & Wang S S (2007) Evaluation of candidate methylation markers to detect cervical neoplasia. *Gynecologic Oncology* **107:** 549-553

Singh N, Senapati S & Bose K (2016) Insights into the mechanism of human papillomavirus E2-induced procaspase-8 activation and cell death. *Sci Rep* **6:** 21408

Skyldberg B, Fujioka K, Hellstrom A C, Sylven L, Moberger B & Auer G (2001) Human papillomavirus infection, centrosome aberration, and genetic stability in cervical lesions. *Mod Pathol* **14:** 279-284

Solinas-Toldo S, Durst M & Lichter P (1997) Specific chromosomal imbalances in human papillomavirus-transfected cells during progression toward immortality. *Proceedings of the National Academy of Sciences, USA* **94:** 3854-3859

Sorm F & Vesely J (1968) Effect of 5-aza-2'-deoxycytidine against leukemic and hemopoietic tissues in AKR mice. *Neoplasma* **15:** 339-343

Steenbergen R D, Snijders P J, Heideman D A & Meijer C J (2014) Clinical implications of (epi)genetic changes in HPV-induced cervical precancerous lesions. *Nature Reviews: Cancer* **14:** 395-405

Steger G & Corbach S (1997) Dose-dependent regulation of the early promoter of human papillomavirus type 18 by the viral E2 protein. *Journal of Virology* **71:** 50-58

Steinbeck R G (1997) Proliferation and DNA aneuploidy in mild dysplasia imply early steps of cervical carcinogenesis. *Acta Oncol* **36:** 3-12

Stich M, Ganss L, Puschhof J, Prigge E S, Reuschenbach M, Guiterrez A, Vinokurova S & von Knebel Doeberitz M (2016) 5-aza-2'-deoxycytidine (DAC) treatment downregulates the HPV E6 and E7 oncogene expression and blocks neoplastic growth of HPV-associated cancer cells. *Oncotarget*

Strauss M J, Shaw E W & et al. (1949) Crystalline virus-like particles from skin papillomas characterized by intranuclear inclusion bodies. *Proc Soc Exp Biol Med* **72:** 46-50

Stubenrauch F & Laimins L A (1999) Human papillomavirus life cycle: active and latent phases. *Seminars in Cancer Biology* **9:** 379-386

Stubenrauch F, Lim H B & Laimins L A (1998) Differential requirements for conserved E2 binding sites in the life cycle of oncogenic human papillomavirus type 31. *Journal of Virology* **72:** 1071-1077

Su J H, Wu A, Scotney E, Ma B, Monie A, Hung C F & Wu T C (2010) Immunotherapy for cervical cancer: Research status and clinical potential. *BioDrugs* **24:** 109-129

Taby R & Issa J P (2010) Cancer epigenetics. *CA Cancer J Clin* **60:** 376-392

Tan Y, Wang Y, Li L, Xia J, Peng S & He Y (2015) Chemokine-like factor 1-derived C-terminal peptides induce the proliferation of dermal microvascular endothelial cells in psoriasis. *PLoS One* **10:** e0125073

Tang A L, Hauff S J, Owen J H, Graham M P, Czerwinski M J, Park J J, Walline H, Papagerakis S, Stoerker J, McHugh J B, Chepeha D B, Bradford C R, Carey T E & Prince M E (2012) UM-SCC-104: a new human papillomavirus-16-positive cancer stem cell-containing head and neck squamous cell carcinoma cell line. *Head Neck* **34:** 1480-1491

Tefferi A & Vardiman J W (2009) Myelodysplastic syndromes. *N Engl J Med* **361:** 1872-1885

Thain A, Jenkins O, Clarke A R & Gaston K (1996) CpG methylation directly inhibits binding of the human papillomavirus type 16 E2 protein to specific DNA sequences. *Journal of Virology* **70:** 7233-7235

Thierry F (2009) Transcriptional regulation of the papillomavirus oncogenes by cellular and viral transcription factors in cervical carcinoma. *Virology* **384:** 375-379

Thomas L K, Bermejo J L, Vinokurova S, Jensen K, Bierkens M, Steenbergen R, Bergmann M, von Knebel Doeberitz M & Reuschenbach M (2014) Chromosomal gains and losses in human papillomavirus-associated neoplasia of the lower genital tract - a systematic review and meta-analysis. *Eur J Cancer* **50:** 85-98

Thompson S L & Compton D A (2008) Examining the link between chromosomal instability and aneuploidy in human cells. *J Cell Biol* **180:** 665-672

Tsai H C, Li H, Van Neste L, Cai Y, Robert C, Rassool F V, Shin J J, Harbom K M, Beaty R, Pappou E, Harris J, Yen R W, Ahuja N, Brock M V, Stearns V, Feller-Kopman D, Yarmus L B, Lin Y C, Welm A L, Issa J P, Minn I, Matsui W, Jang Y Y, Sharkis S J, Baylin S B & Zahnow C A (2012) Transient low doses of DNA-demethylating agents exert durable antitumor effects on hematological and epithelial tumor cells. *Cancer Cell* **21:** 430-446

Vinokurova S & von Knebel Doeberitz M (2011) Differential methylation of the HPV 16 upstream regulatory region during epithelial differentiation and neoplastic transformation. *PLoS One* **6:** e24451

von Knebel Doeberitz M, Reuschenbach M, Schmidt D & Bergeron C (2012) Biomarkers for cervical cancer screening: the role of p16(INK4a) to highlight transforming HPV infections. *Expert Review of Proteomics* **9:** 149-163

Wang F, Li Y, Zhou J, Xu J, Peng C, Ye F, Shen Y, Lu W, Wan X & Xie X (2011) miR-375 is down-regulated in squamous cervical cancer and inhibits cell migration and invasion via targeting transcription factor SP1. *American Journal of Pathology* **179:** 2580-2588

Weber J, Salgaller M, Samid D, Johnson B, Herlyn M, Lassam N, Treisman J & Rosenberg S A (1994) Expression of the MAGE-1 tumor antigen is up-regulated by the demethylating agent 5-aza-2'-deoxycytidine. *Cancer Research* **54:** 1766-1771

Weidenfeld I, Gossen M, Low R, Kentner D, Berger S, Gorlich D, Bartsch D, Bujard H & Schonig K (2009) Inducible expression of coding and inhibitory RNAs from retargetable genomic loci. *Nucleic Acids Research* **37:** e50

Welman A, Barraclough J & Dive C (2006) Generation of cells expressing improved doxycycline-regulated reverse transcriptional transactivator rtTA2S-M2. *Nat Protoc* **1:** 803-811

Wentzensen N, Sherman M E, Schiffman M & Wang S S (2009) Utility of methylation markers in cervical cancer early detection: appraisal of the state-of-the-science. *Gynecologic Oncology* **112:** 293-299

Wentzensen N, Vinokurova S & von Knebel Doeberitz M (2004) Systematic review of genomic integration sites of human papillomavirus genomes in epithelial dysplasia and invasive cancer of the female lower genital tract. *Cancer Research* **64:** 3878-3884

White A E, Livanos E M & Tlsty T D (1994) Differential disruption of genomic integrity and cell cycle regulation in normal human fibroblasts by the HPV oncoproteins. *Genes & Development* **8:** 666-677

Wilting S M, Verlaat W, Jaspers A, Makazaji N A, Agami R, Meijer C J, Snijders P J & Steenbergen R D (2013) Methylation-mediated transcriptional repression of microRNAs during cervical carcinogenesis. *Epigenetics* **8:** 220-228

Wu E W, Clemens K E, Heck D V & Munger K (1993) The human papillomavirus E7 oncoprotein and the cellular transcription factor E2F bind to separate sites on the retinoblastoma tumor suppressor protein. *Journal of Virology* **67:** 2402-2407

Yan J W, Lin J S & He X X (2014) The emerging role of miR-375 in cancer. *International Journal of Cancer* **135:** 1011-1018

Yang A S, Estecio M R, Doshi K, Kondo Y, Tajara E H & Issa J P (2004) A simple method for estimating global DNA methylation using bisulfite PCR of repetitive DNA elements. *Nucleic Acids Research* **32:** e38

Yao J C, Wang L, Wei D, Gong W, Hassan M, Wu T T, Mansfield P, Ajani J & Xie K (2004) Association between expression of transcription factor Sp1 and increased vascular endothelial growth factor expression, advanced stage, and poor survival in patients with resected gastric cancer. *Clinical Cancer Research* **10:** 4109-4117

Yee C, Krishnan-Hewlett I, Baker C C, Schlegel R & Howley P M (1985) Presence and expression of human papillomavirus sequences in human cervical carcinoma cell lines. *American Journal of Pathology* **119:** 361-366

Yoshida T, Sano T, Kanuma T, Owada N, Sakurai S, Fukuda T & Nakajima T (2008) Immunochemical analysis of HPV L1 capsid protein and p16 protein in liquid-based cytology samples from uterine cervical lesions. *Cancer* **114:** 83-88

Yuan P, Wang L, Wei D, Zhang J, Jia Z, Li Q, Le X, Wang H, Yao J & Xie K (2007) Therapeutic inhibition of Sp1 expression in growing tumors by mithramycin a correlates directly with potent antiangiogenic effects on human pancreatic cancer. *Cancer* **110:** 2682-2690

Zeman M K & Cimprich K A (2014) Causes and consequences of replication stress. *Nat Cell Biol* **16:** 2-9

Zerfass K, Schulze A, Spitkovsky D, Friedman V, Henglein B & Jansen-Durr P (1995) Sequential activation of cyclin E and cyclin A gene expression by human papillomavirus type 16 E7 through sequences necessary for transformation. *Journal of Virology* **69:** 6389-6399

Zhang B, Chen W & Roman A (2006) The E7 proteins of low- and high-risk human papillomaviruses share the ability to target the pRB family member p130 for degradation. *Proceedings of the National Academy of Sciences, USA* **103:** 437-442

Zhang C, Deng Z, Pan X, Uehara T, Suzuki M & Xie M (2015) Effects of Methylation Status of CpG Sites within the HPV16 Long Control Region on HPV16-Positive Head and Neck Cancer Cells. *PLoS One* **10:** e0141245

Zimmermann H, Degenkolbe R, Bernard H U & O'Connor M J (1999) The human papillomavirus type 16 E6 oncoprotein can down-regulate p53 activity by targeting the transcriptional coactivator CBP/p300. *Journal of Virology* **73:** 6209-6219

zur Hausen H (1974) [Latency and reactivation of herpes group viruses]. *Med Klin* **69:** 309-312

zur Hausen H (1975) Oncogenic Herpes viruses. *Biochimica et Biophysica Acta* **417:** 25-53

zur Hausen H (2002) Papillomaviruses and cancer: from basic studies to clinical application. *Nature Reviews: Cancer* **2:** 342-350

6. Appendix

6.1. Supplementary Figures

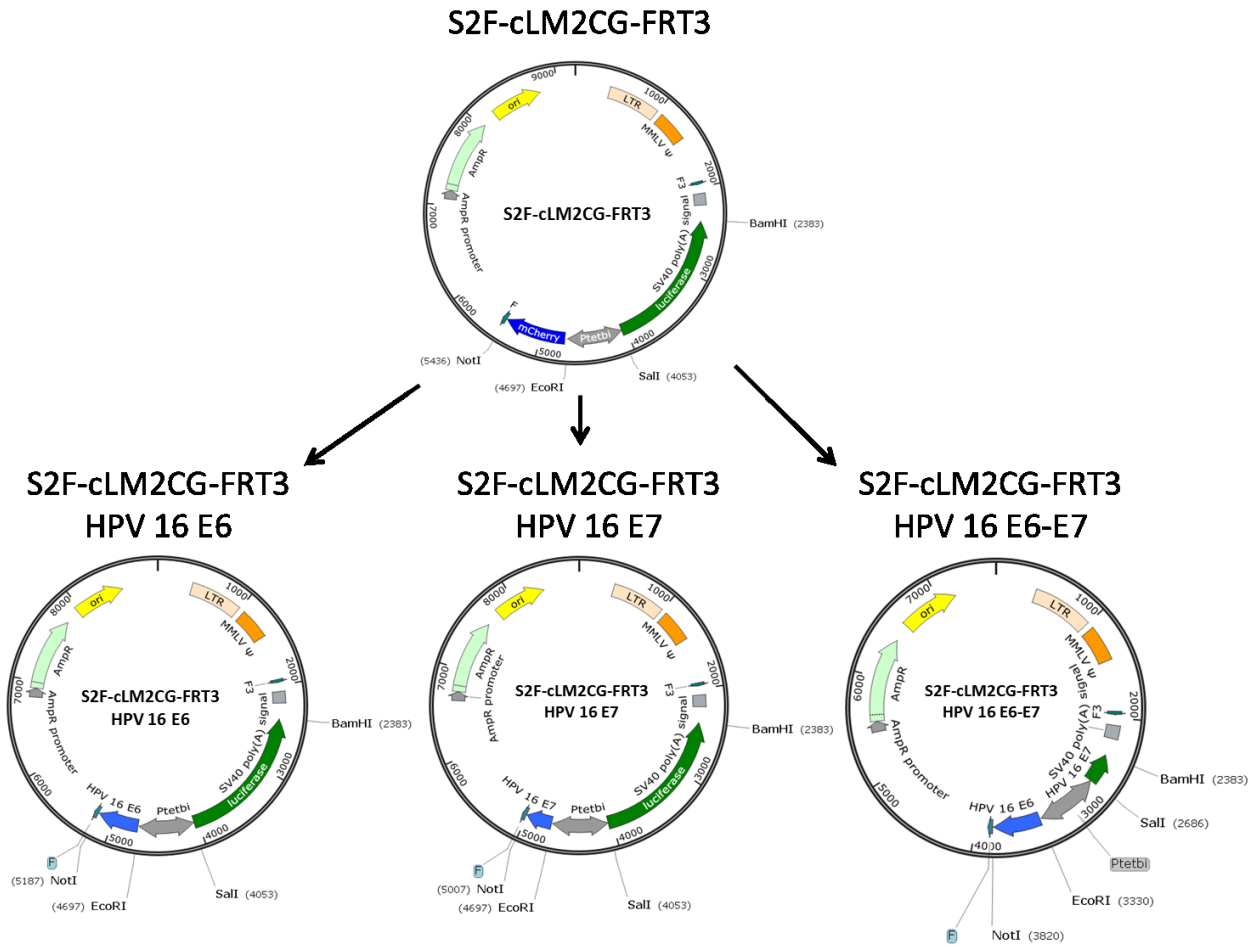

Supplementary Figure 1: Schematic illustration of the vectors used for RMCE.
The vector S2F-cLM2CG-FRT3 was used to generate vectors that allow dox-inducible expression of the HPV 16 oncogenes. S2F-cLM2CG-FRT3 contains a tet-controlled bidirectional promoter (Ptetbi) regulating the expression of firefly luciferase and the red fluorescent protein mCherry. This expression unit is flanked by the two heterospecific Flp-recognition sites F and F3 allowing RMCE upon expression of Flp recombinase. For the generation of the vector S2F-cLM2CG-FRT3 HPV 16 E6 the mCherry fragment was replaced by the sequence encoding HPV 16 E6 (GenBank: K02718.1, nt 83-560). Therefore, the *NotI* and *EcoRI* integration sites were used. The same strategy was performed to integrate HPV 16 E7 (GenBank: K02718.1, nt 562-858) into the vector resulting in the generation of S2F-cLM2CG-FRT3 HPV 16 E7. Expression of both HPV 16 oncogenes in combination was facilitated by replacing the mCherry fragment by HPV 16 E6 and the firefly luciferase encoding region by HPV 16 E7. Thereby, the bidirectional HPV 16 E6 and E7 vector S2F-cLM2CG-FRT3 HPV 16 E6-E7 was generated.

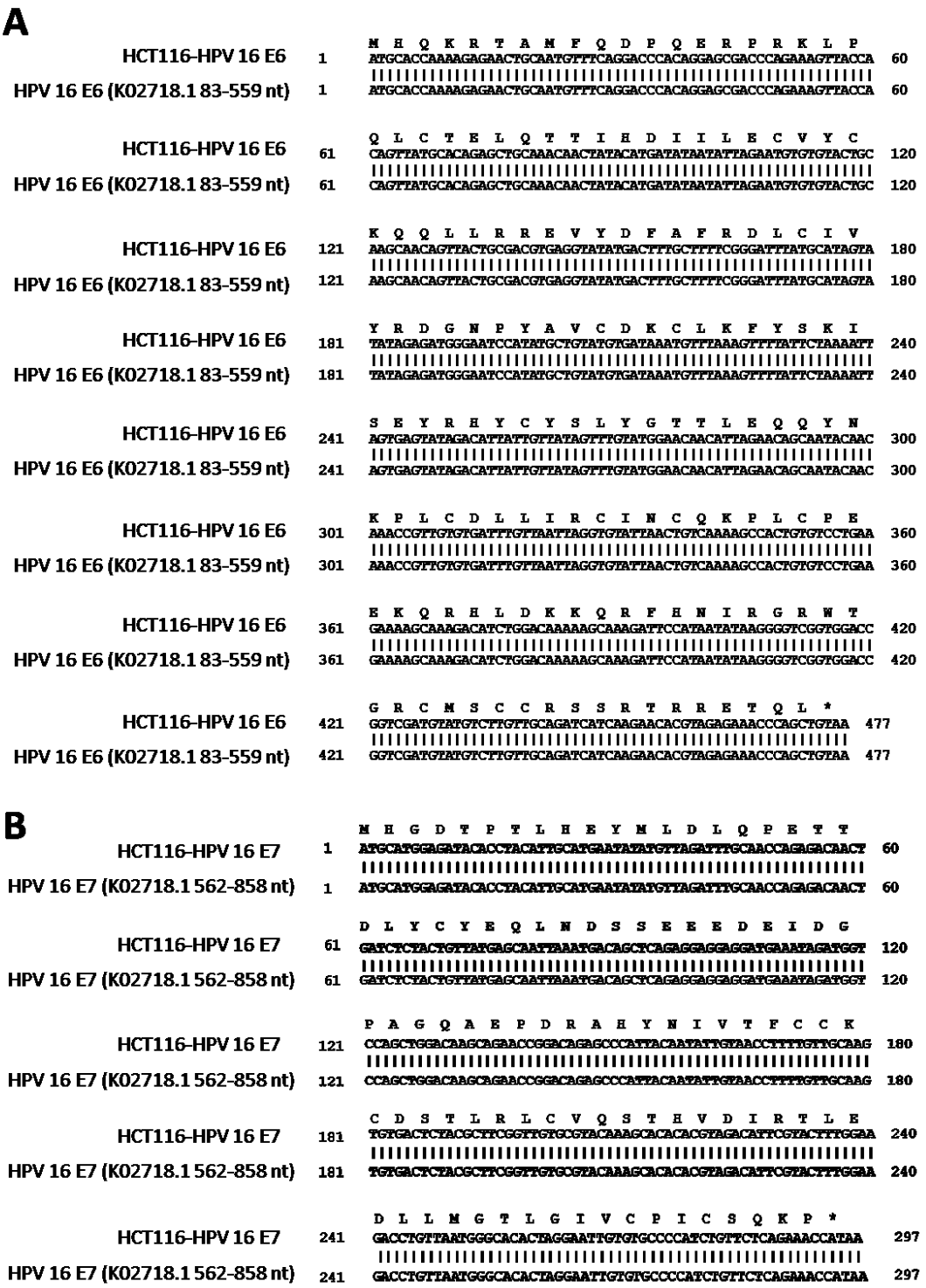

Supplementary Figure 2: Alignment of HPV 16 E6 and E7 mRNA expressed after induction of HCT116 clones with the published sequences.

Sequence identity between the HPV 16 E6 and E7 mRNA expressed from the respective HCT116 clone was confirmed by cDNA sequencing and subsequent alignment with either the published sequence of **(A)** HPV 16 E6 (GenBank: K02718.1, nt 83-560) or **(B)** HPV 16 E7 (GenBank: K02718.1, nt 562-858).

6.2. Supplementary Tables

Supplementary Table 1: Densiometric quantification of Western blot bands presented in Figure 7B.

Fold Change	CaSki			UM-SCC-47			C4-1		
	E7	p53	p21	E7	p53	p21	E7	p53	p21
DMSO	1	1	1	1	1	1	1	1	1
0.1 µM DAC	0.85	11.34	2.54	0.09	7.38	2.95	0.59	80.05	3.17
0.5 µM DAC	0.24	14.74	3.33	0.16	6.28	3.13	0.60	138.60	3.68
1.0 µM DAC	0.05	17.07	3.39	0.05	2.53	0.89	0.57	111.45	2.95

Fold Change	SiHa			UM-SCC-104			SW756		
	E7	p53	p21	E7	p53	p21	E7	p53	p21
DMSO	1	1	1	1	1	1	1	1	1
0.1 µM DAC	0.68	5.20	7.75	0.27	43.71	1.34	0.93	2.63	1.70
0.5 µM DAC	0.32	13.26	8.15	0.06	63.93	2.65	0.25	4.98	1.84
1.0 µM DAC	0.28	12.86	9.66	0.08	112.97	4.59	0.07	6.18	2.11

Supplementary Table 2: Densiometric quantification of Western blot bands presented in Figure 12B.

Fold Change	HPV 16 E7	
	CaSki	SiHa
Untreated	1.29	1.38
Non specific control	1	1
miR-375 mimics	0.35	0.07